

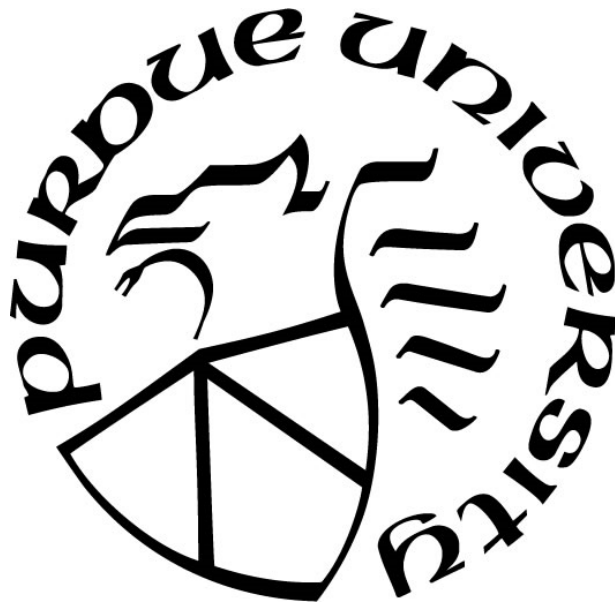
**A NOVEL MECHANISM FOR PROSTATE CANCER PROGRESSION:
FROM POLO-LIKE KINASE 1 TO EPIGENETICS**

by
Ruixin Wang

A Dissertation

*Submitted to the Faculty of Purdue University
In Partial Fulfillment of the Requirements for the degree of*

Doctor of Philosophy



Department of Biochemistry
West Lafayette, Indiana
December 2019

**THE PURDUE UNIVERSITY GRADUATE SCHOOL
STATEMENT OF COMMITTEE APPROVAL**

Dr. Timothy Ratliff

College of Veterinary Medicine

Dr. Xiaoqi Liu

University of Kentucky

Dr. James Forney

College of Agriculture

Dr. Shihuan Kuang

College of Agriculture

Approved by:

Dr. Andrew D. Mesecar

Dr. Jason R. Cannon

Dedicated to people that I love

ACKNOWLEDGMENTS

First and foremost, I would like to extend my gratitude to my mentor, Dr. Xiaoqi Liu, an extraordinary scientist and wise advisor. Without his guidance, intelligence, and support I would not have made it through graduate school. He has taught me foundational skills in science that I will use in the rest of my career. He has also granted me the freedom to test my own ideas as part of the training process. I would also like to show my gratefulness to my co-mentor, Dr. Timothy Ratliff, who is a charming leader of cancer center and a kind friend. Without his excellent expertise in prostate cancer study, it would be difficult for me to move my project forward. I would also like to thank my committee members, Dr. James Forney and Dr. Shihuan Kuang. Their suggestions and guidance on my project have been very valuable; and they also served in my prelim exam committee, many thanks to them for letting me pass the prelim.

I would like to thank all present and past members in Dr. Liu's Lab. They have lent their expertise and years of help to make me achieve new findings. I feel incredibly honored to have such wonderful lab mates. I sincerely acknowledge all my collaborators for the support from different aspects, bioinformatics, histopathological analysis, xenograft experiments and et al. I also want to extend my tremendous thanks to the Department of Biochemistry and PULSe program, as you let me become a graduate student at Purdue to pursue my Ph.D. degree; more importantly, all the faculty, staff and students here have been amazing and supportive. There are too many people to name, but I just cannot thank them enough.

Finally, words are powerless to express how indebted I am to my parents. Without their unending love and support I would not have survived my darkest moments. I truly wish we have all the time in the world ahead of us to spend together.

May God bless all that I love and treasure.

TABLE OF CONTENTS

LIST OF TABLES.....	8
LIST OF FIGURES	9
ABSTRACT.....	11
CHAPTER 1. EPIGENETIC REGULATION OF PROSTATE CANCER	13
1.1 Epigenetic modification in cancer	13
1.2 Phosphorylation of epigenetic modifiers in cancer.....	16
1.3 EZH2 methyltransferase and its phosphorylation in prostate cancer.....	18
1.4 Conclusions.....	20
CHAPTER 2. POLO-LIKE KINASE 1(PLK1) PROMOTES ADVANCED PROSTATE CANCER AND ITS METASTASIS IN MICE VIA IL4/IL13/STAT6- INDUCED ELEVATION OF M2 MACROPHAGES.....	22
2.1 Materials and methods	24
2.1.1 TCGA data.....	24
2.1.2 Tumor microarray (TMA) construction.....	24
2.1.3 Mice and breeding strategy.....	24
2.1.4 Autopsy and histopathology	25
2.1.5 Survival curve.....	25
2.1.6 Mouse prostate organoid culture	25
2.1.7 Bone marrow derived macrophages culture	26
2.1.8 Primary cells from mouse prostates.....	26
2.1.9 Immunohistochemistry and immunofluorescence staining	26
2.1.10 Western blot analysis	26
2.1.11 Quantitative real-time PCR	27
2.1.12 Flow cytometry analysis.....	27
2.1.13 Cell culture	27
2.1.14 Cell migration transwell assay	27
2.1.15 Colony formation assay.....	28
2.1.16 Measurement of IL4 secretion.....	28
2.1.17 Statistical analysis	28

2.2	Results.....	28
2.2.1	PLK1 expression is relevant to human prostate cancer progression and patients' poor survival.	28
2.2.2	Establishment of prostate-specific PLK1 overexpression and PTEN deletion mouse model.	29
2.2.3	PLK1 overexpression accelerates formation of invasive prostate adenocarcinoma in mice.	30
2.2.4	PLK1 is required for castration resistance in mice.....	31
2.2.5	PLK1 overexpression increases incidence of metastasis and induces epithelial-to-mesenchymal transition.	33
2.2.6	Murine prostate stem cell-derived organoids displays similar features presenting in original mice.....	34
2.2.7	PLK1 upregulates IL4/IL13/STAT6 pathway and lead to elevated population of M2 macrophage in murine prostate.....	35
2.2.8	PLK1-mediated activation of IL4/IL13/STAT6 pathway is targetable by STAT6 inhibitors.....	37
2.3	Discussion.....	38
CHAPTER 3. PLK1-DEPENDENT PHOSPHORYLATION OF EZH2 CONTRIBUTES TO ITS ONCOGENIC ACTIVITY IN CASTRATION-RESISTANT PROSTATE CANCER.....		67
3.1	Materials and methods	68
3.1.1	TCGA data.....	68
3.1.2	Cell culture and transfection.....	69
3.1.3	Western blot analysis.....	69
3.1.4	Immunoprecipitation.....	69
3.1.5	Recombinant protein purification.....	69
3.1.6	Kinase assay.....	70
3.1.7	Quantitative real-time PCR.....	70
3.1.8	Colony formation assay.....	70
3.1.9	Tumor microarray (TMA) construction.....	70
3.1.10	Immunohistochemistry and immunofluorescence staining.....	71
3.1.11	LuCaP35CR xenograft model.....	71

3.1.12	Serum PSA measurement.....	71
3.1.13	CRISPR.....	71
3.1.14	Statistical analysis.....	71
3.2	Results.....	72
3.2.1	Inhibition of PLK1 increases H3K27 trimethylation but not EZH2 expression in CRPC cells.....	72
3.2.2	PLK1 phosphorylates EZH2 at T144.	73
3.2.3	Blocking PLK1-mediated phosphorylation of EZH2 results in higher sensitization of CRPC cells to treatment of EZH2 inhibitors.	74
3.2.4	PLK1-mediated phosphorylation induce EZH2 functional switch from a repressor depending on PRC2 to a transcriptional co-activator of AR.	75
	It has been well accepted that	75
3.2.5	Co-targeting PLK1 and EZH2 shows a synergetic efficacy in CRPC cells.	76
3.2.6	Co-treatment of BI2536 and EPZ6438 synergistically inhibit tumor growth in CRPC patient-derived xenograft.....	76
3.2.7	High phosphorylation of EZH2 at T144 can be detected in both PLK-overexpressing mouse prostates and human advanced prostate cancers.	77
3.3	Discussion.....	77
	REFERENCES	97
	VITA.....	105
	PUBLICATIONS.....	106

LIST OF TABLES

Table 2-1 Reagents	65
Table 2-2 Primers.....	66
Table 3-1 Reagents	95
Table 3-2 Primers.....	96

LIST OF FIGURES

Figure 1.1 The dynamic epigenetic modifications on DNA and histone tail.	21
Figure 1.2 A model of the EZH2 functional switch by its hyper phosphorylation in CRPC..	21
Figure 2.1 PLK1 expression is relevant to human prostate cancer progression and patients' poor survival.....	44
Figure 2.2 Establishment of prostate-specific PLK1 overexpression and PTEN deletion mouse model.....	45
Figure 2.3 Venn diagram showing the overlap between PLK1-associated gene set and PI3K/AKT/mTOR pathway-related gene set.....	47
Figure 2.4 PLK1 overexpression accelerates formation of invasive prostate adenocarcinoma in mice.....	48
Figure 2.5 PLK1 overexpression accelerates formation of mPIN in PTEN heterozygous depletion mice.....	50
Figure 2.6 PLK1 is required for castration resistance in mice.....	51
Figure 2.7 PLK1 overexpression in LNCaP cells increases resistance to hormone-deprived culture.	52
Figure 2.8 PLK1 overexpression increases incidence of metastasis and induces epithelial-to-mesenchymal transition.	53
Figure 2.9 PLK1 overexpression in LNCaP cells is associated with EMT..	55
Figure 2.10 Gating strategy of enriched stem cells isolation.....	56
Figure 2.11 Mouse prostate stem cell-derived organoids displays similar features present in original mice..	57
Figure 2.12 PLK1 upregulates IL4/IL13/STAT6 pathway and lead to elevated population of M2 macrophage in murine prostate.....	58
Figure 2.13 Experimental scheme of Fig 2.12L-M and Fig 2.13E.....	60
Figure 2.14 Heat map of expression pattern of genes within the EMT-related gene set.....	61
Figure 2.15 PLK1-mediated activation of IL4/IL13/STAT6 pathway is targetable by STAT6 inhibitors.	62
Figure 2.16 PLK1 promotes prostate adenocarcinoma and its metastasis in mice via IL4/IL13/STAT6-induced elevation of M2 macrophages.....	64
Figure 3.1 Inhibition of PLK1 increases H3K27 trimethylation but not EZH2 expression in CRPC cells.	81
Figure 3.2 PLK1 phosphorylates EZH2 at T144.	83

Figure 3.3 Blocking PLK1-mediated phosphorylation of EZH2 results in higher sensitization of CRPC cells to treatment of EZH2 inhibitors.	85
Figure 3.4 PLK1-mediated phosphorylation induce EZH2 functional switch from a repressor depending on PRC2 to a transcriptional co-activator of AR.	87
Figure 3.5 Co-targeting PLK1 and EZH2 shows a synergetic efficacy in CRPC cells.	89
Figure 3.6 Co-treatment of BI2536 and EPZ6438 synergistically inhibit tumor growth in CRPC patient-derived xenograft.	91
Figure 3.7 High phosphorylation of EZH2 at T144 can be detected in both PLK-overexpressing mouse prostates and human advanced prostate cancers.	93
Figure 3.8 Model for EZH2 functional switch from a transcriptional repressor within PRC2 complex to a transcriptional activator working with AR in CRPC.	94

ABSTRACT

Prostate cancer is (PCa) the second leading cause of cancer death in males in the United State, with 174,650 new cases and 31,620 deaths estimated in 2019. Polo-like kinase 1 (PLK1) has been postulated to have a pro-tumorigenesis function, besides its critical role in regulation of cell cycle, and to be overexpressed in various types of human cancer, including prostate cancer (PCa). However, our understanding remains unclear regarding the pro-tumor properties of PLK1 partially due to a lack of proper animal model. Integrating our recently generated prostate-specific PLK1 knock-in genetically engineered mouse model (GEM) and the transcriptome data of human PCa patients, we identify an oncogenic role of PLK1 in the prostate adenocarcinoma progression, castration resistance and metastatic dissemination. To elucidate the underlying mechanism, we investigate the link between PLK1 and tumor microenvironment in PCa using the transgenic mouse model, and find that PLK1 overexpression enable the macrophages polarization towards M2 phenotype via driving the activation of IL4/IL13/STAT6 pathway. These findings first validates PLK1 as a critical oncogene closely associated with PCa progression *in vivo*, and uncover a novel function of PLK1 to facilitate IL4/STAT6 signaling and M2 macrophage polarization. Importantly, these findings suggest an efficient therapeutic strategy targeting STAT6 for treatment of advanced PCa which usually possessing a high level of PLK1 expression. To further explore the molecular mechanism underlying PLK1-induced PCa progression and resistance to therapy, we turned our eyes to epigenetic modifications. It has been documented that epigenetic deregulation such as histone modification and DNA methylation contributes to PCa initiation and progression. Enhancer of zeste homologue 2 (EZH2), the catalytic subunit of Polycomb-repressive complex 2 (PRC2), plays a critical role in repressing gene expression by tri-methylation of histone 3 at lysine 27 (H3K27me3). Emerging data have demonstrated that there is a link between EZH2 and oncogenesis as EZH2-mediated methylation acts as an important factor in epigenetic silencing of tumor suppressor genes in cancer. Expression of EZH2 is often upregulated in castration-resistant prostate cancer (CRPC), thus EZH2 has been proposed as a target for CRPC. Importantly, it has been demonstrated that EZH2 becomes hyperphosphorylated in CRPC cells. Further, it has been shown that the oncogenic function of EZH2 is usually regulated by the post-translational modifications. PLK1 acting as a serine/threonine kinase to regulate multiple signaling pathways in human cancer, however, whether PLK1 is involved in EZH2 phosphorylation is not known.

Herein, we show that Plk1 physically interacts with EZH2 and negatively regulates H3K27 trimethylation (H3K27me₃). Furthermore, Plk1 can phosphorylate EZH2 at T144, and Plk1-mediated phosphorylation of EZH2 is involved in inhibiting EZH2 activity toward H3K27me₃. More importantly, EZH2 phosphorylation by Plk1 is inhibitory for PRC2-mediated gene repression but required for transcriptional activation toward oncogenesis. Finally, by combination with Plk1 inhibitor BI2536, we show a robust sensitization of EZH2 inhibitors in CRPC cell lines, as well as in CRPC xenograft tumors. Our findings provide a new mechanism to define the oncogenic activity of EZH2 and suggest that inhibition of Plk1-mediated EZH2 activity may provide a promising therapeutic approach for CRPC.

CHAPTER 1. EPIGENETIC REGULATION OF PROSTATE CANCER

While a majority of studies have demonstrated that accumulation of genetic mutations will result in cancer initiation and progression, epigenetic changes without altering DNA sequences, which have been under intensive research in recent years, also contribute to activation of oncogenes and inactivation of tumor suppressors, and subsequently leading to the development of cancer [1]. Epigenetics is usually defined as a heritable change in gene expression without alteration in DNA sequence, including three primary epigenetic mechanisms - DNA methylation, covalent modification of histones and non-coding RNAs. It has been noted that heritable epigenetic marks can be dynamically regulated in response to any change in physiological conditions. Therefore, failure of the appropriate maintenance of these marks will highly possibly result in disease states such as cancer [2]. Epigenetic modifiers refer to adding or removing DNA methylation or histone modifications, which are defined as writers or erasers respectively. Besides writers and erasers, some epigenetic effectors can also be recruited, and affect the final epigenetic programs which we call them “readers”. Increasing data has shown that the activity of these epigenetic modifiers are also under regulation of some posttranslational modifications, such as phosphorylation, which might determine the final biological outcome [3]. In this review, we will take a comprehensive look of current findings of the regulation of the epigenetic modifiers by phosphorylation during carcinogenesis. We will also further discuss phosphorylation of one critical “writer”- enhancer of zeste homolog 2 (EZH2), which is a histone methyltransferase mainly mediating tri-methylation of histone H3 at Lys 27 (H3K27me3), in prostate cancer, and the idea of therapeutic strategies based on EZH2 phosphorylation in prostate cancer treatment.

1.1 Epigenetic modification in cancer

DNA methylation aberrations have been firstly and mostly linked to cancer initiation and progression among the epigenetic alterations, which is featured with genome-wide hypomethylation and hypermethylation of clusters of CpGs, known as CpG islands [4]. The role of global DNA hypomethylation in tumorigenesis has been well established. It occurs in various cancers and becomes an important reason resulting in increased genomic instability and inappropriate activation of oncogenes [5]. Hypermethylation of CpG islands in the promoters of

tumor suppressor genes to silence their expressions has been well noted to contribute to tumorigenesis. Many tumor suppressor genes, which are usually involved in various tumor-associated cellular processes including DNA repair, cell cycle, apoptosis, etc., have been observed to undergo CpG island hypermethylation. These genes, such as cell cycle related gene RB, the DNA repair protein BRCA1, and the tumor suppressor p53, are observed in different types of cancer like esophageal cancer, colorectal and gastric cancers, in which they are commonly mutated [6-9].

DNA methylation is maintained by a family of enzymes which are called DNA methyltransferases (DNMTs). There are four members of the DNMT family, including DNMT1, DNMT3A, DNMT3B and DNMT3L. Among them, DNMT1 plays the main role in maintaining the methylation status of DNA; at the same time, DNMT3A and DNMT3B are known to encode the de novo methyltransferases which will methylate the unmethylated DNA, while DNMT3L, unlike the other DNMTs, has no enzymatic activity [10]. A number of studies have demonstrated a relationship between alterations of DNMTs and tumorigenesis. Overexpression of DNMTs has been well reported in a variety of human cancers via correlating with aberrant DNA methylation. Consequently, overexpression of DNMTs tends to result in increased metastasis and poor prognosis. Highly expressed DNMT1 has been found in numerous patient specimens such as esophageal squamous cell carcinoma and pancreatic cancer. Similarly, increased DNMT3A or DNMT3B is involved in liver cancer, BRCA1-mutated breast tumor, intestinal neoplasia and prostate tumors [11-17]. In addition to overexpression of DNMTs, somatic mutations in DNMTs are also reported as an important contributor to malignant transformation. These mutations have been observed in colon cancers or acute myeloid leukemia, thus leading to disruption of normal DNA methylation and subsequently tumor promotion [18-20]. While deletion of DNMTs in mouse models has shown a lethal phenotype, several recent studies based on the conditional knockout approach demonstrated that loss of DNMTs also participates in development of peripheral T cell lymphoma (PTCL) or AML [21-23].

The N-terminal tails of histones, in which lysine and arginine residues are distributed, are subject to a variety of covalent posttranslational modifications (PTMs), such as acetylation, phosphorylation and methylation [24]. PTMs of proteins are highly dynamic in response to the

altered contexts to ensure the histone modification in balance which is critical for maintaining genome integrity [25]. Many different combinations of PTMs on multiple residues, which defined as “histone code” and regulated by enzymes as “writers” and “erasers”, can precisely govern specific cellular responses, such as cell cycle or signal transductions [26, 27].

Misregulation of histone PTMs, including acetylation, methylation and phosphorylation, have been extensively linked to a variety of cancer types [28]. In tumors, such a misregulation results in the abnormal activation of oncogenes or the repression of tumor suppressors. And the PTMs-induced inappropriate activation or inactivation depends on which residues are modified and which types of modifications occur [29]. Generally speaking, lysine acetylation can open up chromatin structure and subsequently tend to activate the transcription of its target genes [24]. Therefore, histone acetyltransferase (HATs) should promote transcription whereas histone deacetylases (HDACs) should be anti-transcriptional. Alterations and mutations occur on HATs (e.g. MOZ or CBP/EP300) or HDACs have been reported to correlate with a poor clinical outcome in cancer patients [30-32]. Besides the histone acetylation “writers” HATs or “erasers” HDACs, the histone acetylation “readers” the BET (bromodomain and extraterminal domain) proteins, such as BRD4, show increased expression in a variety of cancers. Consequently, the BET inhibitors, like JQ1, have demonstrated great therapeutic efficacy for the treatment of cancers, such as leukemia [33, 34]. Unlike histone acetylation, histone methylation will not exclusively act as a transcriptional activator or repressor; the activation or inactivation depends upon the open or close of the chromatin structure arising from which residue is modified and the degree of its methylation [35]. Similar with histone acetylation, tumor cells are also found common alterations of histone methylation and its histone methyltransferases (HMTs). For example, H3K27 trimethylation contributes to the aberrant silencing of multiple tumor suppressor genes and is associated with poor diagnosis of patients, and correspondingly, its main HMT, EZH2, is overexpressed in these cancers such as prostate cancer and breast cancer [36]. Similarly, the dysregulation of other HMTs and the methylation patterns (e.g. G9a and H3K9me3), have been found in cancers as well [37]. Histone demethylases have been recently identified to have a linkage to cancer. For example, LSD1, the demethylase for H3K4 and H3K9 residues, has been found overexpressed in many types of cancer [38]. Histone phosphorylation is a dynamic process catalyzed by several distinct kinases that are depending on different amino acid residues in histone [39]. Histone phosphorylation

occurs with the change of many cellular processes, such as cell cycle, DNA damage repair, and apoptosis, therefore its dysregulation often leads to tumorigenesis. Accordingly, the kinases regulating the histone phosphorylation are always found overexpressed in cancers. For example, high PRK1 level, which mediates H3T11 phosphorylation, correlates with high stages of prostate cancer [40]. (Fig 1.1)

1.2 Phosphorylation of epigenetic modifiers in cancer

Epigenetic modifiers, including “writers”, “erasers” and “readers”, play a crucial role in maintaining the dynamic balance of epigenetic modification patterns, usually depending on their activities. It has been well established that these modifiers are also under regulation of posttranslational modifications (PTMs), and their activity are affected by these PTMs consequently [3]. Among the PTMs, the importance of phosphorylation contributing to epigenetic events in response to environmental changes has been widespread accepted. These phosphorylation is catalyzed and mediated by many kinases including protein kinase B (PKB/Akt), cyclin-dependent kinases (CDKs), polo-like kinase 1(PLK1), protein kinase A (PKA), AMP-activated protein kinase (AMPK), casein kinase 2 (Ck2) and ataxia telangiectasia and Rad3 related kinase (ATR), etc. Phosphorylation-mediated regulation of modifiers may directly activate or suppress their enzymatic activity, or indirectly regulate the interaction between modifiers with other proteins or RNAs, or make chromatin structure tight or loose [41]. And several epigenetic modifiers have been found either aberrantly hyperphosphorylated or hypophosphorylated in cancer cells, including DNA methyltransferases, histone methyltransferases, histone demethylases, histone acetyltransferases and deacetylases.

DNMTs especially DNMT1 have been known to be phosphorylated to regulate the protein stability and enzymatic activity. AKT and PKC kinases were reported to phosphorylate DNMT1 at Ser127/143 and Ser127, respectively, which will disrupt the interactions of DNMT1 with PCNA and UHRF1 in human cells to promote tumorigenesis [42, 43]. In addition, it has been reported that GSK3 β can interact with DNMT1 and then phosphorylate DNMT1 at Ser410 and Ser414, and finally promote β TrCP-induced proteasomal degradation of DNMT1 [44]. There are not many reports showing the phosphorylation of DNMT3s, however, the kinase CK2 tends to phosphorylate DNMT3A, and decrease the global genomic methylation levels [45].

The histone methyltransferase EZH2 has been shown to be phosphorylated by several kinases, such as AKT, AMPK, CDKs, or Janus kinase 3 (JAK3), in various types of cancer. AKT-mediated phosphorylation of EZH2 at Ser21 results in loss of methylation of H3K27 and increase of expressions of genes used to be silent by H3K27me3. The AKT-mediated phosphorylation of EZH2 promotes expression of several critical oncogenes, and is involved in the development of prostate cancer, uterine cancer and glioblastoma tumorigenesis [46-48]. AMPK can also phosphorylate EZH2 at Thr311 to disrupt the polycomb repressive complex 2 (PRC2), in which EZH2 is the core component, and thus suppresses methyltransferase activity in both ovarian and breast cancers [49]. In addition, CDK1/2 have also been reported to phosphorylate EZH2 at Thr350 and Thr487, which will not only inhibit the enzymatic activity, but also block EZH2 binding to its target region, and will highly increase the risk of tumorigenesis [50, 51]. Phosphorylation of EZH2 by JAK3 induces a noncanonical function of EZH2 to promote transcriptional activation in natural killer/T-cell lymphoma [52]. Collectively, regulation of EZH2 by phosphorylation is highly correlated with tumorigenesis with regard to its activity. We will further discuss about the role of EZH2 and its phosphorylation in prostate cancer and castration-resistant prostate cancer (CRPC) in the subsequent session.

Although contribution to cancer by the phosphorylation of H3K27 histone methyltransferase has been extensively studied, phosphorylation of histone methyltransferases that add methyl groups to other residues of histone tail, such as H3K4, was also reported. For instance, ATR phosphorylates MLL (H3K4 methyltransferase) on Ser516 in response to environmental stress in the S phase, resulting in its degradation and finally contributing to human MLL leukaemia [53]. Several studies also demonstrated the unusual phosphorylation events occurring on arginine methyltransferases. For example, in myeloproliferative neoplasms, Janus kinase 2 (JAK2) oncogenic mutant V617F can phosphorylate protein arginine methyltransferase 5 (PRMT5), consequently decreasing its activity and increasing expression of genes that are inhibited by PRMT5 [54].

Histone demethylases also appear to be regulated by phosphorylation, although how phosphorylation affects the activities still remains to be elucidated. Protein kinase A (PKA)-induced phosphorylation of H3K9me2 demethylase PHD finger protein 2 (PHF2) at Ser1056

results in its increased binding to a DNA-binding protein ARID5B, reduction of methylation on ARID5B, and decrease of gene transcription [55]. CDK1 can catalyze phosphorylation of another demethylase, PHD finger protein 8 (PHF8) at Ser33 and Ser84, leading to disruption of PHF8 with chromatin in acute promyelocytic leukemia [56].

Phosphorylation can also regulate the activities of HATs and HDACs, and therefore affect the gene transcription via histone acetylation patterns. The histone acetyltransferase CBP is phosphorylated by CDK2 in a cell cycle-dependent manner. One study demonstrated that the DNA-dependent protein kinase (DNA-PK) phosphorylates hGCN5, which possesses HAT activity, and the phosphorylation suppresses its HAT activity [57]. In addition, in response to DNA damage, the HAT activity of activating transcription factor 2 (ATF2) is phosphorylated [58]. The PI3K/AKT pathway also stimulates p300 phosphorylation at Ser1834 and its transcriptional activator potential [59].

Like HMTs, HDACs have been commonly believed that their activities are tightly regulated by phosphorylation. The HDAC family members, including HDAC1, HDAC2, HDAC3, HDAC4, HDAC5, HDAC6 and HDAC8, are phosphorylated by many kinases, such as CK2, PKA, extracellular signal regulated kinase (ERK1/2), etc. within different residues, to influence the structure, stability, acetyltransferase activity, binding with partners, or cellular localization, and ultimately leading to either pro- or anti-tumorigenesis [60, 61]. I will take two recent findings as examples. Activated PI3K/AKT pathway in breast cancer cells can lead to the phosphorylation of the p70 S6 kinase (S6K1) and transcriptionally regulate estrogen receptor α (ER α) expression [62]. Moreover, c-Jun N-terminal kinase (JNK)-mediated phosphorylation of HDAC3 in triple-negative breast cancer (TNBC) might affect the sensitivity of HDAC inhibitors in treatment [63].

1.3 EZH2 methyltransferase and its phosphorylation in prostate cancer

In 2019, prostate cancer (PCa) has become the most common cancer with 174,650 newly diagnosed cases and the second leading cause of death associated with cancer or cancer-related factors in males in the United States with estimated 31,620 deaths [64]. Androgen deprivation therapy (ADT) is the routinely used approach to treat PCa patients. Although patients initially respond to ADT well, castration-resistant prostate cancer (CRPC) eventually occurs in most of

these patients after several years and then develops into even worse metastasis [65]. It has been well established that androgen receptor (AR) signaling is enhanced and plays an important role in CRPC [66]. Subsequently, the AR inhibitors, such as enzalutamide and abiraterone, have been approved by the Food and Drug Administration (FDA) for the treatment of late stage PCa [67]. However, enzalutamide resistance eventually develops for almost all cases, making the disease almost incurable. Therefore, how to overcome enzalutamide resistance of CRPC has been under intensive research, and new targets and mechanism-based strategies are urgently needed to treat these patients [68-70].

As we described above, EZH2, the catalytic subunit of PRC2 complex, plays a critical role in repressing gene expression by mediating H3K27me3. Many studies have demonstrated that there is a tight linkage between EZH2 and oncogenesis, and that EZH2-mediated trimethylation triggers silencing of tumor suppressor genes in cancer [71]. Besides acting as a transcriptional suppressor, emerging evidence has shown the uncanonical role of EZH2 towards transcription activation of some genes, whose expression seems to be PRC2-independent. EZH2 has been identified as either a direct transcription activator or coactivator binding with other transcription factors to promote expression of several oncogenes. For example, the transcription levels of genes in NOTCH pathway, NF- κ B pathway or Wnt pathway are directly or indirectly regulated by EZH2 in breast cancer and colon cancer, respectively, which are independent of EZH2 methyltransferase activity [72-75].

In PCa especially in CRPC, EZH2 is overexpressed and promotes cancer cell proliferation and invasion, making EZH2 an attractive anti-cancer drug target. Similar with other types of cancer, aberrant PTMs, such as phosphorylation, of EZH2 are also found in PCa (Fig 1.2). For example, AKT-mediated phosphorylation of EZH2 at Ser21 induces a functional switch from a PRC2-dependent transcription repressor to a PRC2-independent transcription coactivator working with AR to promote the development of CRPC [46, 76]. In addition to AKT kinase, CDK1/2 can also phosphorylate EZH2 at Thr350 during S and G2/M phases. Phosphorylation of Thr350 promotes PCa cell proliferation and migration. Consequently, blocking Thr350 phosphorylation is important for abrogation of the oncogenic activity of EZH2 [50, 51].

Polo-like kinase 1 (PLK1), a regulator of various stages of mitosis, has been shown to be overexpressed in various types of cancers. Our lab has made a series of discoveries to show that Plk1 plays a critical role in different aspects of PCa, including its initiation, progression and therapy resistance [77]. It was shown that PLK1 directly phosphorylates SUZ12, another component of PRC2 complex, and that PLK1 phosphorylation of SUZ12 abolishes its interaction with EZH2 and the PRC2 function [78]. Whether PLK1 also directly phosphorylates EZH2 is unknown.

1.4 Conclusions

PCa is the most commonly diagnosed malignant neoplasm of males in the United States, and ADT is an effective treatment for patients with PCa. However, most patients ultimately develop resistance and cancer relapse. Treatment for CRPC is very limited. Therefore, exploring novel cellular mechanisms controlling progression of PCa is very critical for identifying new targets and eventually developing efficient strategies to treat CRPC. Expression of EZH2 is often upregulated in CRPC, thus EZH2 has been proposed as a target for CRPC. Importantly, it has been demonstrated that EZH2 becomes hyperphosphorylated in CRPC cells [48]. However, very few studies reported the effect of PLK1-dependent phosphorylation on epigenetic modifications. Our ongoing study is expected to fill in this knowledge gap by determining whether and how PLK1-dependent phosphorylation of various epigenetic regulators contributes to PCa progression and drug resistance.

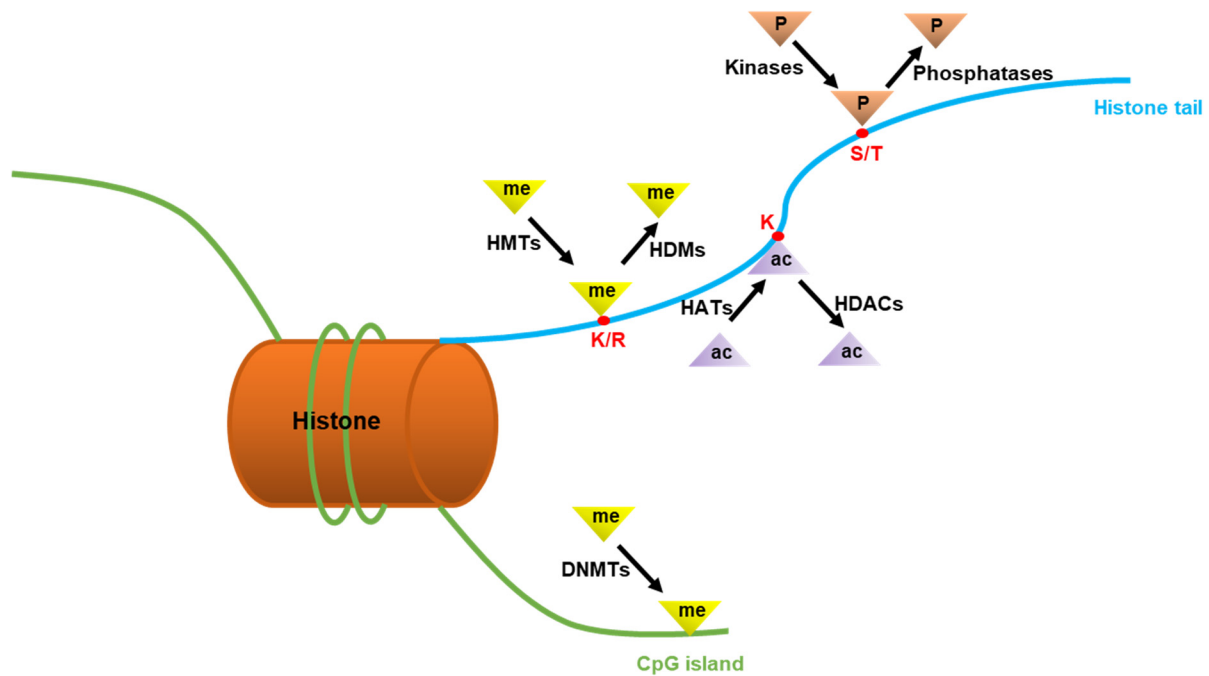


Figure 1.1 The dynamic epigenetic modifications on DNA and histone tail. Enzymes coordinately regulate the epigenetic modifications by adding or removing epigenetic hallmarks. Deregulation of the enzymes can lead to oncogenesis.

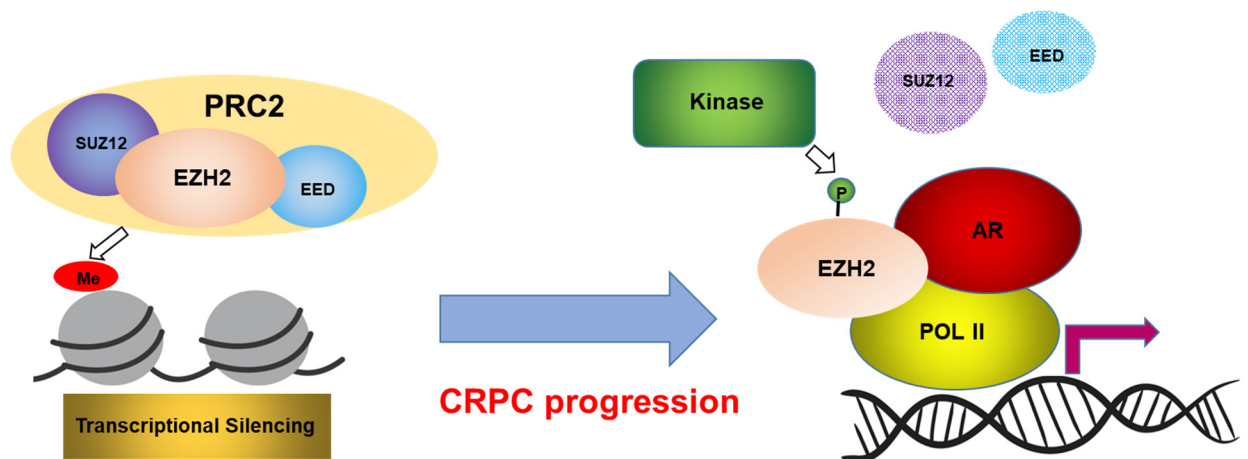


Figure 1.2 A model of the EZH2 functional switch by its hyper phosphorylation in CRPC. Deregulation of EZH2 phosphorylation can change EZH2 from a transcriptional repressor depending upon PRC2 to a transcriptional co-activator cooperating with AR which is independent of PRC2, finally contributing to CRPC progression.

CHAPTER 2. POLO-LIKE KINASE 1(PLK1) PROMOTES ADVANCED PROSTATE CANCER AND ITS METASTASIS IN MICE VIA IL4/IL13/STAT6-INDUCED ELEVATION OF M2 MACROPHAGES

Begin a new chapter here. Each chapter must begin on a new page. If you are pasting in previously published articles, you will need to reformat the articles to match the guidelines that are set in this template. You will also want to use the heading styles above even though you may have previously applied styles in the original document. The styles above will ensure you meet the Graduate School requirements.

Prostate cancer (PCa) is the top diagnosed type of human cancer in males in United States with 174,650 new cases in 2019. Patients with advanced prostate cancer have very poor five- year survival rates despite recent therapeutic and pharmaceutical advances. Therefore, PCa remains the second leading cause of cancer-induced death in United States[64]. Current standard of treatment for patients with advanced PCa is androgen-deprivation therapy (ADT) including surgery or androgen receptor (AR) inhibitors such as enzalutamide and abiraterone. While a majority of patients possess an initial response to these agents, Castration-resistant prostate cancer (CRPC), which is usually with an aberration in AR signaling such as mutations of AR and AR splice variants, is ultimately developed and leads to more than 90% occurrence of bone metastases [79, 80].

The tumor microenvironment (TME) has been demonstrated to play an emerging role in the initiation and progression of PCa [81]. Cancers are a dynamic complex in which malignant cells and many other cells in the microenvironment create a reciprocal interaction in which abnormal changes in the non-transformed cells could drive a tumor-promoting events and in turn transformed cells would enhance these changes in TME by cytokines, chemokines, and growth factors secretion and inflammatory responses at all stages of tumorigenesis [82-84]. Recent studies have revealed that abnormally increasing numbers of tumor-associated macrophages (TAMs) is correlated with poor prognosis of Patients with advanced PCa, especially M2 subtype of TAMs whose population is elevated in high stage tumor and Gleason scores [85-87]. M2 macrophages are shown to promote docetaxel resistance and metastases in PCa patients, therefore therapies aimed to block M2 macrophages and the signaling pathways that drive its increase have shown the

potential for elongating the survival of patients with advanced PCa. M1 and M2 macrophages polarization is a dynamic process regulated by a network of signaling transcriptionally and post-transcriptionally [88]. For M2 macrophages, interleukin 4 (IL-4) and interleukin 13(IL-13) have considered to lead to its activation state via signal transducers and activators of transcription 6 (STAT6) [89].

Accumulating evidence suggests that polo-like kinase 1 (PLK1), whose main function is to regulate mitosis, is involved in multiple aspects of PCa initiation and progression and remains a valid target for patients therapy [90]. Many our previous studies revealed that PLK1 contributes to advanced PCa via its kinase activity inducing phosphorylation on oncogenes or tumor suppressors or its cooperation with oncogenic transcription factors to regulate pro-tumor signaling such as AR pathway and WNT/ β -catenin pathway [77, 91]. Reports about the role PLK1 plays in TME and inflammatory cytokines production are rare. Emerging evidence has shown that PLK1 is involved in the regulation of interaction between malignant cells and immune cells in TME. For example, PLK1 regulates innate immunity and inflammation by affecting NF- κ B [92]; another article shows that PLK1 expressed in monocytic THP-1 cells participates in production of Tumor necrosis factor alpha (TNF- α) by activation of Toll-like Receptor (TLR) [93]. However, more roles PLK1 plays in TME network need further exploration, and underlying mechanism how PLK1 promotes tumorigenesis via activating pathways associated with production of pro-tumor cytokines is uncertain. Lack of a proper pre-clinical model for PLK1 is one major fence to achieve it as in vivo study represents TME to the greatest extent.

Herein, we developed a transgenic mouse model with conditionally overexpression of PLK1 based on a Cre-loxp system. In this study, we used prostate-specific overexpression of PLK1 to show that Plk1 accelerates murine PIN and cancer formation and is highly required for castration resistance and metastasis via activation of IL4/IL13/STAT6 pathway and elevation of M2 macrophages in mice.

2.1 Materials and methods

2.1.1 TCGA data

TCGA prostate adenocarcinoma patient data containing 52 normal prostate tissues and 475 primary prostate tumors (original 498 cases, we combined those from same patient) was obtained from The Cancer Genome Atlas (TCGA, <https://cancergenome.nih.gov/>); complete Clinical Data set was collected from level 2, and the RNA-seq data were collected from Level 3 (for Segmented or Interpreted Data, IlluminaHiSeq_RNASeqV2 of TCGA). The correlation between Gleason score and the gene of interest was constructed using the boxplot package in R. Gene Set Enrichment Analysis (GSEA) (<http://software.broadinstitute.org/gsea/index.jsp>) was applied to determine gene pathway enrichment variation between two groups based on expression level of the gene of interest. The online software MORPHEUS was used to build a heatmap of gene expression, and hierarchical clustering was used to determine sample similarity.

2.1.2 Tumor microarray (TMA) construction

TMA was obtained from the archives of formalin fixed paraffin-embedded tissue blocks in which there are 165 prostate cancer specimens and 34 benign controls from patients who underwent radical prostatectomy at the University of Kentucky (KY, USA), and constructed by the Markey Biospecimen and Tissue Procurement Shared Resource Facility. The use of human prostate specimens was approved by University of Kentucky Institutional Review Board.

2.1.3 Mice and breeding strategy

Animal protocol was approved by the Purdue University Animal Care and Use Committee (Protocol no. 1111000133E001) and Institutional Animal Care and Use Committee of University of Kentucky (Protocol no. 2018-3023). PTEN loxp/loxp (PTEN^{-/-}) mice (strain name: B6.129S4-Ptentm1Hwu/J; genetic background: 129S4/SvJae-BALB/c, backcrossed onto the C57BL/6J background for at least five generations) were purchased from the Jackson Laboratory[94]. Probasn-Cre (PbCre) mice [strain name: Tg (Pbsn-cre) 4Prb; genetic background: C57BL/6] were purchased from the Jackson Laboratory [95]. Inducible conditional PLK1 KI mice (genetic background: C57BL/6NTac, backcrossed with C57BL/6J wild-type mice for at least five generations) were generated by Taconic Biosciences (Germany) (Fig 2.2.A). The breeding strategy

is shown in Fig 2.2.C. DNA was extracted from the left ear biopsy for PCR genotyping (see primer sequences in Supplementary Table S1).

2.1.4 Autopsy and histopathology

Mice were sacrificed at 12, 30 and 54 weeks of age. The genitourinary bloc (consisting of the prostate lobes, seminal vesicles, bladder, and proximal urethra, et al.) was harvested [96]. The GU blocs were photographed, weighed, fixed in 10% buffered Formalin for 12 hr., transferred to 70% alcohol, and finally embedded in paraffin. The paraffin-embedded tissues were sectioned (4 μ m) and stained with hematoxylin and eosin (H&E) for histopathologic assessment by pathologists according to Mouse Prostate Harbor Classification [97].

2.1.5 Survival curve

15 mice from each genotype were monitored up to 1 year age for survival analysis. When mice were found dead spontaneously or sacrificed due to profoundly ill, they were marked as a death. Finally, Kaplan Meier survival curve was generated by Graphpad Prism software.

2.1.6 Mouse prostate organoid culture

The mouse prostate organoid culture was performed as previously described [98]. Prostate glands were isolated from 30 weeks old mice, and then digested by Collagenase Type IV (Sigma) and trypsin (Gibco). To eliminate aggregates, digested prostates were passed through 21G syringe 5 times and 40mm cell strainers. Cell suspensions were incubated with CD45-FITC, CD31-FITC Sca1-APC, and CD49f-PE, then subjected to live cell sorting on the BD FACS Aria in sterile condition to isolate LSC population ((CD45/CD31)⁻ Sca1⁺CD49f⁺). Gating strategy is shown in Fig 2.10.A. Sorted LSC cells was resuspended in 12-well plates, with a density of 10,000 cells/well, and incubated in 2:1 Matrigel/Prostate Epithelial growth medium (PrEGM) for 7 days. Half medium was changed every 3 days. The organoids were observed and counted under microscope at the day of 7. Next, the organoids in Matrigel were fixed in 10% buffered Formalin for 1 hr. and transferred to 70% ethanol for another 1 hr. All fixed organoids were embedded in paraffin and sectioned. H&E staining and IHC staining were performed as standard protocol.

2.1.7 Bone marrow derived macrophages culture

Isolation and differentiation of bone marrow derived macrophages were performed as described earlier [99]. Isolated bone marrow-derived cells were cultured in the presence of Macrophage Colony-Stimulating Factor from mouse (Sigma). Differentiated macrophages were incubated with supernatants from indicated genotype primary mouse prostate cells

2.1.8 Primary cells from mouse prostates

Generation of mouse primary prostate cell clones were performed as described earlier [100]. Freshly dissected prostate glands (Ventral, Dorsal and lateral lobes) were minced with scalpel to ~1mm cubes and subjected to digestion with collagenase Type IV (Sigma) and trypsin (Gibco). Cell suspensions passed through 100 μ m and 40 μ m cell strainers (BD Bioscience) and then was cultured in medium DMEM containing 10% FBS, 25 μ g/mL bovine pituitary extract (Invitrogen), 5 μ g/mL insulin (Sigma-Aldrich) and 6 ng/mL recombinant human epidermal growth factor (rhEGF) (Invitrogen). After cell colonies with epithelial morphology were formed, cells were trypsinized, and cultured separately to expand the population. Culture medium was changed every 3 days.

2.1.9 Immunohistochemistry and immunofluorescence staining

DAB-immunohistochemistry (IHC) and Immunofluorescence (IF) were performed as previously described [101]. Antibodies and reagents used for IHC and IF are listed in Supplemental Material.

2.1.10 Western blot analysis

Extract was prepared by sonicating prostate tissues or cell lysates in buffer containing 50 mM Tris, 150 mM NaCl, 1% NP-40, 0.5% sodium deoxycholate, 0.2% SDS, protease inhibitors, and phosphatase inhibitors (Sigma). After quantification with BCA assay, the equal amounts of protein were subjected to western blot according to standard protocol. Antibodies and reagents used for western blot are listed in Supplemental Material.

2.1.11 Quantitative real-time PCR

Total RNA from mouse prostates was extracted by RNeasy Mini Kit (Qiagen). The first-strand cDNA was generated by iScript cDNA Synthesis Kit (Bio-Rad). Real-time PCR reactions were performed with a SYBR green PCR kit (Roche Applied Science) and a Roche LightCycler 96 thermocycler (Roche Diagnostics Corp.). All individual reactions were performed in triplicate. All genes' expressions were quantified by $2^{-\Delta\Delta C_t}$ relative quantification method and normalized to GAPDH expression. Primers used for real-time PCA are listed in Supplemental Material.

2.1.12 Flow cytometry analysis

Cell suspensions were obtained from prostates by digestion with collagenase Type IV (Sigma) and trypsin (Gibco), and stained with CD45-Alex 488, F4/80-BV605, CD68-APC, and CD163-PE. Flow cytometry analyses were performed at CytoFLEX (BECKMAN) cytometer, and the results were analyzed by FlowJo software. The antibodies used for FACS are listed in Supplemental Material.

2.1.13 Cell culture

Human PCa cell line LNCaP purchased from American Type Culture Collection and cultured in RPMI-1640 medium contained 10% of fetal bovine serum (Atlanta Biologicals, GA, USA), under a humidified atmosphere at 37 °C, with 5% CO₂.

2.1.14 Cell migration transwell assay

Cell migration was measured using transwells (6.5 mm diameter; 8 μm pore size polycarbonate membrane, Corning). 1×10^5 Cells were placed in the upper chamber under medium with 0.5% serum, whereas the lower chamber contained the medium with 10% FBS. After 24 hr. of incubation at 37°C with 5% CO₂, cells migrated through transwell membrane were photographed under microscopy

2.1.15 Colony formation assay

1,000 cells were seeded in 6-well plate and followed with indicated treatment for 14 days. The medium was changed every 3 days. Then the colonies were fixed by 10% formalin and stained with 5% crystal violet. After washing twice by PBS, colonies were photographed.

2.1.16 Measurement of IL4 secretion

5×10^5 primary prostate cells from indicated genotype mouse were cultured for 3 days, and supernatants from cultured cells were collected, filtered, centrifuged and stored at 20°C for further use. IL4 was measured from supernatants using Mouse IL4 ELISA Kit (Abcam) following the manufacturer instruction and analyzed by GloMax Discover Microplate Reader (Promega)

2.1.17 Statistical analysis

The Kaplan-Meier method and the log rank test were used to compare patient's survival time and time to tumor progression between high and low gene expression subgroups. False discovery rate (FDR) q values were calculated for GSEA analysis, a gene set was considered significantly enriched if its normalized enrichment score (NES) has an FDR $q < 0.25$. Statistical analyses were performed with Student t test (two-tailed) for single comparison or One-way ANOVA for multiple comparisons. All data were shown as mean values \pm SD ($n > 3$), and statistical significance was defined as * $p < 0.05$; ** $p < 0.01$; *** $p < 0.001$; n.s., not significant.

2.2 Results

2.2.1 PLK1 expression is relevant to human prostate cancer progression and patients' poor survival.

PLK1 has been postulated to be an oncogene associated with cancer progression by its kinase activity to regulate multiple aspects of cell signaling pathway including DNA damage response, cell division and survival [102, 103]. PLK1 is usually upregulated in various cancers, including PCa [104]. To examine the relevance of PLK1 expression to clinical outcome of patients with PCa, we analyzed the RNA-Seq gene expression and clinical data for 475 tumors and 52 adjacent normal tissues from PCa patients obtained from The Cancer Genome Atlas (TCGA) data portal. Expression of PLK1 was found negatively correlated with time to tumor progression (TTP)

and overall survival in PCa patients (Fig 2.1.A-B). To identify correlation of PLK1 with disease progression, we explored mRNA levels of PLK1 and its associated genes in adjacent normal prostate tissues and primary tumors, respectively. We found that PLK1 mRNA expression was gradually increased with disease progression (Gleason score from 6 to 10) compared with normal tissues (Fig 2.1.C). In the meanwhile, upregulation of PLK1-associated genes was likely observed in primary PCa (Fig 2.1.D). To further validate protein expression shift of PLK1 with PCa progression, Immunohistochemistry (IHC) with the antibody against PLK1 was performed on PCa tissue microarray. Consistently with mRNA expression, tumors in high-grade (Gleason score \geq 8) was shown a much higher and both nucleus/cytoplasmic protein expression level of PLK1 compared with adjacent normal tissues and low-graded tumors (Gleason score $<$ 8) (Fig 2.1.E).

2.2.2 Establishment of prostate-specific PLK1 overexpression and PTEN deletion mouse model.

PLK1 has been found to be overexpressed in both mRNA and protein aspects in PCa and correlated with poor diagnosis and survival of patients; however, there is still lack of direct evidence to prove this notion, one of the main hurdle to achieve it is the lack of proper animal models. Our lab previously generated a conditional PLK1 knock-in (KI) mice in which the KI allele includes a CAG promoter sequence, a loxP-flanked transcription termination cassette (STOP) and mouse PLK1 ORF. To over-express PLK1, Cre recombinase will mediate deletion of the STOP cassette [105] (Fig 2.2.A). To define the oncogenic roles of PLK1 in prostate cancer initiation and progression, we established a prostate-specific PLK1 overexpression mouse model by crossbreeding our generated female PLK KI mice with male Probasin Cre (PbCre) mice which induce prostate-specific expression or deletion of genes of interest after their sexual maturity. Compared with PbCre only mice, PbCre/PLK1KI mice have shown PLK1 overexpression mainly in dorsal and lateral lobes, and ventral lobes, but not in anterior lobes via immunofluorescent staining (Fig 2.2.B). However, PLK1 overexpression alone in prostate might not be sufficient to trigger any significantly histological difference in any lobes at least during 3 months after sexual maturity (Fig 2.3.A). To help drive disease initiation, prostate-specific PTEN conditional null mice, which could recapitulate the human prostate adenocarcinoma progression, were crossbred with PLK1 KI mice to ultimately generate PbCre/PTEN^{+/-} mice, PbCre/PLK1/ PTEN^{+/-} mice, PbCre/PTEN^{-/-} mice and PbCre/PLK1/ PTEN^{-/-} mice [101](Fig 2.2.C); Male mice were genotyped

right after weaning (Fig 2.2.D). PLK1 overexpression and its activation indicated by phosphorylation at threonine 210 were confirmed in PbCre/PLK1/ PTEN^{+/-} mice and PbCre/PLK1/ PTEN^{-/-} mice by western blot; in the meanwhile, PTEN loss and it induced activation of PI3K/AKT/mTOR pathway indicated by phosphorylation of AKT were also confirmed by western blot and immunofluorescent staining (Fig 2.2.E-F). 61 PLK1-associated genes were shown in Venn diagram overlapped within PI3K/AKT/mTOR pathway (Fig 2.3.B). Together, our prostate-specific PLK1 overexpression and PTEN deletion mouse should be an ideal model to define the role of PLK1 in PCa development.

2.2.3 PLK1 overexpression accelerates formation of invasive prostate adenocarcinoma in mice.

As shown in Fig 2.2.C, genitourinary blocs (GU blocs) where mouse prostates are located were dissected from indicated genotype mice at the age of 12 weeks, 30 weeks and 54 weeks. The GU blocs from PbCre/PLK1/ PTEN^{-/-} mice were obviously bigger than those from PbCre/PTEN^{-/-} mice at the age of 30 weeks; further, PbCre/PLK1/ PTEN^{-/-} mice burden significantly larger tumors, not limited to local prostate, compared with PbCre/PTEN^{-/-} mice over one year age; in the meanwhile, both genotypes mice showed abnormally swollen seminal vesicles with pus in it (Fig 2.4.A). Histological observation indicated that murine PIN (mPIN) featured with stratification of the epithelial layer with atypia within prostatic ducts and acini were formed in both PbCre/PTEN^{-/-} and PbCre/PLK1/ PTEN^{-/-} mice at 12 weeks; notably, more inflammatory cell infiltration were observed upon PLK1 overexpression (Fig 2.4.B); in addition, in the PLK KI mice, malignant cells have extended through fibromuscular layer, and more invasive sites were observed, as shown by the laminin immunostaining in Fig 2.4.D. At age of 30 weeks, invasive prostate adenocarcinomas were developed at different rates and in varying degrees among these two genotypes mice; prostatic glands from PbCre/PLK1/ PTEN^{-/-} mice presented with invasive prostate adenocarcinomas were much larger than those from PbCre/PTEN^{-/-}, and importantly, malignant cells upon PLK1 overexpression were poorly differentiated (Fig 2.4.B). This difference in degrees of malignancy among two genotypes mice was more distinct at the age of 54 weeks. As shown in the Fig 2.4.B, not only did prostatic glands with PLK1 overexpression show a much larger occupied tumor area, they also presented adenocarcinoma accompanied by pleomorphic sarcomatoid areas which is a rare and aggressive malignancy [106] (Fig 2.4.B). When compared

the mouse prostates among PTEN heterozygous mice with or without PLK1 overexpression, similarly with what we found in PTEN homozygous knock-out (KO) mice, PLK1 increased prostate tumor burden and accelerated the formation of invasive prostate adenocarcinomas (Fig 2.5.A-C). In addition, we continuously followed the health status and death of 15 mice from each genotypes (in total 60 mice) for 60 weeks and drew the survival curve among them; as shown in Fig 2.4.C, PLK overexpression is negatively correlated with mouse survival, which is consistent with our finding in clinical database in Fig 2.1.B.

To further explore the possible cause of the differences in PCa initiation and development among these mice, immunostaining of Ki67, AR and CD31 were performed on the prostates at the age of 12 weeks. We found that there were more Ki67 positive cells in PLK1 KI prostates than in PTEN knock-out only prostates, which indicated that PLK1 overexpression enhanced cellular proliferation in mouse prostates (Fig 2.4.D). One hallmark of prostate adenocarcinoma is aberrantly upregulation of androgen receptor (AR), as shown in Fig 2.4., AR signaling was significantly increased in the prostates from PbCre/PLK1/ PTEN^{-/-} mice but not from PbCre/PTEN^{-/-} mice (Fig 2.4.F). Angiogenesis level is another hallmark for tumor formation, thus we assessed blood vessels by staining CD31 and found that PLK1 KI prostates possessed a higher level of angiogenesis than PTEN deletion only prostates (Fig 2.4.G, Fig 2.5.D). These results combined together suggested that PLK1-promoted adenocarcinoma formation was due to increased cell proliferation, AR signaling and angiogenesis in mouse prostates.

2.2.4 PLK1 is required for castration resistance in mice.

Localized PCa is commonly treated by surgery or radiotherapy; when cancer cells spread outside of prostate, this so-called advanced PCa is treated by androgen-deprivation therapy (ADT). However, regression of cancer ultimately occurs after ADT treatment even though patients initially respond to it well. This stage is known as Castration-resistant prostate cancer (CRPC), and revealing underlying mechanism of CRPC development is critical for its treatment [107]. To assess the role of PLK1 play in the development of castration resistance, we castrated PbCre/PTEN^{-/-} and PbCre/PLK1/ PTEN^{-/-} mice at 18 weeks when invasive adenocarcinoma has formed, and checked the long-term response of mice to castration by harvesting prostates at 54 weeks (Fig 2.6.A). For PLK1 KI mice, 3 out of 4 prostates remained adenocarcinoma; in contrast, all 4 PTEN KO only

mice were cured after castration (Fig 2.6.B). As shown in Fig 2.2.C, GU blocs appeared significantly larger in the castrated PbCre/PLK1/ PTEN^{-/-} mice than in the castrated PbCre/PTEN^{-/-} mice. The former presented solid tumor, and the latter, in contrast, showed obvious non-tumor phenotype but small and shrinking prostates. Histological analysis demonstrated that castrated PTEN KO prostates shown no clear evidence of mPIN, adenocarcinoma, and even epithelial hyperplasia, but PLK1 KI prostates with castration resistance presented a substantial number of malignant cells indicating that PCa with PLK1 overexpression benefited from ADT (Fig 2.6.D). We found a number of apoptotic cells in castrated PbCre/PTEN^{-/-} prostate by immunostaining of cleave-caspase 3, which suggested that, in response to androgen deprivation, the murine prostatic epithelial cells undergone elevated cell death by lack of hormone for their growth which will result in a shrink of prostate volume; but in the PbCre/PLK1/ PTEN^{-/-} mice, apoptotic response could be hardly detected (Fig 2.6.E). Further, we also detected a dramatically increased AR-positive cells in castrated PbCre/PLK1/ PTEN^{-/-} prostates which suggesting that PLK1 overexpression leads to hormone-independent cell growth due to persistent activation of AR following castration (Fig 2.6.F). Therefore, these results revealed a critical role of PLK1 plays in malignant cells survival from absence of hormone and eventual development of castration resistance.

We confirmed PLK1 contributing to androgen independent growth of human PCa cells *in vitro*. Hormone-sensitive PCa cell line-LNCaP cells were infected by lentivirus to overexpress PLK1. After puromycin antibiotic selection, PLK1 overexpressing LNCaP cell line was established, and this overexpression was confirmed via western blot (Fig 2.7.A). To mimic hormone deprivation *in vitro*, the Fetal Bovine Serum (FBS) in culture medium for LNCaP PLK1 overexpressing cell line and lentivirus control cell line was replaced with Charcoal Stripped Fetal Bovine Serum overnight, and then the androgen-dihydrotestosterone (DHT) were added back into hormone deprived medium. In the absence of hormone, cell growth and colony formation ability of LNCaP control cells were significantly inhibited, and were partially rescued by adding back DHT; notably, LNCaP PLK1 overexpressing cells still possessed significantly higher levels of cell proliferation and colony formation than control cells under hormone starvation (Fig 2.7.B-C). These results from human PCa cells were consistent with what we found *in vivo*.

2.2.5 PLK1 overexpression increases incidence of metastasis and induces epithelial-to-mesenchymal transition.

PLK1 has been postulated to stimulate cell migration and invasion by inducing epithelial-to-mesenchymal transition (EMT) in prostate cancer cells [108]. However, currently the pro-metastatic function of PLK1 has not been confirmed in animal model. Using our prostate-specific PLK1 overexpression mouse model, we found that PLK1 could dramatically increase the incidence of metastasis (Fig 2.8.A). We have observed the metastatic tumors in distant sites from PLK1 KI prostates; majority of them were in the lung alveolar space, meanwhile one case was found nearby the left thigh, which showed classic prostate adenocarcinoma phenotype via histological observation (Fig 2.8.B-C). Fig 2.8.D presented that the tumor cells in the lung remained positive signaling of AR indicating a prostate cancer derivation. To examine whether PLK1 enhanced prostate cancer metastasis via causing cells undergo EMT, prostate glands from PbCre/PTEN^{-/-} and PbCre/PLK1/ PTEN^{-/-} mice at age of 12 weeks, when invasive adenocarcinoma has been formed, were immunostained with epithelial marker-E-cadherin and mesenchymal marker-Vimentin. As shown in Fig 2.8.E-F, Vimentin was upregulated, and meanwhile E-cadherin was downregulated upon PLK1 overexpression in prostates. In agreement with the results obtained from IHC, PLK1 induced reduction of epithelial Markers (E-cadherin and ZO1) and increasing of mesenchymal markers (Vimentin, β -catenin and N-cadherin) at protein level via western blot (Fig 2.8.G). Taken together, these results recovered the key role of PLK1 in enabling a switch of prostate cells from epithelial-like phenotype to mesenchymal phenotype. This finding was further supported by TCGA database analysis shown in the Fig 2.8.H heat map which demonstrated that the EMT-related genes were likely upregulated in PCa specimens with high PLK1 expression (higher than median of PLK1 expression among 475 human PCa specimens from TCGA). In addition, the cell adhesion pathway and focal adhesion pathway, which are highly related with metastasis, were found enriched in high PLK1 expressing PCa from TCGA by Gene Set Enrichment Analysis (GSEA) (Fig 2.9.A-B).

We also examined PLK1-mediated EMT and the cell motility using our generated LNCaP PLK1 overexpressing cell line. Similarly with the results obtained from mouse prostates, western blot showed that LNCaP cells with PLK1 overexpression remarkably decreased the expression of E-cadherin and increased expressions of N-cadherin and Vimentin compared with LNCaP control

cells (Fig 2.9.C). Moreover, upregulation of PLK1 significantly increased planar migration ability of LNCaP cells via transwell migration assay (Fig 2.9.D). Combined results from our animal model and human PCa cell line together, PLK1 as a crucial molecular effector leading to EMT was fully highlighted.

2.2.6 Murine prostate stem cell-derived organoids displays similar features presenting in original mice.

The organoid culture system has been well applied as a promising model to study carcinogenesis as it can genetically and functionally recapitulate the development of tumor where it was derived. Recent work has successfully established organoid culture systems for mouse and human prostates [109-111]. To further characterize the correlation between PLK1 expression and PCa progression, we generated mouse PCa organoid model. We adapted and further modified a recently published protocol to generate organoid cultures from prostates isolated from PbCre/PTEN^{-/-} and PbCre/PLK1/ PTEN^{-/-} mice[109]. Within the protocol, instead of basal cells or luminal cells, we enriched murine prostate stem cells ((CD45/CD31)⁻ Sca1⁺CD49f⁺), which has been reported to possess 60-fold higher level of prostate sphere formation capacity, via fluorescence-activated cell sorting (FACS) [98]. Enriched stem cells (Sca-1⁺ CD49f⁺) were sorted and subjected to organoid culture (detailed protocol in Materials and Methods). After 7 days culture, organoids were observed under microscope (Fig 2.10.B). The number of organoids from 10,000 sorted stem cells from PLK1 overexpressing mice was significantly higher than the one from PTEN KO only mice, even though organoids from both were morphologically similar to each other after H&E staining (Fig 2.11.A-B). Immunostaining of PLK1 indicated its overexpression in organoids derived from PLK1 KI prostates; and these PLK1 overexpression organoids showed increased levels of Ki67 and AR which are similar to their in vivo counterpart (Fig 2.11.D-E). Interestingly, although organoids from both indicated genotype prostates showed an intensive E-cadherin staining due to their epithelial cells-derived enrichment, a positive staining of Vimentin could also be detected upon PLK1 overexpression, indicating that PLK1 overexpressing organoids underwent EMT transition to a certain degree that resembled their corresponding prostates observed in the mice (Fig 2.11.F-G).

2.2.7 PLK1 upregulates IL4/IL13/STAT6 pathway and lead to elevated population of M2 macrophage in murine prostate.

Fig 2.4.B has shown a dramatic increasing of immune cells infiltration in PLK1 overexpressing prostates indicating that the influence of PLK1 was not only on malignant cells but also on other cells in the tumor microenvironment (TME). Thus, in order to investigate whether PLK1 regulates TME network-associated molecular programs and inflammatory cytokines production and consequentially contributes to PCa development, we performed gene set enrichment analysis (GSEA) from TCGA PCa patient data to detect TME and inflammatory response-associated pathways enrichment. Among them, cytokine pathway gene set, T helper 1 and 2 (Th1/Th2) pathway gene set and TGF β pathway gene set were enriched in high PLK1 expressing group (Fig 2.12.A-C). Notably, interleukin 4 (IL4) was positively involved in these three signaling pathways; And IL4 or interleukin 13 (IL13) could activated STAT6 and STAT6-mediated macrophage polarization towards M2 macrophage subtypes which has been reported occurred in the PCa and promoted its development [87, 88]. Pro-tumor role of M2 macrophages were validated by a positive correlation between CD163, which is the marker of M2 macrophages, and Gleason score of PCa patients from TCGA data; and this correlation is much more significant than the one between M1 macrophages marker-CD68 and Gleason score although the latter is positive as well. Therefore, these results raised the possibility that PLK1 modulated inflammatory responses of PCa via triggering the IL4/IL13/STAT6 activation and M2 macrophages upregulation. To test this hypothesis, we compared the mRNA expressions of M2 macrophages stimulators-IL4 and IL13, M2 mainly secreted cytokine- interleukin 10 (IL10), and M1 main product- interleukin 12 (IL12) between PbCre/PTEN^{-/-} and PbCre/PLK1/ PTEN^{-/-} prostates. As shown in Fig 2.12.F, the transcriptional levels of IL4, IL13 and IL10 were upregulated, and the one of IL12, in contrast, was downregulated in prostates from PbCre/PLK1/ PTEN^{-/-} mice. Furthermore, prostate glands from indicated genotype mice at age of 12 weeks were immunostained with arginase-1 (Arg1), which is the marker for mouse M2 macrophages, and nitric oxide synthase 2 (NOS2), which is used to define M1 macrophages [112]. As shown in Fig 2.12.G-H, PLK1 overexpression induced an increasing of Arg1 and a decreasing of NOS2 in prostates. Since Arginase 1 production, a hallmark of M2 polarization, is transcribed by STAT6 whose activation is due to IL4-induced phosphorylation, we performed immunostaining and western blot of STAT6 and its phosphorylation at Y641 on prostate glands from PbCre/PTEN^{-/-} and PbCre/PLK1/ PTEN^{-/-} mice

[113, 114]. A significant increasing of STAT6 as well as phosphorylation of STAT6 was detected by both approaches indicating an obvious activation of this pathway (Fig 2.12.I-K). In addition, to distinguish M1 and M2 populations in prostate glands, FACS analysis was performed with antibodies against M2 marker-CD163 and M1 marker-CD68, conjugated with different fluorescence, on gated CD45⁺F4/80⁺ cells in PbCre/PTEN^{-/-} and PbCre/PLK1/ PTEN^{-/-} prostate tissues. As expected, the percentage of CD163 positive cells were dramatically increased upon PLK1 overexpression in prostates based on FACS analysis results (Fig 2.12.L). Taken together, these results suggested that the activation of IL4/IL13/STAT6 signaling is mediated by PLK1 and able to stimulate inflammatory response of M2 macrophages and attenuate M1 macrophages response in prostate TME.

To further validate our findings obtained from mouse model, we designed an *in vitro* experimental protocol shown in Fig 2.13.A. Ventral, dorsal and lateral prostate lobes, within PLK1 was overexpressed based on Fig 2.2.B, were isolated from PbCre/PTEN^{-/-} and PbCre/PLK1/ PTEN^{-/-} mice at age of 30 weeks and digested for primary cell culture (Details in Methods); Three clones of each genotype were ultimately established. All the clones possessed homozygous deletion of PTEN, and meanwhile three from PbCre/PLK1/ PTEN^{-/-} prostates had PLK1 overexpression via a genotyping analysis (Fig 2.13.B). Based on growth curve result, all six clones hosted similar levels of proliferation, however, colony formation assay indicated a higher capacity of cell clones with PLK overexpression (Fig 2.13.C-D). To determine whether PLK1 induces secretion of IL4 from tumor cells, the supernatant from cultured medium of these primary cells was harvested and subjected to enzyme-linked immunosorbent assay (ELISA). We found that increased mouse IL4 was secreted from PLK1 overexpressing prostate tumor cells into medium, indicating an activation of IL4 by PLK1 (Fig 2.12.M). We then stimulated mouse bone marrow cells to differentiate into M0 macrophages by adding L cell-derived colony-stimulating factor 1 (CSF-1); When most cells were macrophages, the original medium was replaced by the supernatant from PbCre/PTEN^{-/-} primary cells or the one from PbCre/PLK1/ PTEN^{-/-} primary cells, respectively. After 1 week culture, the bone marrow derived macrophages under different culture medium were subjected to FACS analysis using CD163 and CD68 to identify M2 and M1 populations. As shown in Fig 2.12.N, the ratio of CD163⁺/CD68⁺ skyrocketed in the PbCre/PLK1/ PTEN^{-/-} medium group, suggesting that PLK1-induced high IL4 secretion could skew macrophages toward the M2

polarization. In addition, the phosphorylation of STAT6 was significantly increased in the bone marrow derived macrophages cultured under PbCre/PLK1/ PTEN^{-/-} medium via western blot (Fig 2.13.E). Consistent with the findings from our transgenic mouse model, our in vitro data also suggested that PLK1 promote tumor progression in PCa through activating IL4/IL13/STAT6 and inducing macrophages towards M2 phenotype, which might provide an advantage in the therapy for advanced PCa with high PLK1 by shutting down IL4/IL13/STAT6 signaling and inhibiting M2 macrophage function.

2.2.8 PLK1-mediated activation of IL4/IL13/STAT6 pathway is targetable by STAT6 inhibitors.

We examined whether targeting IL4/IL13/STAT6 pathway would reverse tumor development and metastasis induced by PLK1 overexpression in mouse prostates. The heat map from TCGA PCa patients' database has shown that high STAT6 expression led to upregulation of the EMT-related genes in PCa specimens (higher than median of STAT6 expression among 475 human PCa specimens) (Fig 2.14.). Therefore, we performed pharmacologic inhibition of STAT6 on PbCre/PLK1/ PTEN^{-/-} mice by treatment of the inhibitor-AS1517499 which has been used to treat several animal models including tumor development in carcinoma [115]. The treatment scheme is given in Fig. 7A. PLK1 KI mice at the age of 24 weeks were intraperitoneally injected with vehicle or AS1517499 daily for 21 days; the mice were sacrificed on 21 days after the last treatment when they were 30 weeks age. The GU blocs from inhibitor-treated mice were obviously smaller than mice treated with vehicle, and the average weight of GU blocs of inhibitor-treated mice was also significantly lighter than the vehicle group, indicating a reduction of tumor burden after inhibition of STAT6 in PLK1 KI prostates (Fig 2.15.B-C). Of note, one mouse from vehicle group showed lung metastasis, but no any distant tumor from original organ was found in inhibitor-treated mice (Fig 2.15.B). Histological analysis demonstrated that invasive prostate adenocarcinomas were fully developed in PLK1 overexpressing mice treated with vehicle, which was similar with what we found in the PbCre/PLK1/ PTEN^{-/-} mice 30 weeks age in Fig 2.4.B; in contrast, the pathological process of prostates from STAT6 inhibitor-treated mice was much slower and only at the stage of mPIN (Fig 2.15.E). From immunostaining of Ki67 and cleaved-caspase 3 shown in Fig 2.15.F-G, treatment of AS1517499, as expected, inhibited prostatic cells proliferation and resulted in an increase of apoptotic response. Inhibition of STAT6 could also

slow down the EMT induced by PLK1 overexpression, which represented as a decrease of Vimentin staining in prostates after the inhibitor treatment (Fig 2.15.H). These results suggested an inhibitory effect of AS1517499 on PLK1-promoted PCa progression and metastasis in mice.

To examine whether inhibition of STAT6 shut down IL4/IL13/STAT6 pathway and reversed the switch from M1 to M2 macrophages, we assessed the mRNA expressions of IL4, IL13, IL10 and IL12 in the mouse prostate glands treated with vehicle or AS1517499. The stimulators of M2 polarization-IL4 and IL13, and the product of M2 macrophages-IL10 were attenuated by STAT6 inhibition in transcriptional aspect; meanwhile, the mRNA level of IL12, mainly secreted from M1, was increased (Fig 2.15.D). Consequentially, both western blot and IHC staining showed that phosphorylation of STAT6 was significantly decreased upon AS1517499 treatment, along with a reduction of STAT6 (Fig 2.15.I, Fig 2.15.K-L). Moreover, prostates from vehicle group and STAT6 inhibitor group were subjected to the same FACS analysis as we did in Fig 2.12. to identify M1 and M2 populations, and the results indicated a significant repression of CD163 positive cells upon the inhibitor treatment (Fig 2.15.J). This repression of M2 macrophages by STAT6 inhibition resulted in a downregulated expression of Arg1 and an upregulated expression of NOS2 in prostates via IHC staining (Fig 2.15.M-N). Taken together, PLK1-triggered activation of IL4/IL13/STAT6 and elevation of M2 macrophages were efficiently shot by STAT6 inhibitors treatment, which highlighted a potential targeted therapy for patients with metastatic PCa.

2.3 Discussion

Polo-like kinase 1(PLK1) are essential regulator of mitotic progression, and its expression and enzymatic activity tightly varies with cell cycle and peaks during G2 to M phase [116]. Cell cycle dysregulation is one of hallmarks of human cancer, therefore PLK1 has been highlighted to be overexpressed in various human cancer types, and its overexpression in cancer cells was not only observed in mitosis, but also during interphase, where PLK1 usually shows a low level of expression in normal cells [117]. Considering its upregulation in cancer, PLK1 has been validated as a promising cancer target; consequently, pharmacological inhibition of PLK1 provides an efficient way to kill cancer cells, and therefore a set of small inhibitors have applied into clinical trials [118]. Although PLK1 has been postulated as an oncogene, unexpectedly, recent reports

proposed PLK1 as a potential tumor suppressors in some cancer types with particular genetic background, placing the pro-tumorigenic role of PLK1 under controversy [119]. For example, M. Malumbres' and R. Sotillo's laboratories validated that PLK inducible overexpression in mouse breast glands dramatically reduced the rate of breast cancer appearance driven by *K-Ras* or *Her2* oncogenes [120]. For prostate cancer, PLK1 has been found frequently upregulated, however, direct evidence pointing to its role in PCa progression, pro-tumorigenic or ant-tumorigenic, is still lacking. Therefore, in present study we performed a series of bioinformatics analysis based on the RNA-seq of PCa specimen in TCGA and immunostaining on PCa TMA, and demonstrated a correlation of PLK1 expression with short TTP, poor overall survival and advanced disease progression, which validated PLK1 as a prognostic marker in PCa (Fig 2.1.). Our lab previously reported PLK1 could cooperate with some critical oncogenes, like AR and β -catenin, to promote the proliferation of PCa cell lines, and targeting PLK1 with chemotherapy or ADT therapy should be an efficient way to induce cancer cells death, however, direct evidence of PLK1 being a *bona fide* contributor to PCa progression is still lacking due to a short of proper animal models [77, 91]. Accordingly, we established a GEM mouse line to achieve conditional PLK1 overexpression in prostate glands by the recombination of Probasin Cre with lox sequences (Fig 2.2.A). However, PLK1 overexpression alone is not sufficient enough to drive PCa cancer initiation, indicating additional genetic modifications needed, in our case, PTEN depletion in prostates (Fig 2.3.A). Based on histopathological data, PLK1 overexpression could accelerate the rate of pathological progression in mouse prostate glands, from epithelial hyperplasia, murine PIN to adenocarcinoma, and, to our surprise, was associated with an induction of sarcomatoid carcinoma histological phenotype, which representing epithelial to spindle cell proliferation composed of atypia cells with enlarged nuclei, vesicular chromatin, abundant mitotic figures, and cell necrosis and apoptosis (Fig 2.4.B). Sarcomatoid carcinoma is rare, <1% among all prostate neoplasms, and patients with it hold a remarkably poor extended survival. However, the development of sarcomatoid carcinoma is not clear, but has been shown an association with a prior history of prostate adenocarcinoma based on some reported cases [121-123].

CRPC is the late stage of PCa, and a number of evidence indicated that PLK1 is critical for castration resistance. PLK1 was dramatically upregulated by castration in human PCa xenograft

models; and castration-induced elevations of PLK1 then led to activation of AR signaling which is the main factor contributing to resistance [124, 125]. In our mouse model, we provided compelling data that PLK1 overexpression is required for castration resistant tumors, with an intensively elevated signaling of AR (Fig 2.6.). To mimic the castration *in vitro*, we cultured androgen naïve LNCaP cells with medium without hormones, and the growth of cells with PLK1 overexpression was not obviously affected by the starvation, indicating PLK1's essential role in forcing cells independent of androgen hormone (Fig 2.7.).

Next, our mouse model revealed that activation of PLK1 signaling was linked to PCa metastatic dissemination (Fig 2.8.A-D). EMT has been believed as a key mechanism for metastasis by converting epithelial-like cells into a mesenchymal phenotype. And malignant cells undergoing EMT possess stem cell properties and is usually resistant to cancer treatment [126, 127]. But this transition is not fully completed, cancer cells are in a mixed state with expressions of both epithelial and mesenchymal genes; and this process is also reversible when cancer cells migrate to a long-distant organ to form secondary tumors, which is called mesenchymal-to-epithelial transition (MET) [128]. EMT is featured with downregulation of epithelial markers (e.g. E-cadherin) and upregulation of mesenchymal markers (e.g. Vimentin), and disruption of cell adhesion. These phenotypes have been found in the mouse prostates with PLK1 expression and in the TCGA human PCa database (Fig 2.8.E-H, Fig 2.9.A-B). In agree with the findings of recent paper which demonstrated PLK1 promoting cell mobility via inducing EMT in PCa cell lines, our work identified the pro-metastatic function of PLK1 *in vivo* which highlights PLK1 as a target of interest for metastatic PCa therapy by stopping EMT process[108, 129].

To characterize the oncogenic function of PLK1 in prostate cancer, besides our unique PLK1 KI transgenic mouse lines, we also performed *ex vivo* culture of murine prostate organoids. The use of this three-dimensional culture system provides insight into carcinogenesis within patients due to its capacity of accurately recapitulate the molecular program presenting in their *in vivo* counterpart. Organoid culture has been applied in pancreatic, gastric, and colon cancers [130, 131]. For prostate cancer, the protocol of organoid culture for mouse and human prostates has been well established, and it has allowed for the genomic and functional study in PCa progression [109-

111]. For instant, Wei laboratory used -derived organoids derived from PCa patient harboring *SPOP*- W131R mutation were more resistant to treatment of JQ1, the BET inhibitor [132]. According to recent report, both basal cells (CD49fHi) and luminal cells (CD26+) of prostates are able to form organoids [130]; however, to guarantee a successful establishment of prostate organoids from our transgenic mouse, we performed an upgraded protocol, designed by our collaborators, in which we sorted epithelial prostate stem cells (PSC) or so-called Lin (CD45/CD31)⁻ Sca1⁺CD49f⁺ (LSC) cells, instead of basal cells or luminal cells, for organoid culture as LSC cells possess significant high capacity of prostate sphere formation[98, 109]. Consistent with the results derived from our mouse model, compared with the PTEN KO only organoids, the PLK1 overexpressing organoid exhibited increased proliferative ability and elevated AR signaling (Fig 2.11.D-E). Interestingly, our epithelial-derived organoids was not supposed to show any mesenchymal marker, but upon PLK1 KI, we could still observe positive signaling of Vimentin, even though not very strong, which suggesting the occurrence of PLK1-induced EMT in mouse prostate organoids (Fig 2.11.F).

It has been believed that development of PCa is associated with the abnormal changes in the complex consisting of malignant cells, inflammatory cells such as tumor associated macrophages (TAMs), and non-inflammatory cells such as cancer-associated stromal fibroblasts (CAFs); and these changes produce a microenvironment favorable to tumor growth and migration [82]. EMT has been considered as a key player in promoting metastasis; and in tumor microenvironment (TME), the infiltration of macrophages induces an increase in the secretion of inflammatory cytokines such as TGF- β , IL-6, TNF- α , as well as IL-10, which upregulate potent EMT inducers, like Snail and ZEB1/2 and enhance the stemness properties by activating multiple signaling pathways, including NF- κ B and STAT family, resulting in cancer metastasis and treatment resistance [51, 133]. TAMs are highly plastic and can be stimulated into two polarized states, M1 subtype and M2 subtype, by distinct collections of cytokines and chemokines in the TME. M2 macrophages are polarized by IL-4 and IL-13-induced activation of JAK/STAT6 pathway and regarded as tumor-promoting cells. As we mentioned above, EMT transition in cancer cells can be promoted by TGF- β , IL-6, TNF- α and IL-10, which are the main products of M2 macrophages [133, 134]. In Fig 2.8., we revealed a critical role of PLK1 in promoting EMT and PCa metastasis in mice; combining with the metastasis-initiating function of M2 macrophages in

TME, it raised a possibility that PLK1 is the key factor forcing macrophage polarization towards M2 phenotype and consequentially leads to EMT. This hypothesis was verified by FACS analysis showing an increased population of M2 macrophages (CD45⁺F4/80⁺CD163⁺ cells) in PLK1 KI mouse prostates (Fig 2.12.L). Increasing of M2 macrophages led to increasing expression of IL10 and Arg1, which were produced by M2, and a decrease of IL12 and NOS2, which were secreted by M1 (Fig 2.12.F-H). IL4/IL13/STAT6 pathway is required for M2 macrophages polarization; therefore, it is logical to ask whether PLK1 regulated macrophage polarization via driving IL4/IL13/STAT6 pathway activation [89]. In present study, we unraveled that PLK1 overexpressing prostate glands exhibited robust IL4-STAT6 signaling in macrophage cells as well as epithelial cells, which providing the first evidence *in vivo* of the link between PLK1 and macrophage polarization regulation (Fig 2.12.). To further identify the dynamic process of PLK1-mediated M2 elevation following the interaction between epithelial cells and macrophages, we cultured CSF-1-stimulated macrophages from mouse bone marrow, and incubated them with supernatants from primary prostate epithelial cells with or without PLK1 overexpression. An increase of M2 phenotype was also found in the macrophages under PLK1 KI cells medium in which secreted IL4 was significantly higher, indicating PLK1-mediated abundant IL4 secretion from epithelial cells would lead to M2 polarization by activating STAT6 in macrophages (Fig 2.12. M-N, Fig 2.13.E). The molecular mechanisms of PLK1-mediated direct transcriptional activation of IL-4 and STAT6 remain to be identified. Serine phosphorylation of Stat6 is also believed to involve in the transcriptional activation of STAT6 induced by IL4, so it raised the possibility of STAT6 as a substrate for PLK1 kinase which required further investigation [135]. In addition, our findings also indicated STAT6 as a new target for advanced PCa with metastasis in which PLK1 is usually overexpressed. By treating PLK1 KI mouse with STAT6 inhibitors, PCa development has been largely inhibited with loss of tumor burden, impaired EMT progression, downregulation of STAT6 activity and reducing number of M2 macrophages, which has shown significant efficacy of inhibition of STAT6 in murine models highlighting its potential for human PCa treatment (Fig 2.15.).

In summary, overexpression of PLK1 in mouse prostate epithelial cells leads to increase of STAT6 signaling and its phosphorylation at Y641, and stimulates increasing secretion of IL4 and IL13 from epithelial cells. Increased IL4/IL13 secretion activates STAT6 featured with hyper-

phosphorylation of STAT6 in macrophages. Activation of STAT6 drives elevation of M2 macrophage numbers, and subsequently induces increasing IL10 secretion from macrophages. PLK1-mediated activation of STAT6 in both epithelial cells and macrophages will produce a microenvironment favorable to promote prostate cancer progression and EMT transition. When PLK1 overexpressing mice are treated with STAT6 inhibitors, IL4/IL13/STAT6-induced elevation of M2 macrophages is suppressed, which will ultimately inhibit prostate cancer progression and metastasis (Fig 2.16.). The findings of our work defined the oncogenic roles of PLK1 and uncovered a novel pro-metastatic function of PLK1 from *in vitro*, *in vivo* and pre-clinical aspects. Our finding also bridged the knowledge gap of the critical role of PLK1 in regulating the complex interaction of tumor cells and other immune cells in TME. Finally, we provided preliminary clinical evidence of novel therapeutic strategy targeting TME-associated signaling pathway to significantly improve the poor survival of advanced PCa and CRPC resulted from PLK1 overexpression.

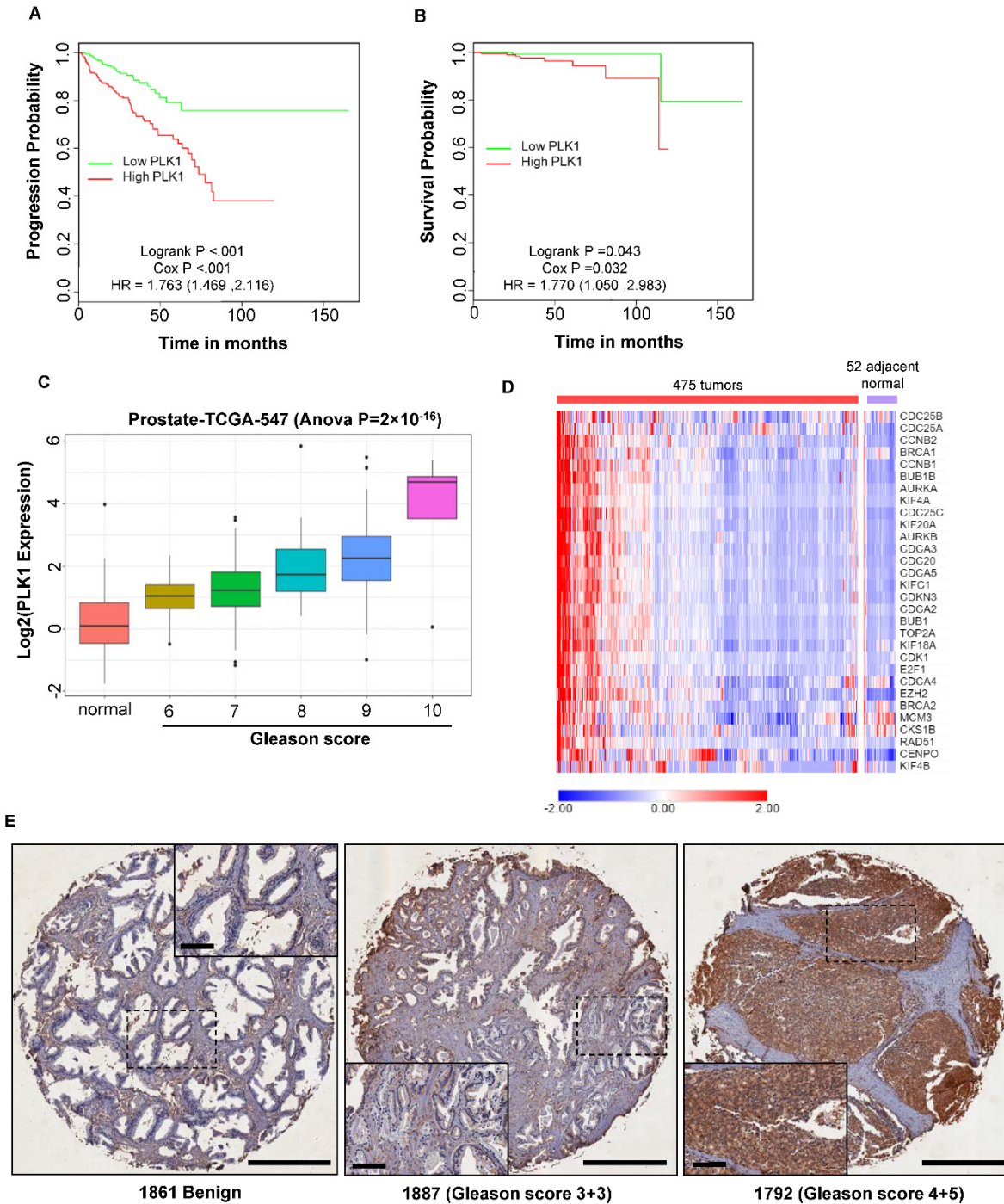
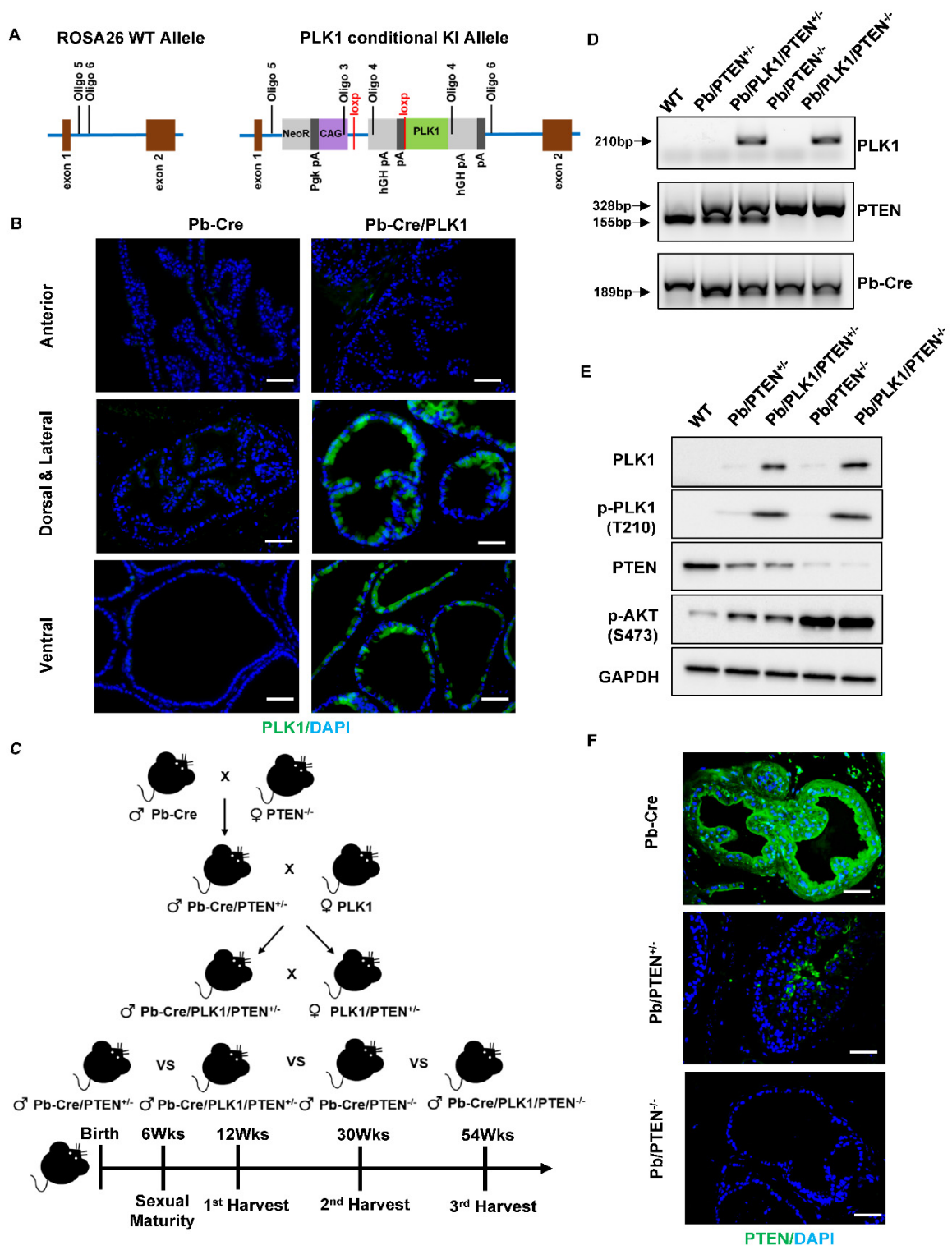


Figure 2.1 PLK1 expression is relevant to human prostate cancer progression and patients' poor survival. (A-B) Probability of progression(A)and survival(B) of PCa patients with expression level of PLK1 (C) Correlation between PLK1 and Gleason score in 52 adjacent normal prostate tissues and 475 primary PCa from TCGA. (D) Heat map of representatively PLK1-associated genes expression pattern compared in 52 adjacent normal prostate tissues and 475 primary PCa from TCGA. (E) Representative images of prostate tissue microarray (TMA) with different Gleason score stained with PLK1.

Figure 2.2 Establishment of prostate-specific PLK1 overexpression and PTEN deletion mouse model. (A) Structure of PLK1 conditional KI allele in mice. The Rosa26 locus has been inserted by following elements using recombination-mediated cassette exchange (RMCE): a CAG promoter sequence, a loxP-flanked transcription termination cassette (STOP) containing the human Growth Hormone polyadenylation signal (hGH pA) and a synthetic polyadenylation signal (pA), the mouse Plk1 ORF together with a Kozak sequence, and the hGH pA and an additional pA. The expression of Plk1 is precluded from the conditional KI allele via the presence of STOP cassette. Plk1 will be expressed following the CAG promoter after Cre-mediated deletion of the STOP cassette. (B) Immunofluorescent staining of PLK1 expression in different prostatic lobes of Pb-Cre and Pb-Cre/PLK1 mice. (C) Breeding strategy of generating prostate-specific PLK1 KI and PTEN homozygous or heterozygous deletion mouse model. (D) Representative gel images of genotyping. (E) Western blot analysis of PLK1 expression, PLK1 activation by p-PLK1 at T210, PTEN expression, and AKT pathway activation by p-AKT at S473 from mouse prostates. (F) Immunofluorescent staining of PTEN in mice with or without PTEN deletion.



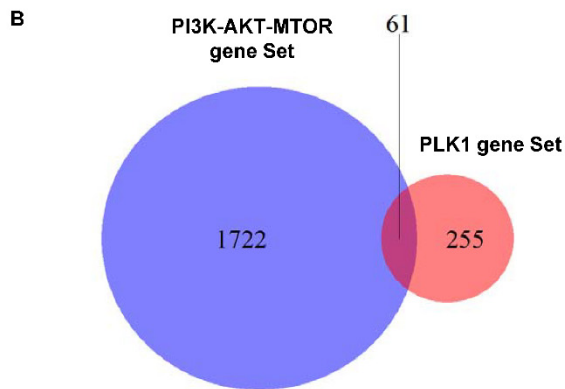
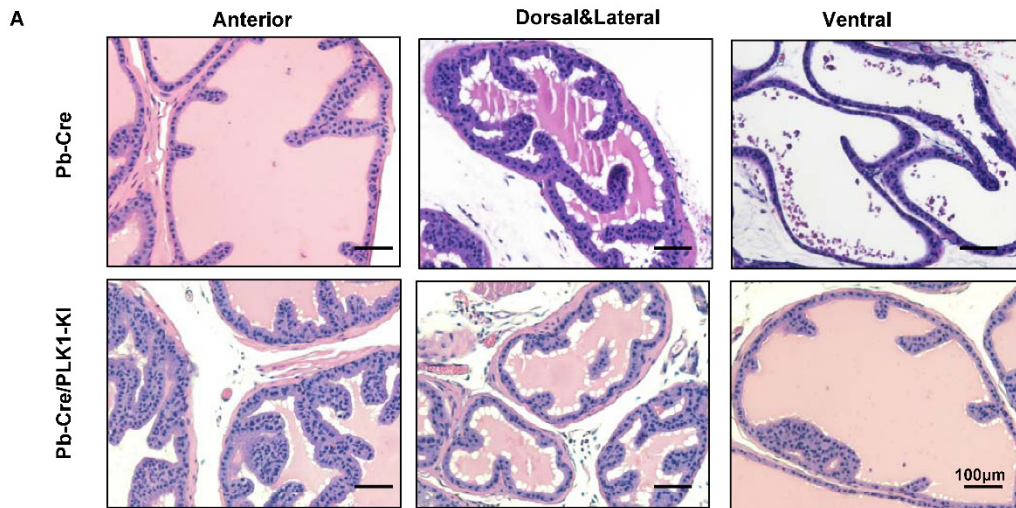
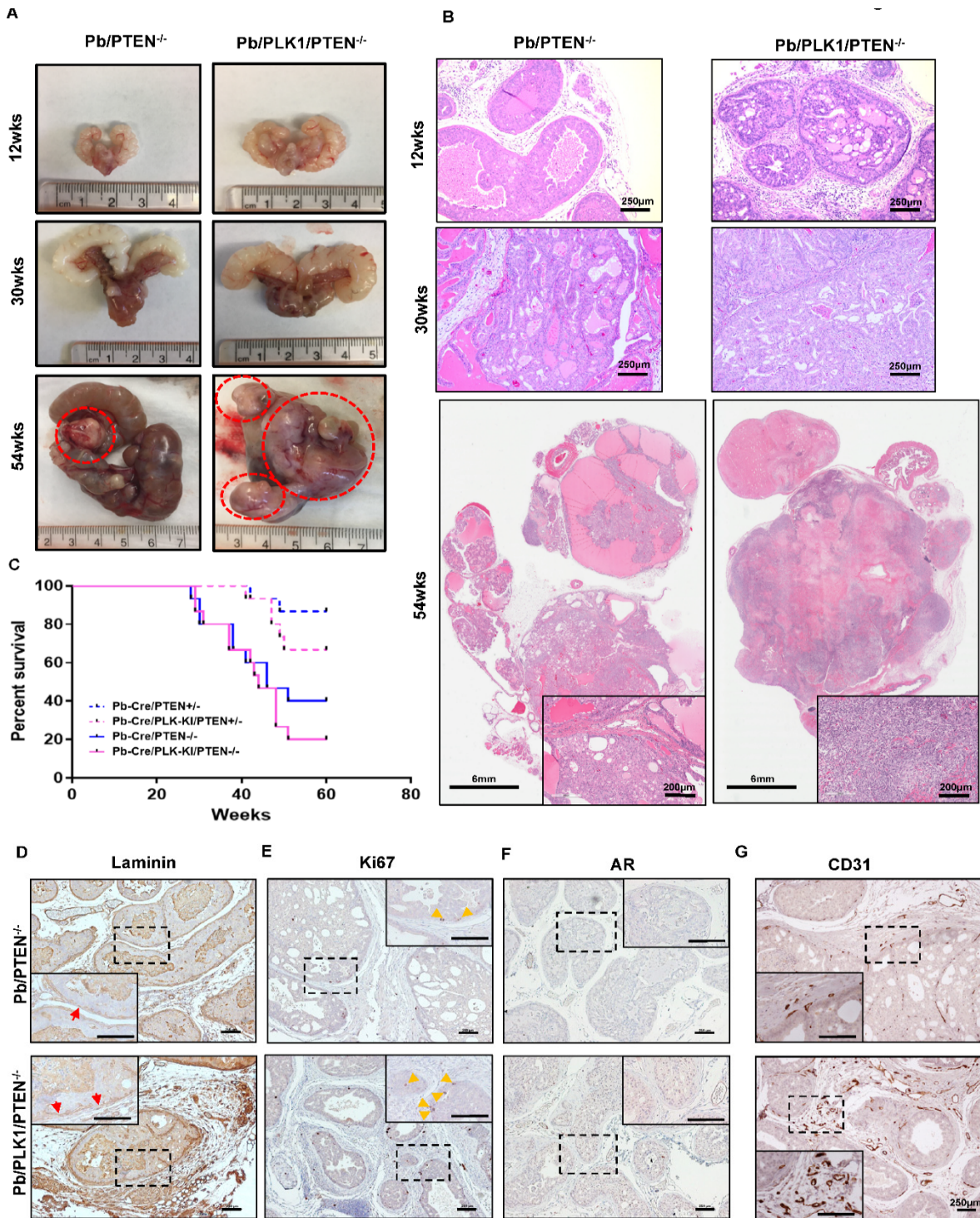


Figure 2.3 (A) Venn diagram showing the overlap between PLK1-associated gene set and PI3K/AKT/mTOR pathway-related gene set. (B) Representative images of anterior, dorsal, and ventral lobes from prostates with or without PLK1 overexpression following with H&E staining.

Figure 2.4 PLK1 overexpression accelerates formation of invasive prostate adenocarcinoma in mice. (A) Representative images of the genitourinary (GU) blocs in PbCre/PTEN^{-/-} and PbCre/PLK1/ PTEN^{-/-} mice at the age of 12 weeks, 30 weeks and 54 weeks respectively. Red circles indicate the solid tumors. (B) Representative images of prostates stained with H&E in PbCre/PTEN^{-/-} and PbCre/PLK1/ PTEN^{-/-} mice at the age of 12 weeks, 30 weeks and 54 weeks respectively. (C) Percent survival of mice with different genotypes (n=15). (D-G) Representative images of prostate from indicated genotype mouse stained with Laminin, Ki67, AR and CD31. Yellow arrows indicate Ki67 positive cells. Red arrows indicate invasive sites.



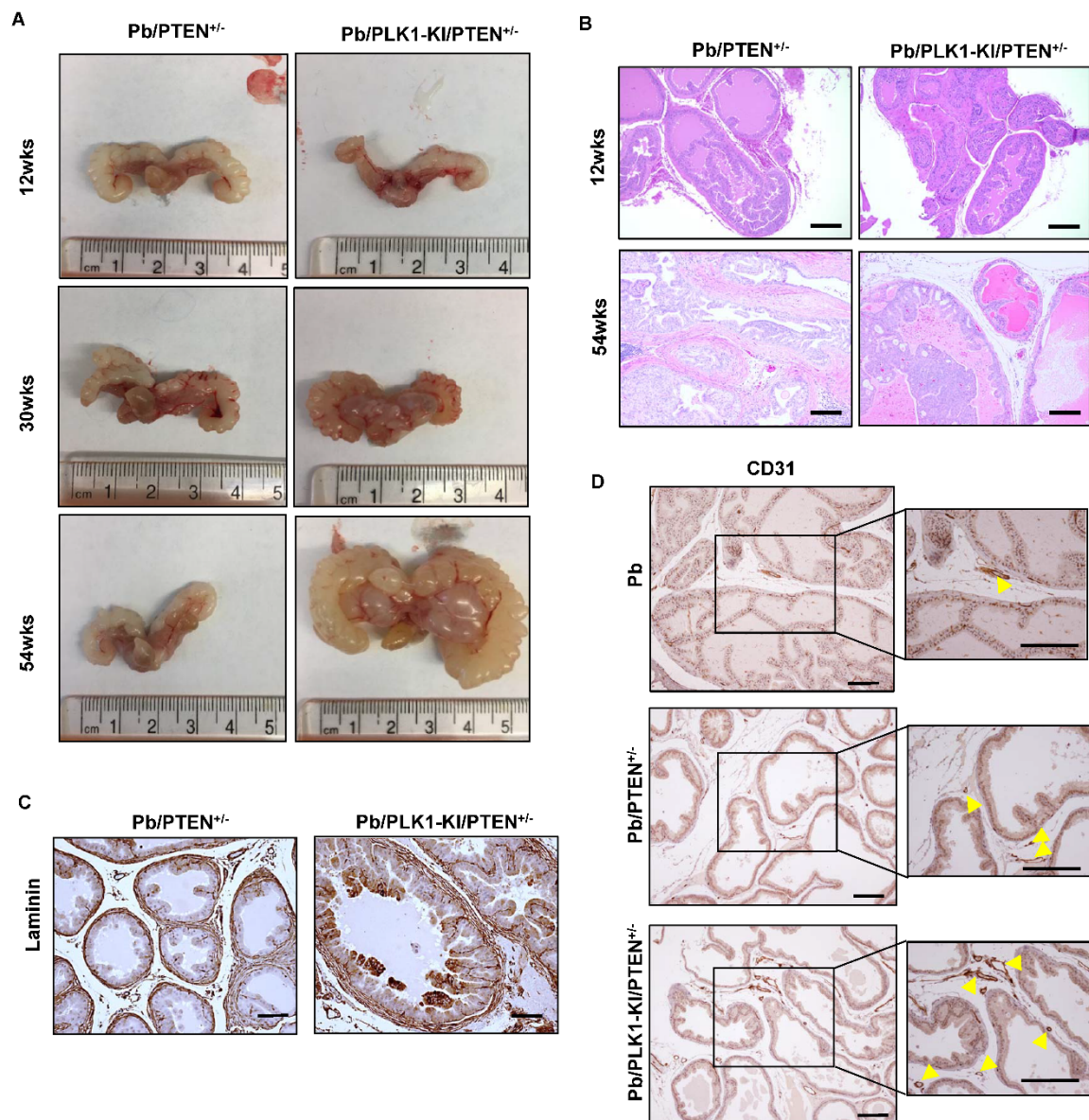


Figure 2.5 PLK1 overexpression accelerates formation of mPIN in PTEN heterozygous depletion mice (A) Representative images of the genitourinary (GU) blocs in PbCre/PTEN^{+/-} and PbCre/PLK1/PTEN^{+/-} mice at the age of 12 weeks, 30 weeks and 54 weeks respectively. (B) Representative images of prostates stained with H&E in PbCre/PTEN^{+/-} and PbCre/PLK1/PTEN^{+/-} mice at the age of 12 weeks and 54 weeks. (C-D) Representative images of prostate from indicated genotype mouse stained with Laminin and CD31. Yellow arrows indicate microvessels.

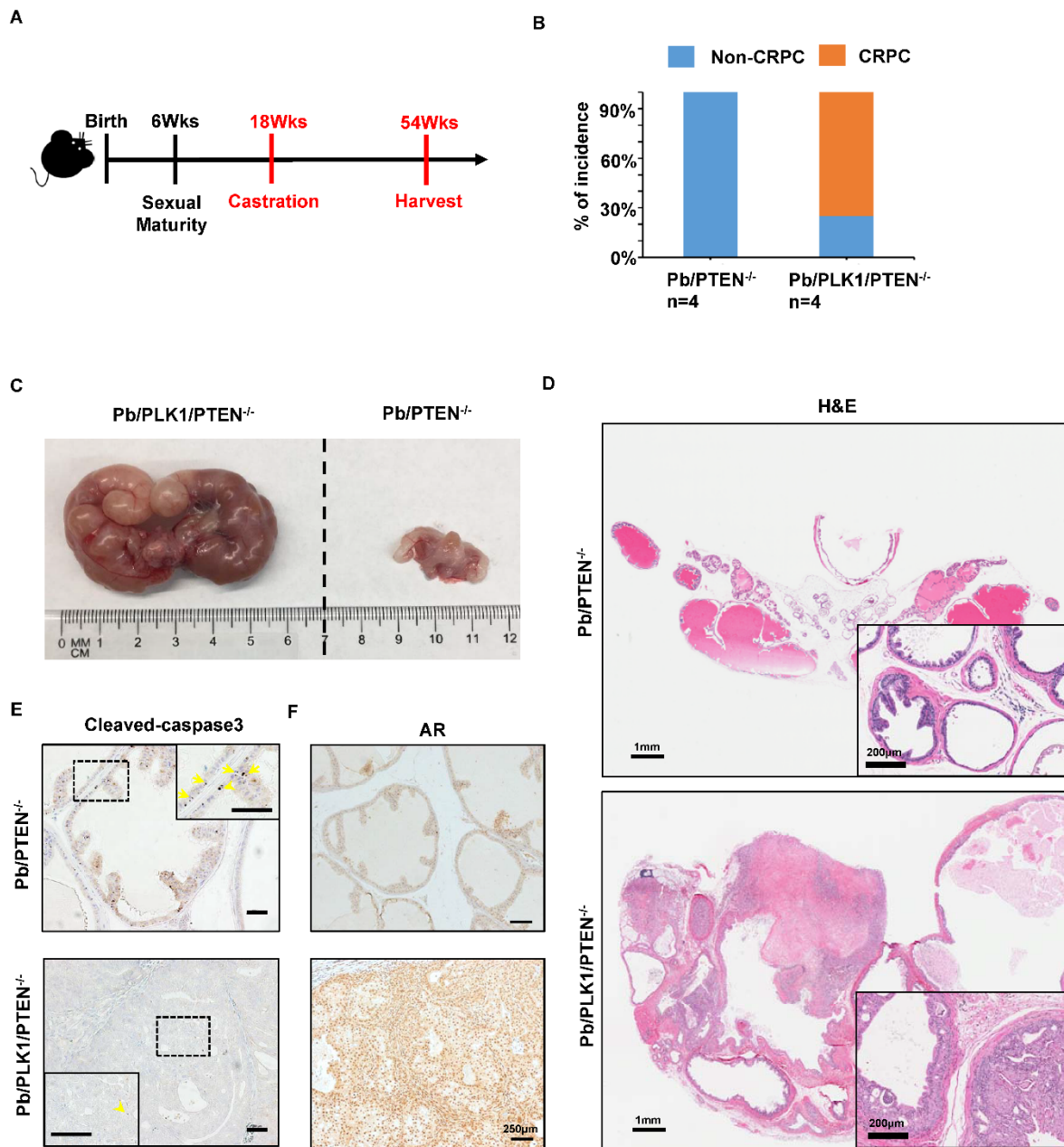


Figure 2.6 PLK1 is required for castration resistance in mice. (A) Schedule of castration in mice. (B) Percent incidence of castration observed in PbCre/PTEN^{-/-} and PbCre/PLK1/PTEN^{-/-} mice (n=4). (C) Representative images of the GU blocs in PbCre/PTEN^{-/-} mice without castration resistance and PbCre/PLK1/PTEN^{-/-} mice with castration resistance. (D) Representative images of H&E staining in PbCre/PTEN^{-/-} prostates without castration resistance, and PbCre/PLK1/PTEN^{-/-} prostates with castration resistance. (E-F) Representative images of prostate from indicated genotype mouse stained with cleaved-caspase 3 and AR. Yellow arrows indicate apoptotic cells.

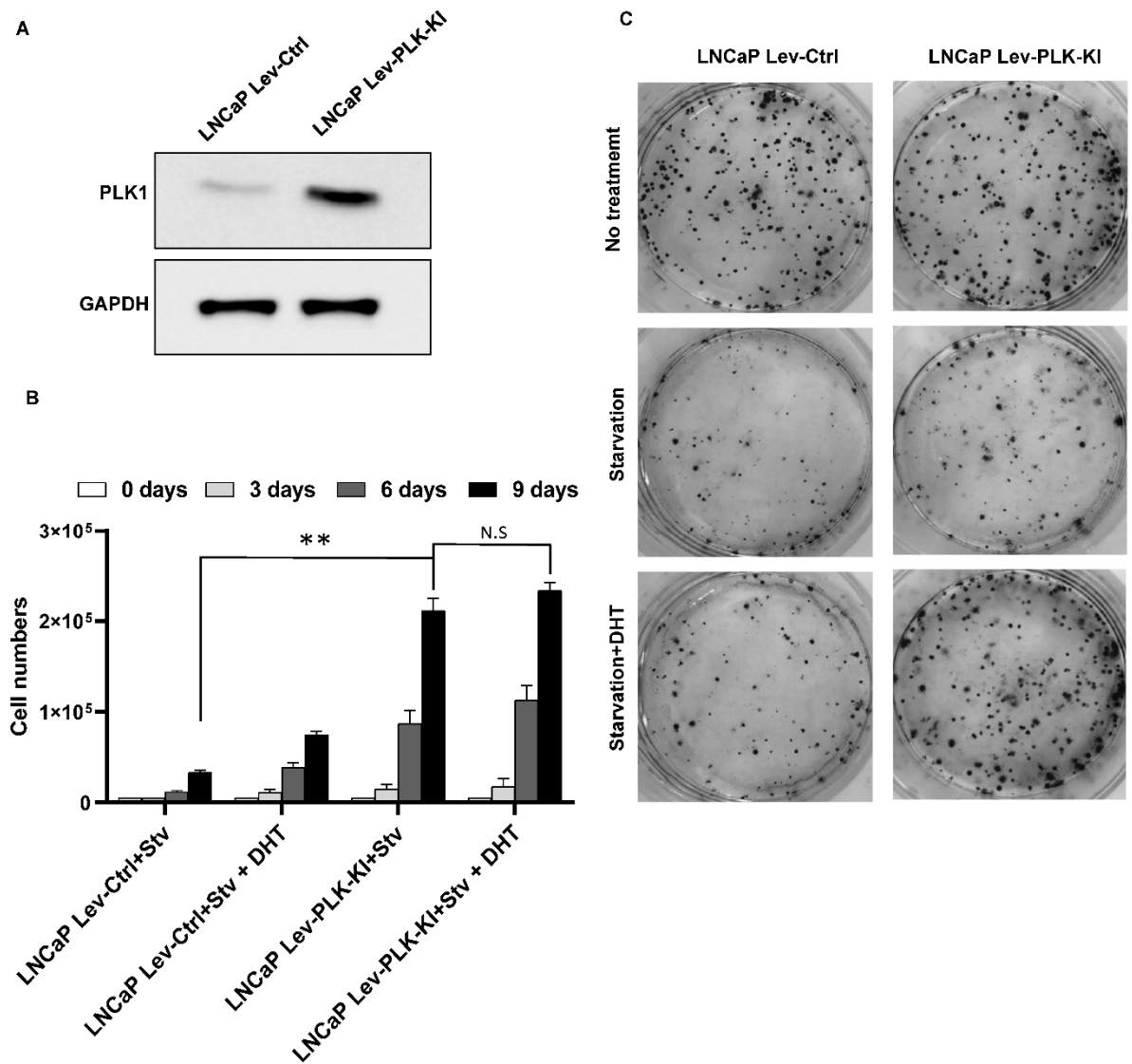
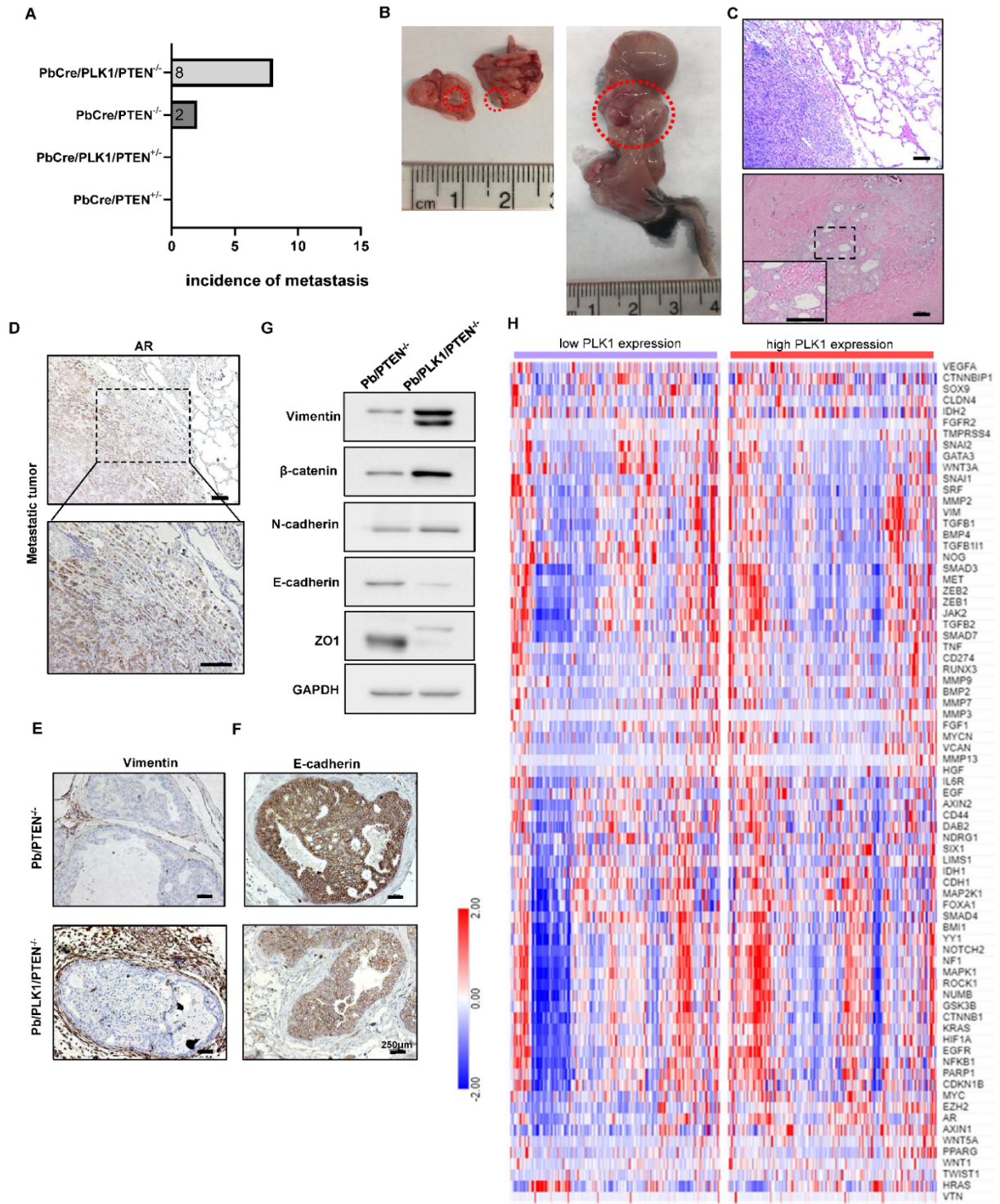


Figure 2.7 PLK1 overexpression in LNCaP cells increases resistance to hormone-deprived culture. (A) LNCaP cells were infected with control and PLK1 KI lentivirus. After puromycin selection, western blot was performed showing the PLK1 overexpression in LNCaP cells. (B-C) The culture medium including 10% Fetal Bovine Serum (FBS) of LNCaP Lev-ctrl cells and LNCaP Lev-PLK-KI cells was replaced with hormone deprived medium (with 5% Charcoal Stripped Fetal Bovine Serum but without FBS) overnight, and then 10nM dihydrotestosterone (DHT) were added into hormone deprived medium. Cell growth (B) and colony formation ability (C) of cells from indicated treatment were measured (** $p < 0.01$). Stv: hormone starvation.

Figure 2.8 PLK1 overexpression increases incidence of metastasis and induces epithelial-to-mesenchymal transition. (A) Overall incidence number of distant tumors observed in indicated genotype mice (n=15). (B) Representative images of distant tumors found in PbCre/PLK1/ PTEN^{-/-} mice. (C) Representative images of H&E staining in distant tumors found in PbCre/PLK1/ PTEN^{-/-} mice. (D) Representative images of lung tumor and adjacent tissue stained with AR in PbCre/PLK1/ PTEN^{-/-} mice. (E-F) Representative images of prostate from indicated genotype mouse stained with Vimentin and E-cadherin. (G) Western blot analysis of Vimentin, β -catenin, N-cadherin, E-cadherin and ZO1 from mouse prostate in PbCre/PTEN^{-/-} and PbCre/PLK1/ PTEN^{-/-} mice. (H) Heat map of expression pattern of genes within the EMT-related gene set compared in human prostate cancers with low PLK1 expression (lower than median of PLK1 expression among 475 human PCa specimens from TCGA) and high PLK1 expression (higher than median of PLK1 expression).



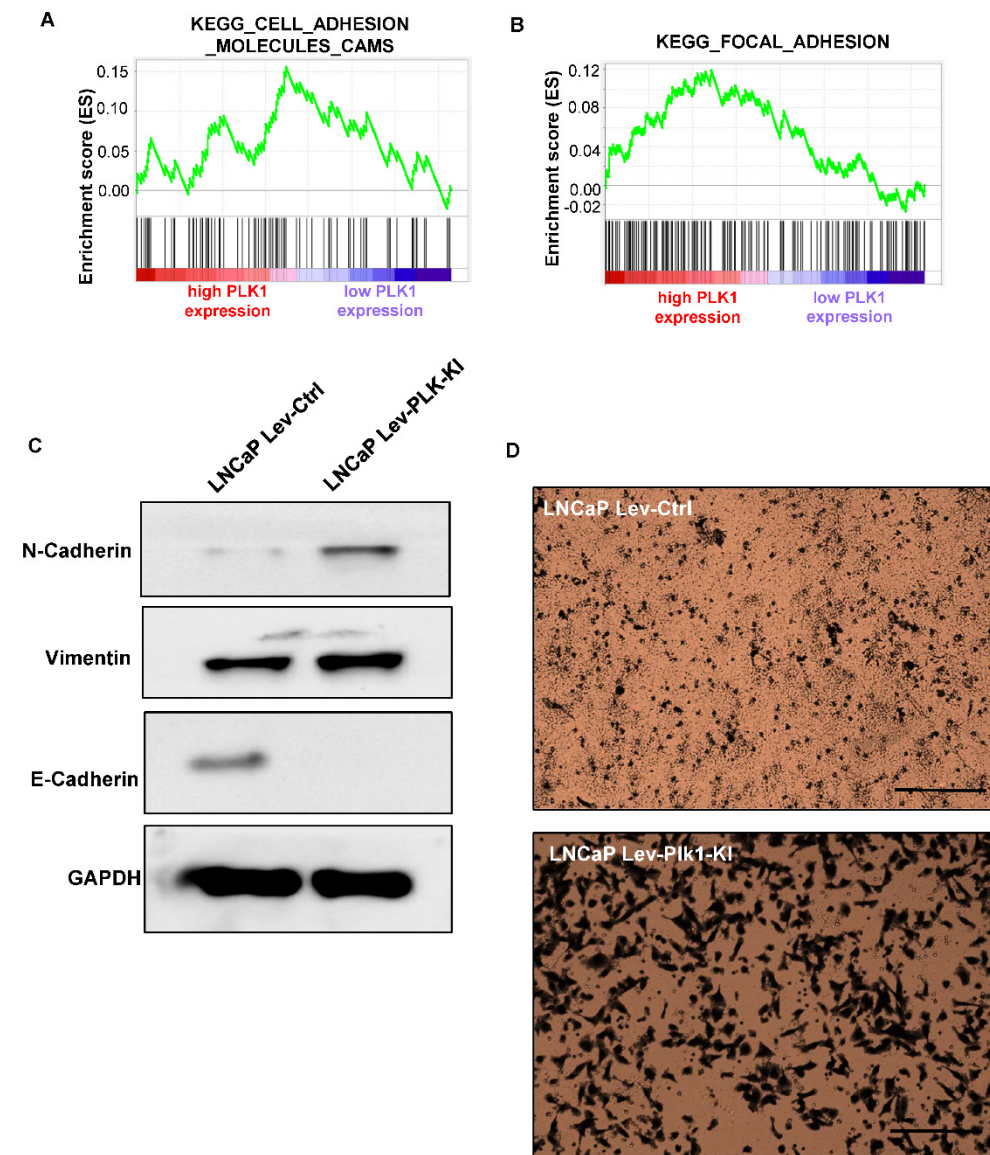


Figure 2.9 PLK1 overexpression in LNCaP cells is associated with EMT. (A-B) GSEA shows the enrichment of cell adhesion gene set (FDR q -val=0.33) and focal adhesion gene set (FDR q -val=0.27) in high PLK1 expression group (above median of PLK1 expression among 475 human PCa specimens from TCGA). (C) Western blot analysis of N-cadherin, Vimentin and E-cadherin from LNCaP Lev-ctrl cells and LNCaP Lev-PLK-KI cells. (D) Representative microscopic images of LNCaP Lev-ctrl cells and LNCaP Lev-PLK-KI cells that migrated through the transwell in the transwell migration assay.

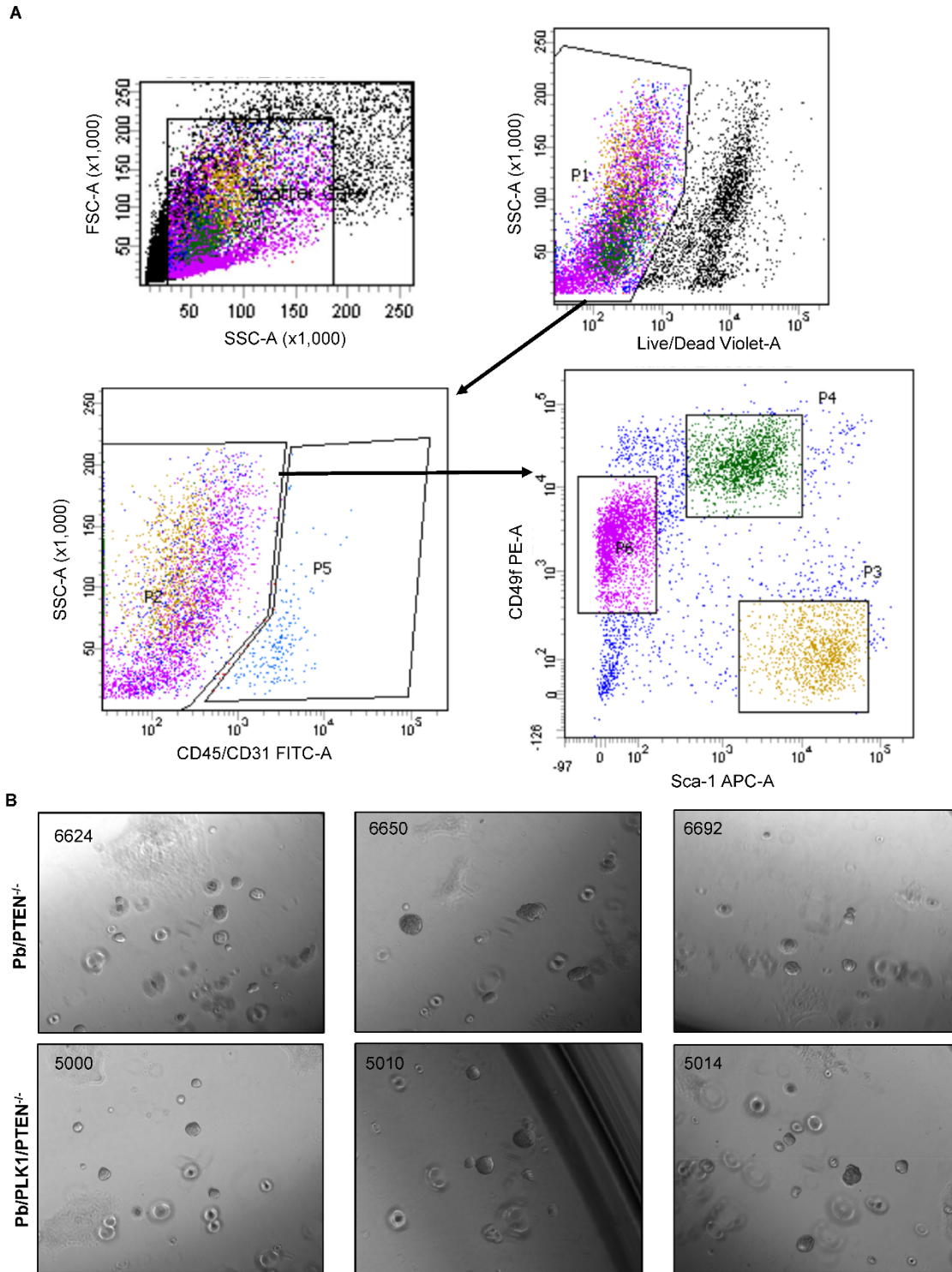


Figure 2.10 (A) Gating strategy of enriched stem cells isolation. Enriched stem cells were subjected to organoid culture shown in Fig 2.11.. (B) Representative microscopic images of prostate stem cell-derived organoids from indicated genotype mouse.

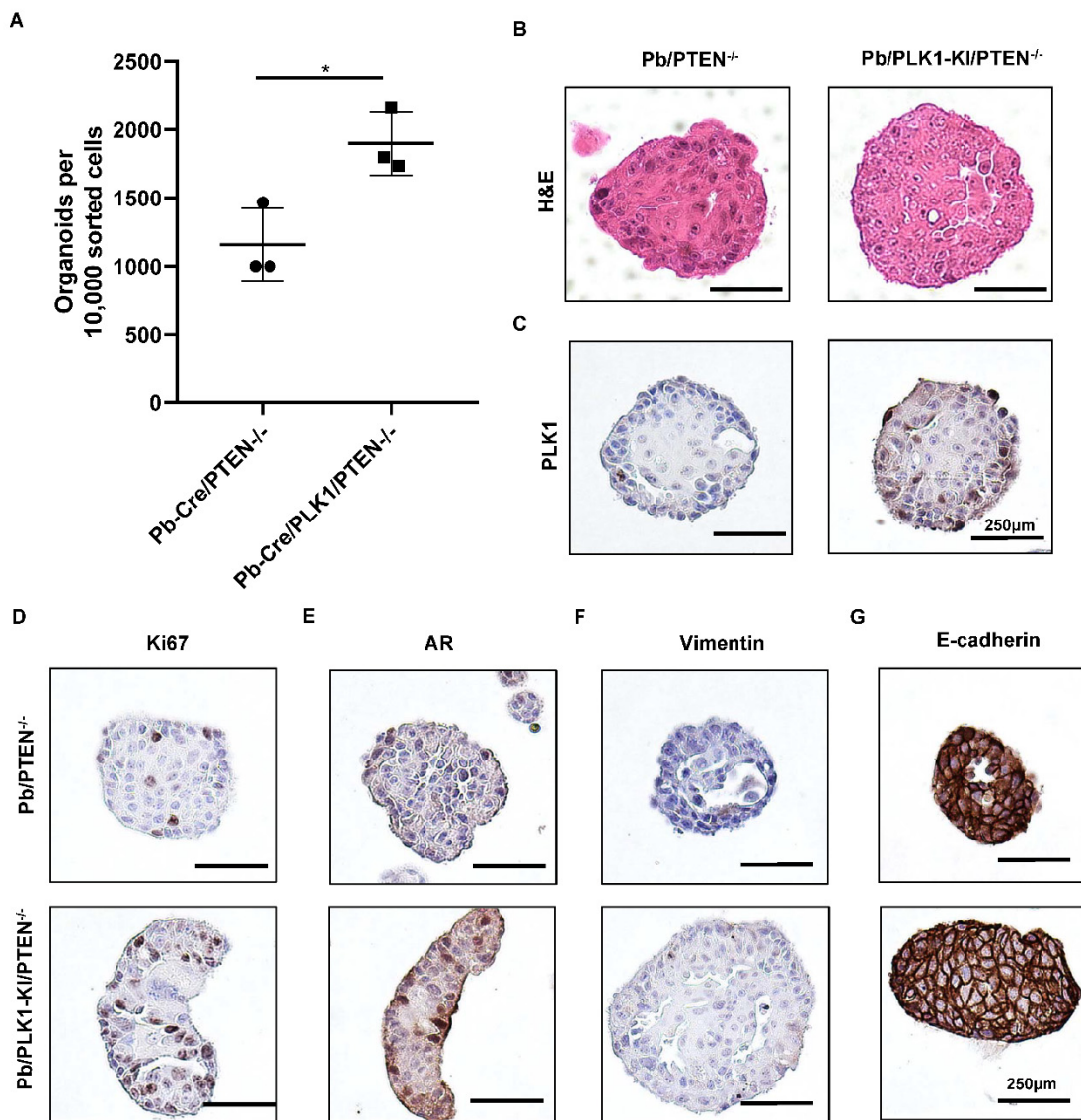
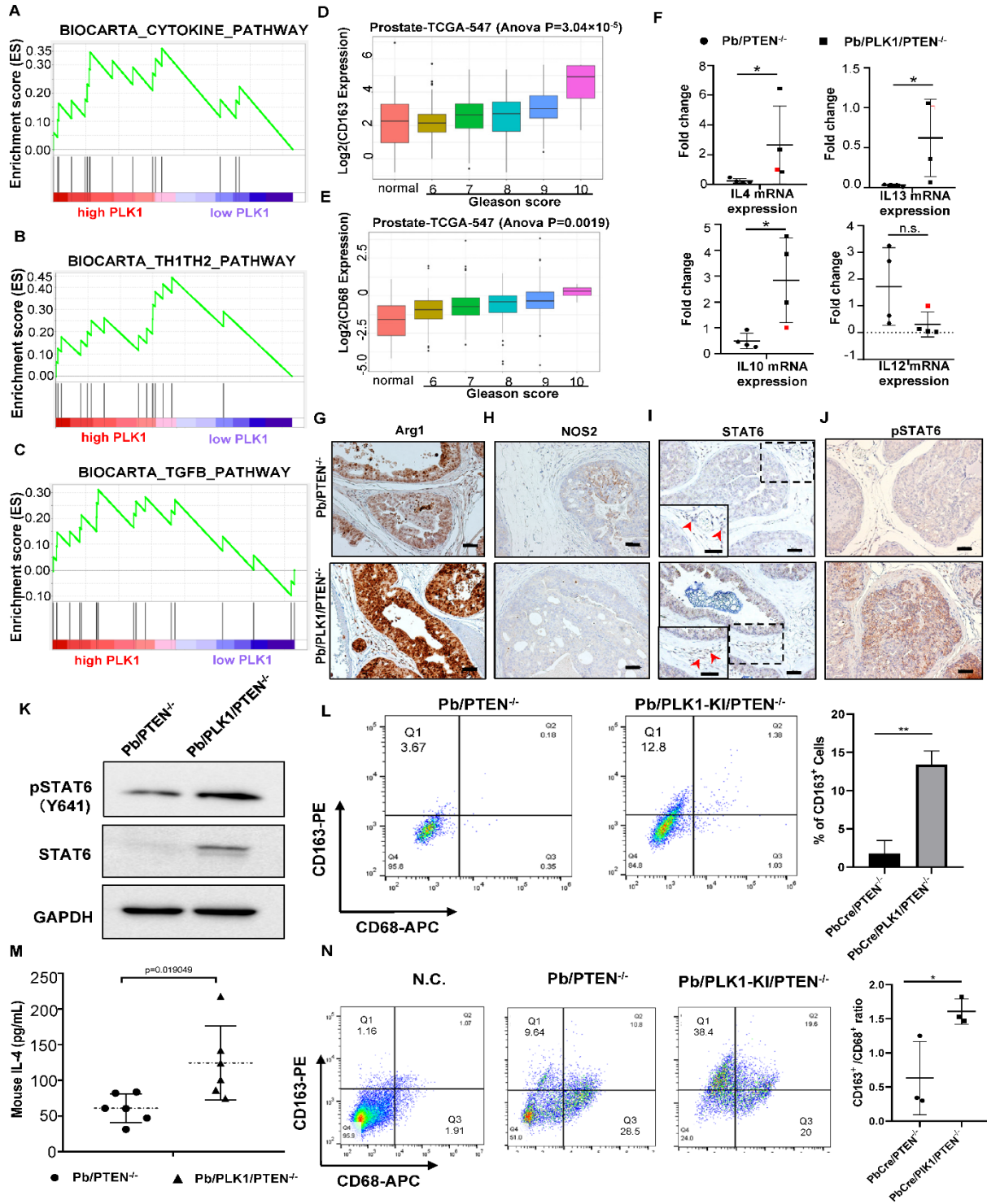


Figure 2.11 Mouse prostate stem cell-derived organoids displays similar features present in original mice. (A) Mouse prostate from indicated genotype mouse were isolated and subjected to enzymatic digestion with collagenase and trypsin. After staining with conjugated antibodies Sca-1 and CD49f, and enriched stem cells (Sca-1⁺ CD49f⁺) were sorted and subjected to organoid culture. The number of organoids from 10,000 sorted stem cells from indicated genotype mouse was counted. (B-G) Representative images of murine prostate stem cell-derived organoids from indicated genotype mouse following H&E staining, PLK1, Ki67, Vimentin and E-cadherin IHC staining.

Figure 2.12 PLK1 upregulates IL4/IL13/STAT6 pathway and lead to elevated population of M2 macrophage in murine prostate. (A-C)GSEA shows the enrichment of cytokine pathway gene set (FDR q-val=0.18), Th1/Th2 pathway gene set (FDR q-val=0.047) and TGF β pathway gene set (FDR q-val=0.30) in high PLK1 expression group (above median of PLK1 expression among 475 human PCa specimens from TCGA). (D) Correlation between CD163 and Gleason score in adjacent normal prostate tissues and primary PCa from TCGA. (E) Correlation between CD68 and Gleason score in adjacent normal prostate tissues and primary PCa from TCGA. (F) mRNA expressions of IL4, IL13, IL10 and IL12 compared in PbCre/PTEN^{-/-} and PbCre/PLK1/ PTEN^{-/-} mice (n=4). (G-J) Representative images of prostate from indicated genotype mouse stained with Arg1, NOS2, STAT6, and p-STAT6 at Y641. Red arrows indicate macrophages. (K)Western blot analysis of STAT6 and phos-STAT6 from mouse prostate in PbCre/PTEN^{-/-} and PbCre/PLK1/ PTEN^{-/-} mice. (L) Representative FACS analysis of M1 macrophages marker-CD68 and M2 macrophages marker-CD163 by gated CD45⁺F4/80⁺ cells in PbCre/PTEN^{-/-} and PbCre/PLK1/ PTEN^{-/-} prostate tissues; Quantification by FACS analysis of CD163⁺ cells (n = 3; **p < 0.01). (M) Following the Experimental scheme in Fig 2.13.A, 1x10⁵ primary prostate cells from 30 weeks age PbCre/PTEN^{-/-} and PbCre/PLK1/ PTEN^{-/-} mice were cultured for 3 days, and supernatants were collected and filtered. Secreted IL4 from supernatants was measured via mouse IL4 ELISA kit (n=6, *p < 0.05). (N) Following the Experimental scheme in Fig 2.13.A, mouse bone marrow was cultured *in vitro* and stimulated into bone marrow derived macrophages (BMDMs) by adding CSF-1 into medium. After one week stimulation, culture medium was replaced with supernatants in the Fig 2.12.M from indicated genotype primary prostate cells. CD68 and CD163 expressions were analyzed in PbCre/PTEN^{-/-} and PbCre/PLK1/ PTEN^{-/-} BMDMs via FACS by gated CD45⁺F4/80⁺ cells. Quantification by FACS analysis of CD163⁺/CD68⁺ ratio (n=3, *p < 0.05).



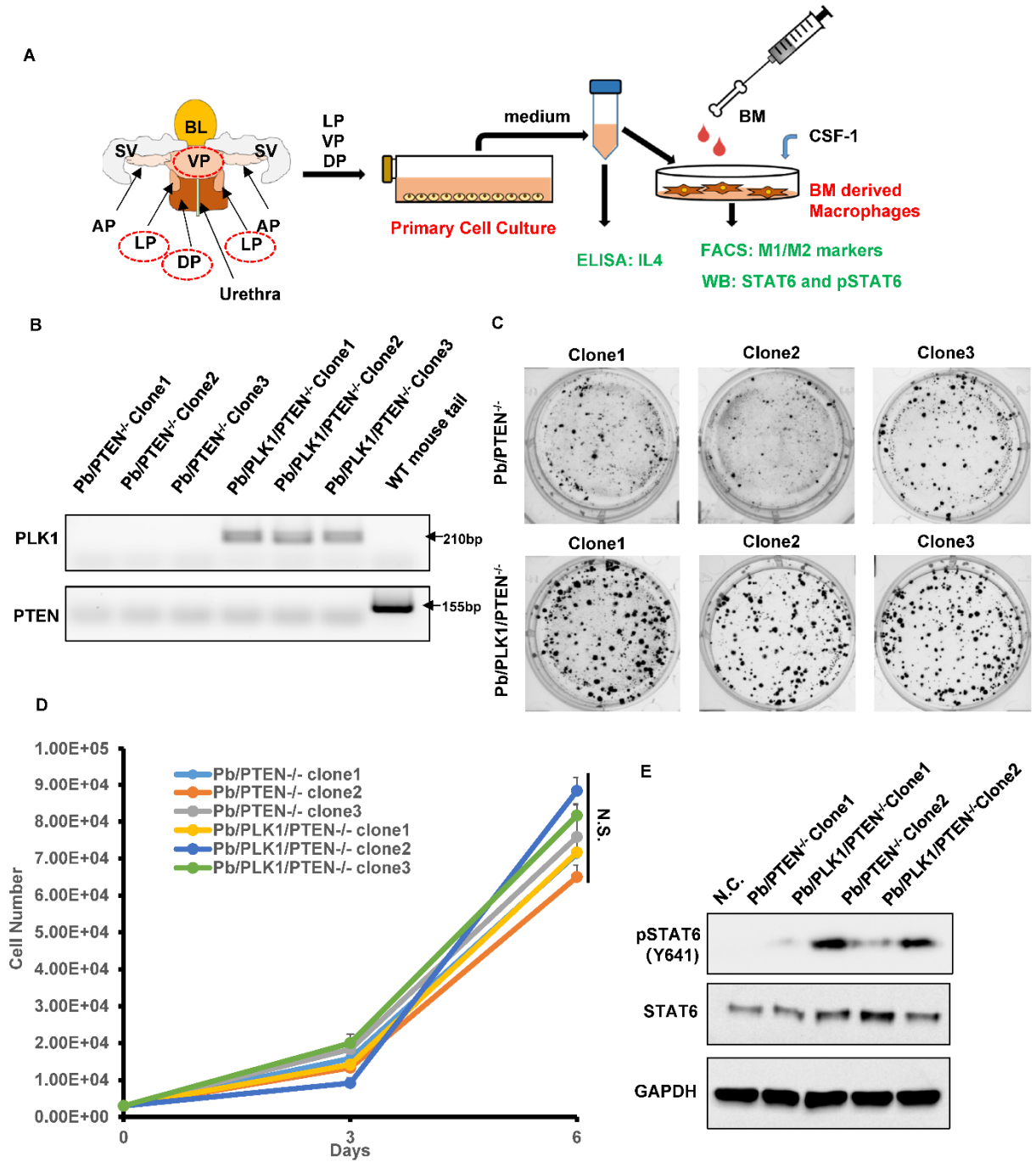


Figure 2.13 (A) Experimental scheme of Fig 2.12L-M and Fig 2.13E. BL: bladder; SV: seminal vesicle; AP: anterior prostate; VP: ventral prostate; DP: dorsal prostate; LP: lateral prostate; BM: bone marrow. (B) Representative gel images of genotyping of primary prostate cell clone from indicated genotype mouse. (C-D) Colony formation (C) and cell growth (D) of primary prostate cell clones from indicated mouse. (E) Western blot analysis of STAT6 and phos-STAT6 from PbCre/PTEN^{-/-} and PbCre/PLK1/PTEN^{-/-} BMDMs.

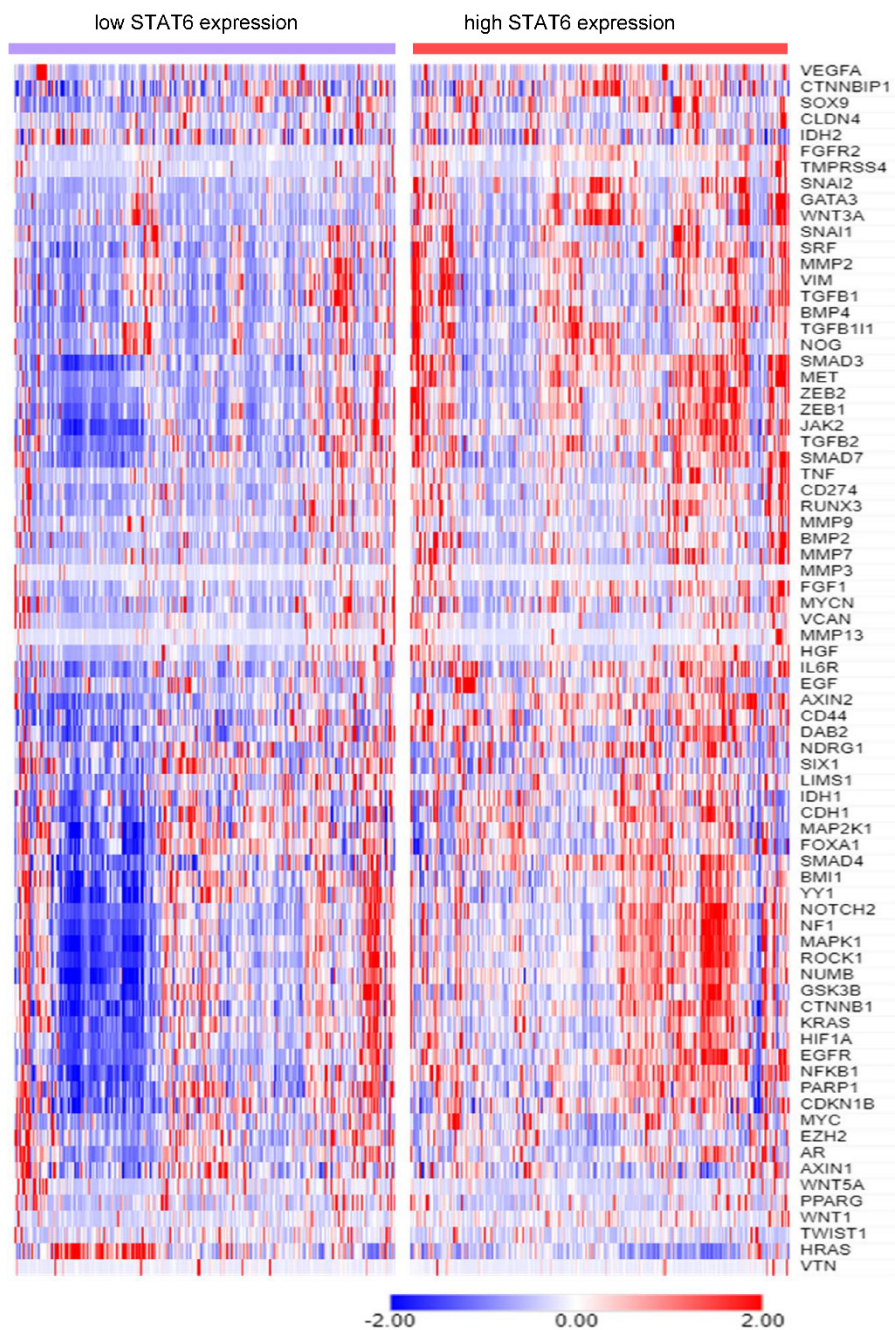
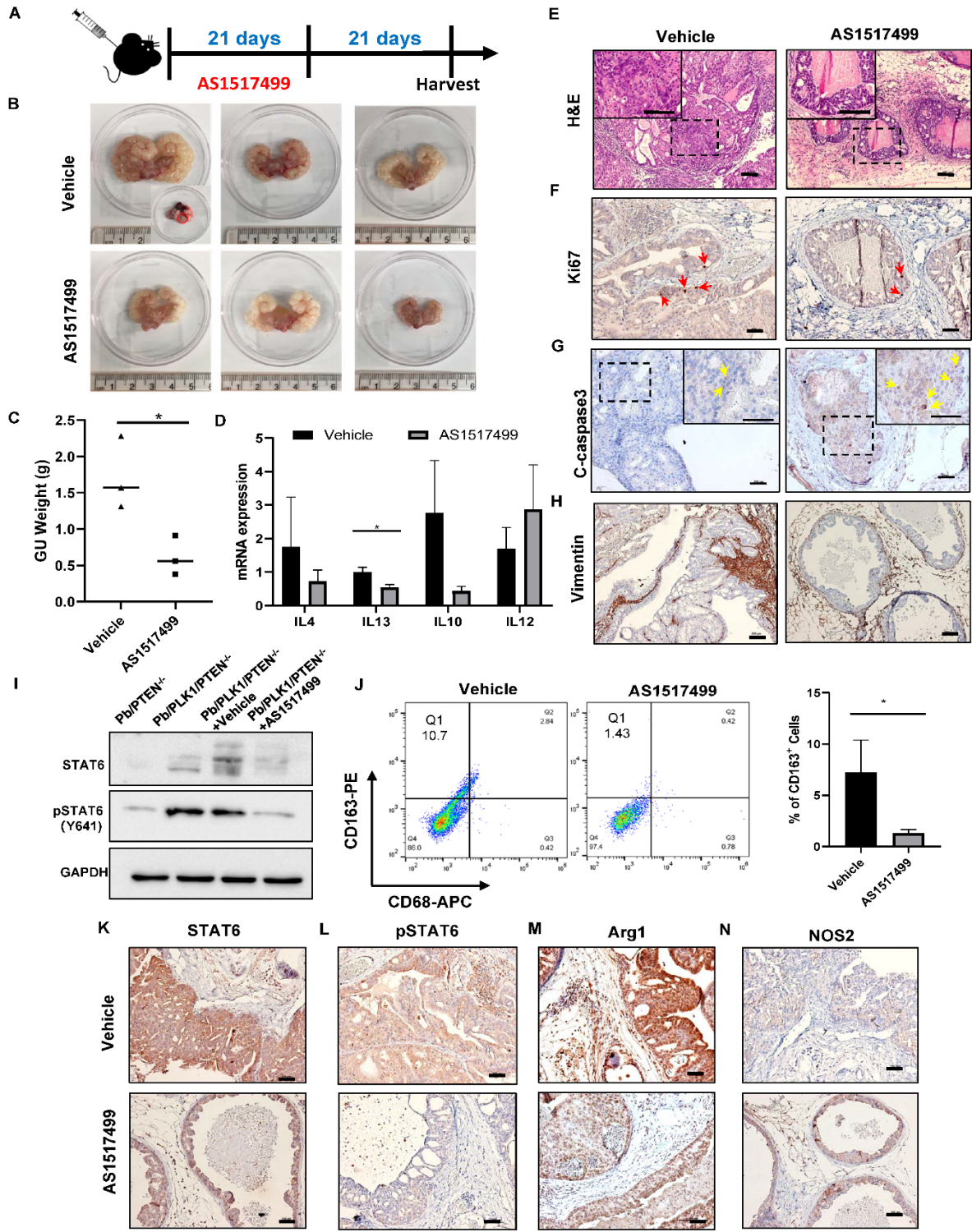


Figure 2.14 Heat map of expression pattern of genes within the EMT-related gene set compared in human prostate cancers with low STAT6 expression and high STAT6 expression.

Figure 2.15 PLK1-mediated activation of IL4/IL13/STAT6 pathway is targetable by STAT6 inhibitors. (A) Schedule of treatment used *in vivo* with the STAT6 inhibitor AS1517499 in PbCre/PLK1/ PTEN^{-/-} mice. Starting from 24 weeks of age, mice were treated daily for 21 days with a dose of 10 mg/kg of AS1517499 (10 mg/kg, i.p., dissolved in 20% DMSO in saline). Mice were euthanized on days 21 after the last day treatment of AS1517499, and then GU blocs were harvested. Vector indicates treatment with 20% DMSO in saline. (B) Representative images of the GU blocs from indicated treatment (n=3). Red circle indicates the tumor found in lung. (C) GU bloc weight was measured (n=3, *p < 0.05). (D) mRNA expressions of IL4, IL13, IL10 and IL12 compared in indicated treatment (n=3, *p < 0.05). (E-H) Representative images of prostate from indicated treatment following H&E staining, Ki67, cleaved-caspase 3 and E-cadherin IHC staining. Red arrows indicate Ki67 positive cells. Yellow arrows indicate apoptotic cells. (I) Western blot analysis of STAT6 and phos-STAT6 from mouse prostate in PbCre/PTEN^{-/-}, PbCre/PLK1/ PTEN^{-/-}, and PbCre/PLK1/ PTEN^{-/-} with vector or AS1517499 treatment. (J) Representative FACS analysis of CD68 and CD163 by gated CD45⁺F4/80⁺ cells in prostate tissues from indicated treatment; Quantification by FACS analysis of CD163⁺ cells (n = 3; *p < 0.05). (K-N) Representative images of prostate from indicated treatment stained with STAT6, p-STAT6 at Y641, Arg1 and NOS2.



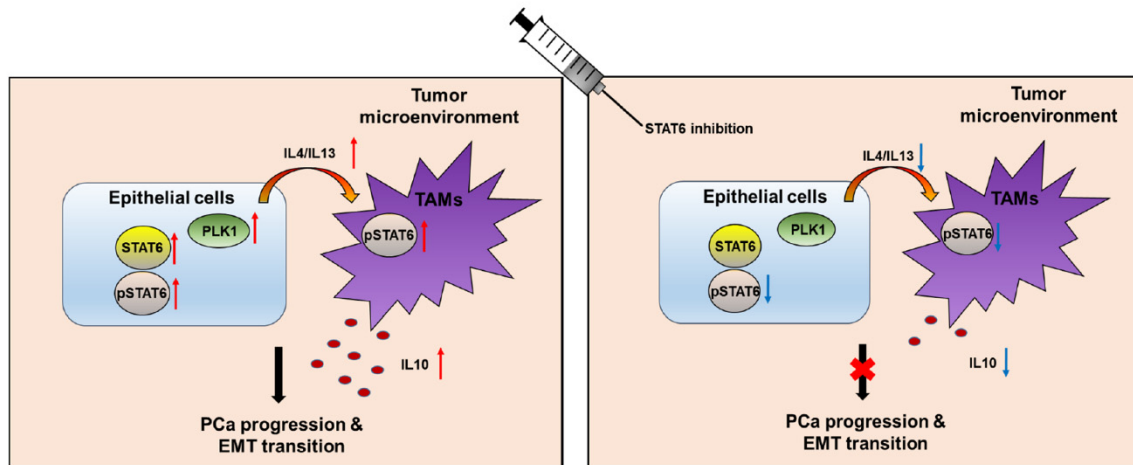


Figure 2.16 PLK1 promotes prostate adenocarcinoma and its metastasis in mice via IL4/IL13/STAT6-induced elevation of M2 macrophages. Probasin cre-mediated overexpression of PLK1 in mouse prostate epithelial cells leads to increase of STAT6 and its phosphorylation at Y641, and also stimulates increasing secretion of IL4 and IL13 from epithelial cells. Increased IL4/IL13 secretion activates STAT6 featured with hyperphosphorylation of STAT6 in macrophages. Activation of STAT6 drives elevation of M2 macrophage population, and subsequently induces higher level of IL10 secretion from macrophages. PLK1-mediated activation of STAT6 in both epithelial cells and macrophages will promote prostate cancer progression and EMT transition. When PLK1 overexpressed mice are treated with STAT6 inhibitors, IL4/IL13/STAT6-induced elevation of M2 macrophages will be suppressed which will ultimately inhibit prostate cancer progression and metastasis.

Table 2-1 Reagents

Designation	Source	Cat#
Primary antibodies		
AR Rabbit mAb	Cell Signaling Technology	5153
Arg1 Chicken polyAb	Sigma Aldrich	ABS535
β -Catenin Rabbit mAb	Cell Signaling Technology	8480
Cleaved Caspase-3 Rabbit mAb	Cell Signaling Technology	9579
CD31 Rabbit mAb	Cell Signaling Technology	77699
E-Cadherin Mouse mAb	Cell Signaling Technology	14472
iNOS Rabbit polyAb	Abcam	ab15323
Ki67 Rabbit mAb	Sigma Aldrich	275R-1
Laminin Rabbit polyAb	Sigma Aldrich	L9393
N-Cadherin Rabbit mAb	Cell Signaling Technology	13116
PLK1 Mouse mAb	Sigma Aldrich	05-844
PTEN Rabbit mAb	Cell Signaling Technology	9188
STAT6 Rabbit mAb	Cell Signaling Technology	5397
Vimentin Rabbit mAb	Cell Signaling Technology	5741
ZO-1 Rabbit mAb	Cell Signaling Technology	13663
Phospho-antibodies		
Phospho-Akt (Ser473) Rabbit mAb	Cell Signaling Technology	4060
Phospho-PLK1 (Thr210) Rabbit mAb	Cell Signaling Technology	9062
Phospho-STAT6 (Tyr641) Rabbit Ab	Cell Signaling Technology	9361
Conjugated-antibodies		
CD163-PE	Invitrogen eBioscience	12-1631-82
CD31-FITC	BD Bioscience	553372
CD45-FITC	BioLegend	103108
CD45- Alexa Fluor® 488	BioLegend	103122
CD68-APC	BioLegend	137008
CD49f-PE	Invitrogen eBioscience	12-0495-83
F4/80-BV605	BioLegend	123133
Sca1-APC	BioLegend	108112
Inhibitors		
AS1517499	Selleckchem	S86855
Critical reagents		
Collagenase Type IV	Sigma Aldrich	C5138
Matrigel	Corning	354230
Prostate Epithelial growth medium	LONZA	CC-3166
Macrophage Colony-Stimulating Factor from mouse	Sigma Aldrich	M9170
bovine pituitary extract	Sigma Aldrich	P1476
insulin	Sigma Aldrich	I9278
recombinant human epidermal growth factor (rhEGF)	Sigma Aldrich	GF144
dihydrotestosterone (DHT)	Sigma Aldrich	D-073
Mouse IL4 ELISA Kit	Abcam	ab221833
Charcoal Stripped Fetal Bovine Serum	Thermo Fisher	12676029

Table 2-2 Primers

Designation	Forward oligo	Reverse oligo
Genotyping Primers		
PLK1	ACTTCGTATAGCATAACATTATACGAA GTTATC	TCCTTTACCCAGAAAGCGC
PTEN	CAAGCACTCTGCGAACTGAG	AAGTTTTTGAAGGCAAGATGC
PbCre	ACCAGCCAGCTATCAACTCG	TTACATTGGTCCAGCCACC
	CTAGGCCACAGAATTGAAAGATCT	GTAGGTGGAAATTCTAGCATCAT CC
qRT-PCR Primers		
Mouse IL4	AGATGGATGTGCCAAACGTCCTCA	AATATGCGAAGCACCTTGGAAGC C
Mouse IL13	TGAGGAGCTGAGCAACATCACACA	TGCGGTTACAGAGGCCATGCAAT A
Mouse IL10	AGAGAAGCATGGCCCAGAAATC	TCATGGCCTTGTAGACACCTTG
Mouse IL12	AGAAAGGTGCGTTCCTCGTAG	AGCCAACCAAGCAGAAGACAG
Mouse GAPDH	GTTGTCTCCTGCGACTTCA	GGTGGTCCAGGGTTTCTTA

CHAPTER 3. PLK1-DEPENDENT PHOSPHORYLATION OF EZH2 CONTRIBUTES TO ITS ONCOGENIC ACTIVITY IN CASTRATION-RESISTANT PROSTATE CANCER

Prostate cancer is the most commonly diagnosed malignant neoplasm of males in the United States, and Androgen deprivation therapy (ADT) or castration is an effective therapeutic approach for patients with advanced PCa. However, most patients initially respond to ADT due to a loss of androgen hormone for tumor cells growth, but the malignant cells ultimately develop resistance to ADT, which results in recurrence of cancer. This so-called castration-resistant prostate cancer (CRPC) is at very late stage and with metastasis, and current options for its treatment is limited [64, 65]. Therefore, exploring novel cellular mechanisms controlling progression of PCa is critical for identifying new targets and developing efficient strategies to treat CRPC. Polo-like kinase 1 (PLK1), which is closely associated with various aspects of cell cycle, regulates a number of cellular signaling pathways via its serine/threonine kinase activity [116]. It has been well demonstrated that PLK1 is overexpressed in a wide range of human cancers and promotes proliferation and invasion of malignant cells, which makes it an attractive anti-cancer drug target [117]. Accumulating evidence indicates that PLK1 plays a promoting role in multiple aspects of PCa initiation and progression, including development of therapy resistance; more importantly, our previous findings provided several therapeutic strategies of combinatory treatment in CRPC, co-targeting PLK1 and other oncogenic pathways, including Androgen Receptor (AR), Poly (ADP-Ribose) Polymerase 1 (PARP1), and WNT/ β -Catenin [77, 90, 136]. However, the molecular mechanism underlying PLK1-induced castration resistance remains unclear.

In recent years, it has been becoming well accepted that epigenetic alterations present in malignant cells transformation. Epigenetics is defined as heritable modifications in expression of genes without changing the DNA sequence, usually including DNA methylation, histone modification and non-coding RNAs. Increasing evidence has uncovered an oncogenic role of dysfunctional epigenetic modifiers in cancer progression by either activating the transcriptions of oncogenes or suppressing transcriptions of tumor suppressors [1]. Dysregulation of covalent modifications of histone is closely linked with poor prognosis of a variety of cancers, and the

molecular outcome of histone modifications relies on which residues on what type of epigenetic groups (e.g. acetylation, phosphorylation, and methylation) are added on or removed from which residues in the N-terminal tails of histones [28, 29]. The methylation on histone lysine residues is usually with closed chromatin structure resulting in gene silencing; and among these histone lysine methylation, trimethylation at lysine 27 in histone 3 (H3K27me3) has been well demonstrated to present in various cancer types and be correlated with poor prognosis and overall survival of patients with these cancers[36]. Enhancer of Zeste Homolog 2 (EZH2) is the main enzyme responsible to H3K27me3. To fulfill its function as a histone methyltransferase, EZH2 need to work with other proteins, such as SUZ12, EED, AEBP2, and et al., as a complex named Polycomb Repressive Complex 2 (PRC2). EZH2 has been reported to be overexpressed in prostate cancer especially advanced PCa, which making EZH2 an attractive anti-cancer drug target [137, 138]. More importantly, EZH2 has been found hyperphosphorylated in CRPC cells, which indicating a PRC2-independent function of EZH2 besides its canonical role in regulation of H3K27me3 [48]. Protein kinase B (also known as AKT), Cyclin-dependent kinase 1 or 2 (CDK1/2) and Janus Kinase 3 (JAK3) have been reported to mediate phosphorylation of EZH2, however, whether PLK1, the critical kinase highly upregulated in CRPC, is involved in EZH2 phosphorylation is not known [46, 50, 51, 76, 139]. Moreover, few studies reported the effect of PLK1-dependent phosphorylation on epigenetic modification.

In present study, we revealed a PLK1-dependent phosphorylation on EZH2 at threonine 144 in CRPC cells. This phosphorylation led to an oncogenic function of EZH2 by disruption of PRC2 complex and a binding of EZH2 with AR to activate its downstream genes. Moreover, this new regulatory mechanism may lead to a novel therapy for CRPC patients by shutting down histone methyltransferase activity of EZH2 as well as its phosphorylation induced by PLK1.

3.1 Materials and methods

3.1.1 TCGA data

TCGA prostate adenocarcinoma patient data containing 52 normal prostate tissues and 475 primary prostate tumors (original 498 cases, we combined those from same patient) was obtained from The Cancer Genome Atlas (TCGA, <https://cancergenome.nih.gov/>); complete Clinical data

set was collected from level 2, and the RNA-seq data were collected from Level 3 (for Segmented or Interpreted Data, IlluminaHiSeq_RNASeqV2 of TCGA). The correlation between Gleason score and the gene of interest was constructed using the boxplot package in R.

3.1.2 Cell culture and transfection

LNCaP, C4-2, and 22Rv1 cells were cultured in RPMI 1640 medium contained 10% of fetal bovine serum (Atlanta Biologicals, GA, USA), under a humidified atmosphere at 37 °C, with 5% CO₂. Transiently transfection with plasmid DNA were conducted via Lipofectamine 3000 transfection reagent (Invitrogen). Cell stably ectopically expressing the gene of interest were obtained after G418 or puromycin selection for 2 weeks.

3.1.3 Western blot analysis

Extract was prepared by sonicating cell lysates in buffer containing 50 mM Tris, 150 mM NaCl, 1% NP-40, 0.5% sodium deoxycholate, 0.2% SDS, protease inhibitors, and phosphatase inhibitors (Sigma). After quantification with BCA assay, the equal amounts of protein were subjected to western blot according to standard protocol. Antibodies and reagents used for western blot are listed in Supplemental Material.

3.1.4 Immunoprecipitation

Equal amounts of protein from cell lysates were incubated with indicated antibodies at 4°C overnight, followed by incubation with protein A/G plus-Agarose beads at 4°C for 2 hr. After several times wash with high salt TBSN (20 mM Tris-HCl, pH 8.0, 0.5% NP-40, 5 mM EGTA, 1.5 mM EDTA, 0.5 mM sodium vanadate and 500 mM NaCl) and low salt TBSN (20 mM Tris-HCl, pH 8.0, 0.5% NP-40, 5 mM EGTA, 1.5 mM EDTA, 0.5 mM sodium vanadate and 150 mM NaCl), the beads were subjected to regular western blot procedure.

3.1.5 Recombinant protein purification

The purification of glutathione *S*-transferase (GST)-tagged proteins was conducted as previously described [77]. Basically, recombinant GST fusion proteins were incubate with glutathione-agarose beads (Sigma), followed by STE buffer (10 mM Tris-HCl (pH 8.0), 1 mM

EDTA, 150 mM NaCl) wash several times, and ultimately eluted into glutathione elution buffer (40 mM glutathione, 50 mM Tris-HCl, 10 mM dithiothreitol (DTT), 200 mM NaCl (pH 8.0)).

3.1.6 Kinase assay

Purified recombinant GST-EZH2 fragments or IP-enriched proteins were incubated with purified PLK1 (R&D) and [γ - 32 P]ATP under the TBMD buffer (50 mM Tris (pH 7.5), 10 mM MgCl₂, 5 mM dithiothreitol, 2 mM EGTA, 0.5 mM sodium vanadate, 20 mM *p*-nitrophenyl phosphate) at 30°C for 30 mins, followed by being mixed with SDS loading buffer, boiled and SDS-PAGE. After coomassie brilliant blue staining, gels were dried by a gel drier and subjected to autoradiography.

3.1.7 Quantitative real-time PCR

Total RNA from mouse prostates was extracted by RNeasy Mini Kit (Qiagen). The first-strand cDNA was generated by iScript cDNA Synthesis Kit (Bio-Rad). Real-time PCR reactions were performed with a SYBR green PCR kit (Roche Applied Science) and a Roche LightCycler 96 thermocycler (Roche Diagnostics Corp.). All individual reactions were performed in triplicate. All genes' expressions were quantified by $2^{-\Delta\Delta C_t}$ relative quantification method and normalized to GAPDH expression. Primers used for real-time PCA are listed in Supplemental Material.

3.1.8 Colony formation assay

1,000 cells were seeded in 6-well plate and followed with indicated treatment for 14 days. The medium was changed every 3 days. Then the colonies were fixed by 10% formalin and stained with 5% crystal violet. After washing twice by PBS, colonies were photographed.

3.1.9 Tumor microarray (TMA) construction

TMA was obtained from the archives of formalin fixed paraffin-embedded tissue blocks in which there are 165 prostate cancer specimens and 34 benign controls from patients who underwent radical prostatectomy at the University of Kentucky (KY, USA), and constructed by the Markey Biospecimen and Tissue Procurement Shared Resource Facility. The use of human prostate specimens was approved by University of Kentucky Institutional Review Board.

3.1.10 Immunohistochemistry and immunofluorescence staining

DAB-immunohistochemistry (IHC) and Immunofluorescence (IF) were performed as previously described [101]. Antibodies and reagents used for IHC and IF are listed in Supplemental Material.

3.1.11 LuCaP35CR xenograft model

LuCaP35CR tumors are a gift from Robert Vessella at the University of Washington. Tumors were minced into 20- to 30-mm³ pieces and then implanted into castrated NSG mice. When tumor volume reached 200 to 300 mm³, mice were randomly separated into 4 groups for indicated treatment. In present study, mice were intravenously injected twice per week with BI2536 (15 mg/kg), EPZ6438 (40 mg/kg), or both, and monitored for 42 days.

3.1.12 Serum PSA measurement

Blood was collected from xenograft mice harvested about every 10 days during the treatments mentioned above, followed by centrifuge to obtain serum. PSA levels were determined using a PSA ELISA kit (Abnova) following manufacturer instruction.

3.1.13 CRISPR

Endogenous EZH2 knock-out in 22RV1 cells was conducted using CRISPR-based EZH2 Human Gene Knockout Kit (Origene, KN202054). After puromycin selection, the single cell-derived colonies were amplified and subjected to western blot for EZH2 KO detection.

3.1.14 Statistical analysis

Statistical analyses were performed with Student t test (two-tailed). All data were shown as mean values \pm SD ($n > 3$), and statistical significance was defined as * $p < 0.05$; ** $p < 0.01$; *** $p < 0.001$; n.s., not significant

3.2 Results

3.2.1 Inhibition of PLK1 increases H3K27 trimethylation but not EZH2 expression in CRPC cells.

EZH2 has been postulated as a critical oncogene contributing to tumorigenesis, and is one of major genes upregulated in advanced PCa especially in CRPC [48, 140, 141]. To validate the association of overexpression of EZH2 with PCa progression, we first analyzed the correlation between mRNA expressions of EZH2 and Gleason scores among 497 PCa specimens from TCGA database. We found that EZH2 mRNA expression was gradually increased with pathological progression (Fig 3.3..1.A). We further investigated the protein expression levels of EZH2 in a panel of human prostate cell lines with diverse genetic backgrounds (Fig 3.3..1.B). Among them, RWPE1 cells are non-transformed immortal prostate cells; DU145 and PC3 cells are AR-null; LNCaP cells are hormone naïve, non-CRPC cells, while C4-2 and 22RV-1 cells are androgen independent, CRPC cells; and MR49F cells are derived from LNCaP cells but show resistance to enzalutamide, a commonly used androgen antagonist [142]. As shown in Fig 3.3..1.C, EZH2 is highly overexpressed in CRPC cell lines-C4-2 and 22RV1, compared with RWPE1 and LNCaP cells. To address whether Plk1 could affect the status of the EZH2 and histone3 methylation, C4-2, 22RV1 and LNCaP cells were treated by different concentrations of BI2536, an ATP competitive PLK1 inhibitor. EZH2 protein expression was not altered upon treatment of PLK1 inhibitor in all three types of PCa cells, and there was no dosage-dependent manner (Fig 3.3..1.D-F). EZH2, the catalytic component of PRC2, enables trimethylation at lysine 27 on histone 3. Given that PLK1 would not affect EZH2 expression, we want to ask whether that modulation of PLK1 could change EZH2 enzymatic activity and consequentially change H3K27 trimethylation. As shown in Fig 3.3..1.G, C4-2 cells treated with BI2536 showed a significant increase of H3K27me3. Similarly, another CRPC cell line, 22RV1 cells also expressed enhanced H3K27me3 after treatment of BI2536 (Fig 3.3..1.H). However, H3K27me3 level was not significantly increased in LNCaP cells, the non-CRPC cell line, treated with BI2536 (Fig 3.3..1.I). To further validate the increase of H3K27me3 was due to the inhibition of PLK1 activity but not the side effect of the inhibitor BI2536, we performed a depletion of PLK1 in C4-2 and 22RV1 cells via a lentivirus-based shRNA. In agreement with BI2536 treatment, depletion of Plk1 resulted in upregulated levels of trimethylation of H3K27 in CRPC cells (Fig 3.3..1.J-K). Taken together, H3K27me3 was inhibited by PLK1 in CRPC cells but not in primary PCa cells, which suggesting

a novel function of JAK3 to negatively regulate H3K27me₃; and EZH2 was not affected by PLK1 which indicated a possibility that PLK1 might mediate a post-translational modification of EZH2.

3.2.2 PLK1 phosphorylates EZH2 at T144.

PLK1 expression is closely associated with PCa progression, and its serine/threonine kinase activity is highly activated in CRPC [124]. However, the interaction between PLK1 and EZH2 signaling in the context of CRPC remains unknown. Given what we found in Fig1 that PLK1 suppressed EZH2 activity toward trimethylation of H3K27, we postulated that PLK1 could induce phosphorylation of EZH2 in CRPC cells. To determine whether EZH2 was a target of PLK1, we first conducted co-immunoprecipitation (co-IP) against PLK1 and EZH2 in 22RV1 cells to explore their possible interactions (Fig 3.3..2.A). As expected, PLK1 was detected in EZH2 immunoprecipitates and vice versa. To further determine the co-localization of PLK1 and EZH2, CRPC cells were transfected with PLK1 tagged with GFP, and then subjected to immunofluorescent staining against EZH2 via Alexa 568. Interestingly, a co-localization of them was found in nucleus as well as cytoplasm (Fig 3.3..2.B). The physiological interaction between PLK1 and EZH2 raised the possibility that PLK1 directly phosphorylated EZH2. Therefore, we first enriched EZH2 protein by immunoprecipitation in HEK293T cells transfected with EZH2 plasmid, and then performed kinase assay with enriched EZH2, purified PLK1 kinase and [γ -³²P] ATP. As shown in Fig 3.3..2.C, EZH2 was a substrate for PLK1 kinase. After in vitro kinase assay using recombinant GST-EZH2 fragments, we then determined that the N terminal region of EZH2 from amino acids (aa) 1 to 200 was targeted by PLK1 (Fig 3.3..2.D). To precisely identify the phosphorylation site(s), threonine 126 or threonine 144 within the aa 1 to 200, were mutated to alanine respectively, and purified aa 1-200 EZH2 proteins carrying WT, T126A mutation or T144A mutation were subjected to in vitro kinase assay (Fig 3.3..2.E). We found that T144A mutant showed a significant reduction of phosphorylation, which suggesting that Plk1 could phosphorylate EZH2 at T144. To confirm T144 is the residue phosphorylated by PLK1, we purified EZH2 fragments (aa 1-125, aa 1-126, aa 1-143, and aa 1-144) and conducted kinase assay; as shown in Fig 3.3..2.F, only aa 1-144, which included the T144 residue, had a strong signal of phosphorylation. EZH2-T144 is highly conserved in different species, and the amino acid sequence around T144 fits the consensus motif for Plk1 phosphorylation (Fig 3.3..2.G). Plk1 phosphorylation of EZH2 at T144 was further confirmed by western blot using our newly

generated phosphor- EZH2 antibody that could recognize phosphorylation at T144 site, both in the context of recombinant GST-EZH2 fragments and IP-enriched EZH2 proteins from 22RV1 cells (Fig 3.3..2.H-I). Next using the pT144-EZH2 antibody, we would like to determine whether phosphorylation of EZH2 at T144 does occur in human CRPC cells and this phosphorylation relies on PLK1 kinase activity. By shRNA-mediated PLK1 knock-down or treatment of BI2536 in 22RV1 cells, the level of T144 phosphorylation of EZH2 was significantly attenuated, which providing the cell biological evidence to support the notion that phosphorylation of EZH2-T144A is dependent on PLK (Fig 3.3..2.J-K).

3.2.3 Blocking PLK1-mediated phosphorylation of EZH2 results in higher sensitization of CRPC cells to treatment of EZH2 inhibitors.

To investigate whether PLK1-dependent phosphorylation of EZH2 could result in the inhibition of H3K27me₃, our generated 22RV1 cell line- A11 with complete EZH2 knock-out by CRISPR were retransfected by different EZH2 constructs (EZH2-WT, EZH2-T144A or EZH2-T144D) to test their rescue abilities towards H3K27me₃. From western blot analysis, we found that blocking the phosphorylation at T144 by alanine mutation led to an increasing level of H3K27 trimethylation, indicating that Plk1 regulates the methylation of H3K27 via direct phosphorylation of EZH2 in CRPC cells (Fig 3.3.B).

Given that EZH2-mediated H3K27me₃ is highly upregulated in human cancers, development of EZH2 inhibitors have been under intense investigation. Most current compounds, such as EPZ6438, GSK126, or DNZeP, target EZH2 methyltransferase activity by competing with S-adenosyl-L-methionine (SAM) to disrupt the methylation process [143]. As CRPC cells expressing different EZH2 constructs (WT or T144A) showed different levels of H3K27me₃, we explored whether Plk1 phosphorylation of EZH2 affects cell response to EZH2 inhibitors. 22RV1 cells expressing EZH2-T144A presented a higher level of apoptotic response and inhibitory colony formation upon the EZH2 inhibitor treatment compared with EZH2-WT or EZH2-T144D (Fig 3.3.C-D).

Our previous studies have shown that hormone naïve PCa cells with overexpression of PLK1 could proliferate under androgen deprivation (data not shown). Therefore, we wanted to further ask whether PLK-induced androgen-independent growth of PCa cells is dependent on its phosphorylation of EZH2. We first established a stabilized LNCaP cell line with overexpression of PLK1 but depletion of endogenous EZH2, and then retransfected these cells with different forms of EZH2 (EZH2-WT, EZH2-T144A or EZH2-T144E) (Fig 3.3.E-F); When under hormone starvation conditions for 9 days, LNCaP cells with PLK1 knock-in still possess a high level of cell proliferation, in contrast, loss of EZH2 resulted in a stagnation of cell growth; more importantly, after restoring EZH2 expression, cell proliferation was rescued; however, the proliferative ability of cells with EZH2-T144A mutation was still highly inhibited in the absence of androgen (Fig.3G).

Taken together, these data suggested that dysregulation of Plk1-induced EZH2 phosphorylation resulted in downregulation of H3K27me3 and development of resistance to castration in PCa.

3.2.4 PLK1-mediated phosphorylation induce EZH2 functional switch from a repressor depending on PRC2 to a transcriptional co-activator of AR.

It has been well accepted that EZH2 performs its pro-oncogenic function through transcriptional silencing of tumor suppressors by H3K27me3 in the context of PRC2 [140, 141]. In addition to its canonical activity, recent studies have demonstrated a PRC2-independent function of EZH2 as a transcriptional activator. Interestingly, this functional switch from a polycomb repressor to an activator, cooperating with AR to promote its downstream targets, was found in CRPC and required hyperphosphorylation of EZH2 [144]. To determine whether PLK1-induced phosphorylation of EZH2 also contributes to this switch to a noncanonical role, we first assessed the interaction between EZH2 with other two main components of PRC2-SUZ12 and EED in 22RV1 cells upon blocking the phosphorylation of EZH2 at T144 via inhibition of PLK1 activity by BI2536 treatment, or depletion of PLK1, or ectopically expressing EZH2 T144A mutants; notably, all these three approaches could enhance the binding between EZH2 with PRC2; on the contrary, T144 phosphorylation of EZH2 interferes with its binding with other PRC2 components, which provides a logical explanation why PLK1 activation is negatively associated with H3K27 trimethylation (Fig 3.4.A-C). Consistently, we observed that EZH2 T144A mutant showed less

transcription level of canonical PRC2-target gene in PCa-DAB2IP due to an elevation of H3K27me3 (Fig 3.4.D) [145]. In the meanwhile, 22RV1 cells expressing EZH2 WT or its T144D mutation exhibited a stronger binding of EZH2 with AR, but T144A mutant impaired this binding, which indicating that T144 phosphorylation of EZH2 promoted the formation of EZH2-AR complex (Fig 3.4.E). The T144 phosphorylation-induced formation of complex was confirmed by an increasing binding between EZH2 T144D/E, which mimic the phosphorylation, and AR in 293T cells (Fig 3.4.F). Furthermore, the mRNA expressions of two downstream targets for transcription activator function of EZH2, TMEM48 and KIA0101, were significantly decreased after cut-off of PLK1, indicating a critical role of PLK1 in EZH2 uncanonical function as a transcription activator (Fig 3.4.G-J).

3.2.5 Co-targeting PLK1 and EZH2 shows a synergetic efficacy in CRPC cells.

As we found in Fig 3.3..2. and Fig 3.3. that inhibition of PLK1 upregulated trimethylation of H3K27, and shutting down PLK1-mediated T144 phosphorylation of EZH2 could make CRPC cells more sensitive in response to EZH2 inhibitors treatment, we would like to ask whether the PLK1 inhibitor and the EZH2 inhibitor could act synergistically to kill CRPC cells. Therefore, C4-2 cells were treated with BI2536, an EZH2 inhibitor (EPZ6438, GSK126, or DNZeP), or a combination with them, and western blot analysis were performed to detect cleaved-PARP, one marker of apoptosis. As expected, co-treatment of the PLK1 inhibitor with the EZH2 inhibitor significantly increased cell death compared with monotherapy (Fig 3.5.A-C). In the meanwhile, this combinatory treatment would not lead to cellular toxicity in normal prostate cells (Fig 3.5.D). In addition, treatment of C4-2 cells or 22RV1 cells with the combination of BI236 and EPZ6438 exhibited a much more significant inhibitory effect on cell proliferation as well as colony formation compared to treatment with BI2536 or EPZ6438 alone (Fig 3.5.E-H). These results suggested a strong synergistic effect when co-targeting PLK1 and EZH2 in CRPC cell *in vitro*.

3.2.6 Co-treatment of BI2536 and EPZ6438 synergistically inhibit tumor growth in CRPC patient-derived xenograft.

To further determine this synergistic efficacy in CRPC, a well-established patient-derived LuCaP35CR xenograft model, which is castration-resistant, was treated with BI2536, EPZ6438, or combinatory treatment [146]. In agreement with what we found *in vitro*, monotherapy either

BI2536 or EPZ6438 did not inhibit dynamic growth of tumor after castration as significant as the combination treatment did (Fig 3.6.A); this strong efficacy was also presented in the sizes and weights of tumors from co-treatment group (Fig 3.6.B-C). Serum PSA levels were also dramatically decreased upon co-treatment (Fig 3.6.D). Histological analyses of these tumors under indicated treatment showed abundant malignant cells with marked mitotic figure in the tumors from control group, however, a remarkable increase of apoptotic bodies with a condensed cytoplasm and pyknotic nuclei in the co-treatment group tumors (Fig 3.6.E). Immunofluorescent staining against cleaved-caspase 3 confirmed the significant increase of apoptosis induced by the combination therapy of BI2536 and EPZ6438 (Fig 3.6.F). These *in vivo* results combining with the finding we obtained from *in vitro* experiments highlight an effective and promising therapeutic strategy to treat CRPC patients by inhibition of Plk1 and EZH2 in CRPC.

3.2.7 High phosphorylation of EZH2 at T144 can be detected in both PLK1-overexpressing mouse prostates and human advanced prostate cancers.

Next we used our transgenic prostate-specific PLK1 overexpression model to determine whether PLK1-induced phosphorylation exists in mouse PCa. The immunostaining of PLK1 confirmed its overexpression in the PLK1 knock-in prostates (Fig 3.7.A); as predicted, a more intense staining of pT144-EZH2 was observed upon PLK1 overexpression (Fig 3.7.B). Our previous study has revealed that PLK1 overexpression in mouse prostate could lead to a more advanced phenotype of prostate adenocarcinoma (data not shown); therefore, using our PLK1 KI mouse model, we not only identified PLK1-dependent phosphorylation of EZH2 at T144 again, but also revealed an association of this phosphorylation with PCa progression. The immunostaining of pT144-EZH2 was also conducted in human prostate cancer patients' tissue microarray (TMA). As shown in Fig 3.7.C, the extent of T144 phosphorylation of EZH2 is positively correlated with Gleason score. Taken together, we preliminarily validated the oncogenic role of PLK1-mediated phosphorylation of EZH2 in PCa development using our preclinical and clinical model, although more evidence needs to be explored.

3.3 Discussion

PCa is the most commonly diagnosed malignant neoplasm of males in the United States, and castration is an effective treatment for patients with late-stage PCa [64]. However, most

patients ultimately experience disease relapse and develop into an advanced stage called CRPC[147]. Treatment for CRPC is very limited, therefore, exploring novel cellular mechanisms underlying progression of CRPC is extremely important. Intensive studies aim to identify new targets and developing efficient strategies to treat CRPC. The notion has been well supported that dysfunction of AR signaling plays a critical role in CRPC occurrence, however, whether AR fulfills its promote-oncogenic function alone or with assistance of other molecules remains unclear [66].

Expression of EZH2, the catalytic subunit of PRC2, was reported to be upregulated in metastatic PCa with an elevation of androgen hormone-refractory; and its overexpression closely correlates with poor prognosis and survival of PCa patients. Thus EZH2 has been proposed as a promising diagnostic marker to distinguish indolent cancers from those with a high potential of lethal malignancy, including CRPC[148]. It has been well accepted that EZH2 promotes the development of disease via inducing silencing of tumor suppressors by trimethylation of H3K27 [140, 141]. More studies reported novel functions of EZH2 besides its canonical activity. For example, EZH2 was positively involved in the transcriptional activation of Wnt target genes, NOTCH1 pathway, and NF- κ B target genes in different human cancer types, which is independent of its histone methyltransferase activity [72-75]. In CRPC, EZH2 working with AR as a transcription coactivator can promote a series of AR downstream targets expressions and ultimately contribute to CRPC progression; and this polycomb-independent activity relies on the phosphorylation of EZH2 [144]. Moreover, it has been demonstrated that EZH2 becomes hyperphosphorylated in CRPC, however, whether PLK1, the serine/threonine kinase, contributing to EZH2 phosphorylation is not known, and very few studies reported the effect of PLK1-dependent phosphorylation on epigenetic modification.

In present study, we found that EZH2 is a novel substrate for PLK1-dependent phosphorylation, and the phosphorylation site T144 was confirmed by multiple approaches, including in vitro kinase assay to detect the loss of phosphorylation signal by alanine mutants, western blot analysis using our homemade phosphor-EZH2 antibody that specifically recognizes T144, and immunostaining against phosphor-EZH2 T144 antibody (Fig 3.2., Fig 3.7.). Phosphorylation is one of the critical steps in regulation of enzymatic activity and transduction of

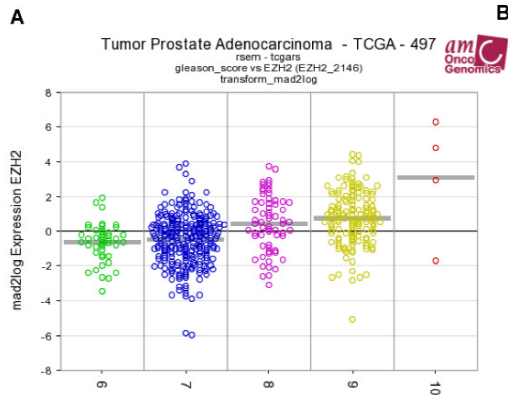
signaling; significantly, our study revealed that this PLK1-mediated post-translational modification of EZH2 could alter the methyltransferase activity towards H3K27 trimethylation. Mechanistically, Plk1 phosphorylation of EZH2 interferes with the binding of components in PRC2 leading to a disruption of this complex (Fig 3.4.). The molecular outcomes of this disruption include 1) a downregulation of H3K27 trimethylation which is independent of PRC2; 2) rescued transcriptional expressions of PRC2 targeted genes; 3) a functional switch of EZH2 from a transcription suppressor to a transcription coactivator forming an EZH2/AR complex; 4) ultimately the activation of oncogenes to promote the development of CRPC (Fig 3.4.).

The novel mechanism underlying the cross talk between PLK1 and EZH2 raised a possibility that co-targeting these two oncogenes might be an efficient way to treat CRPC. Here, we demonstrated that a combination of BI2536 and EPZ6438 significantly inhibited cell proliferation and colony formation of CRPC cells in a synergistic manner (Fig 3.5.). And this synergistic efficacy was also displayed in a castration-resistant LuCaP35CR PDX mouse model (Fig 3.6.). After discovering a strong level of T144 phosphorylation in high graded human PCa via TMA staining against phosphor-EZH2 T144 antibody, we have confidence to predict that the combinatory treatment by inhibition of EZH2 and PLK1 could be applied in clinical therapy (Fig 3.7.).

In summary, we proposed a working model based on the results of this study (Fig 3.8.). In non-CRPC PCa cells in which PLK1 expression is relatively low, EZH2 functions as a histone methyltransferase within PRC2 complex to catalyze trimethylation of H3K27 and consequentially result in genes silence. In contrast, for CRPC cells, high level of PLK1 mediates phosphorylation of EZH2 at T144; this phosphorylation event leads to disruption of PRC2 complex and a functional switch of EZH2 from a polycomb repressor to a transcriptional coactivator binding with AR. The novel oncogenic function of EZH2 promotes transcriptions of a series of oncogenes. In addition, co-targeting PLK1 and EZH2 provides an effective therapeutic approach for CRPC treatment. Inhibition of PLK1 shuts down phosphorylation of EZH2 and ultimately restores EZH2 from PRC2-independence to PRC2-dependence, which upregulates methylation level at H3K27; and treatment of current EZH2 inhibitors can efficiently attenuate H3K27me3. Therefore, combinatory treatment of the PLK1 inhibitor with the EZH2 inhibitor indicates an enhanced efficacy on CRPC.

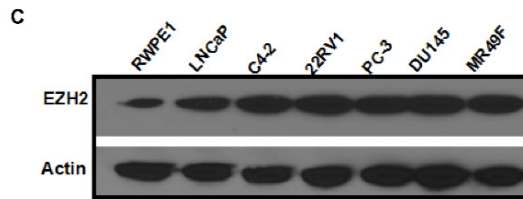
Therefore, the present study will fill in this knowledge gap by determining whether and how PLK1-dependent phosphorylation of EZH2 might alter its histone methyltransferase activity, thus contributing to PCa progression and castration resistance. We revealed that PLK1-dependent phosphorylation is essential for the uncanonical function of EZH2 in CRPC cells. This new regulatory mechanism may lead to novel therapies to shut down the oncogenic function of EZH2 in CRPC.

Figure 3.1 Inhibition of PLK1 increases H3K27 trimethylation but not EZH2 expression in CRPC cells. (A) Correlation between EZH2 and Gleason score in 497 human PCa specimens from TCGA. (B) Genetic backgrounds and biological features of human prostate cell lines used in this study. (C) EZH2 protein expressions in a panel of prostate cell lines. (D-F) PCa cells, including hormone naïve PCa cell line-LNCaP and CRPC cell lines-C4-2 and 22RV1 were treated with 50nM BI2536, the PLK1 inhibitor, for 4 hr., and cell lysates were subjected to western blot against EZH2. (G-I) C4-2, 22RV1 and LNCaP were treated with 50nM BI2536 for 4 hr., and cell lysates were subjected to western blot against H3K27me3. (J-K) C4-2 and 22RV1 were infected with lentivirus carrying shPLK1 and vector control. Western blot analysis of PLK1, EZH2, SUZ12, H3K27me3 and Histone 3. EV: empty vector; Plk-KD: PLK1 Knock-down.

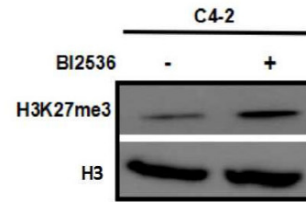


B

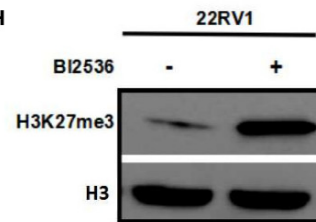
Cell line	PTEN	P53	AR	Androgen dependency	Enzalutamide resistance
RWPE1	+	+	+/-	+	-
LNCaP	mutant	+	+	+	-
C4-2	mutant	+	+	-	-
22RV1	+	mutant	+	-	+
PC3	-	-	-	-	-
DU145	+	mutant	-	-	-
MR49F	mutant	+	+	+	+



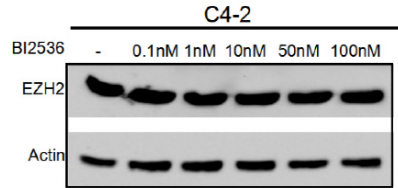
G



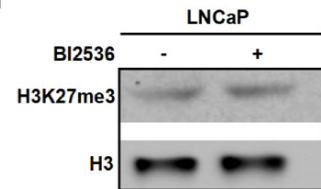
H



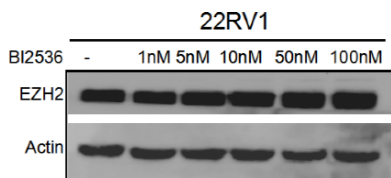
D



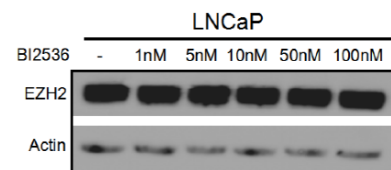
I



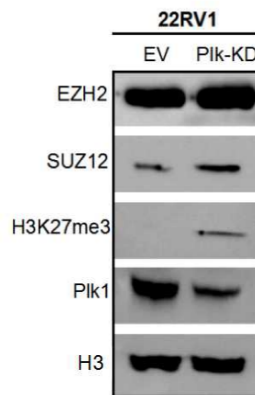
E



F



J



K

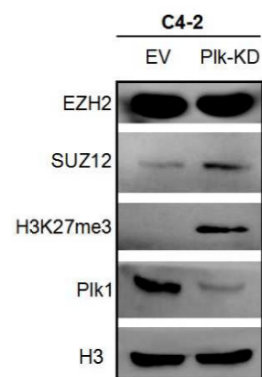


Figure 3.2 PLK1 phosphorylates EZH2 at T144. (A) The physiological interaction between endogenous EZH2 and PLK1 in CRPC cells. Cell lysates from 22RV1 cells were subjected to co-IP of EZH2 and PLK1, and then followed by western blot. (B) 22RV1 cells were transfected with pCMV-GFP-PLK1, and subjected to immunostaining against EZH2 antibody. (C) HEK293T cells were transfected with pCDNA3.0-myc-EZH2, and cell lysates were subjected to anti-myc IP. Kinase assay was conducted using purified PLK1 kinase with beads after IP in the presence of [γ - 32 P] ATP. Beads without incubation with myc antibody were used as negative control. (D) Plk1 targets N-terminal EZH2. Purified PLK1 kinase was incubated with purified GST-EZH2 regions (aa 1 to 200, and aa 201 to 746) in the presence of [γ - 32 P] ATP. (E) S106, S144, T126 and T144 within the N-terminal EZH2 were mutated to alanine. Purified PLK1 kinase was incubated with different recombinant EZH2 regions from aa 1 to 200 (WT, S106A, S114A, T126A mutant, or T144A mutant) and followed *in vitro* kinase assay. (F) Different recombinant EZH2 regions were generated (aa 1 to 125, aa 1 to 126, aa 1 to 143, and aa 1 to 144), and subjected to *in vitro* kinase assay with purified PLK1 kinase. (G) Amino acid sequence context of EZH2 T144 within different species. Red letter indicates phosphorylation site. (H) We generated a phosphor-EZH2 antibody that specifically recognizes T144 of EZH2. Recombinant EZH2 proteins with WT or T144A mutation were incubated with purified PLK1 kinase in the presence of non-radioactive ATP and subjected to western blot using the pT144-EZH2 antibody. (I) 22RV1 cells were transiently transfected with different myc-EZH2 constructs (WT, T144A or T144D) for 48 h, and cell lysates were subjected to anti-myc IP, incubated with purified PLK1 kinase in the presence of cold ATP, and followed with western blot against pT144-EZH2 antibody. (J-K) 22RV1 cells were infected with shPLK1 lentivirous or under BI2536 treatment, then subjected to western blot analysis of pT144-EZH2 antibody.

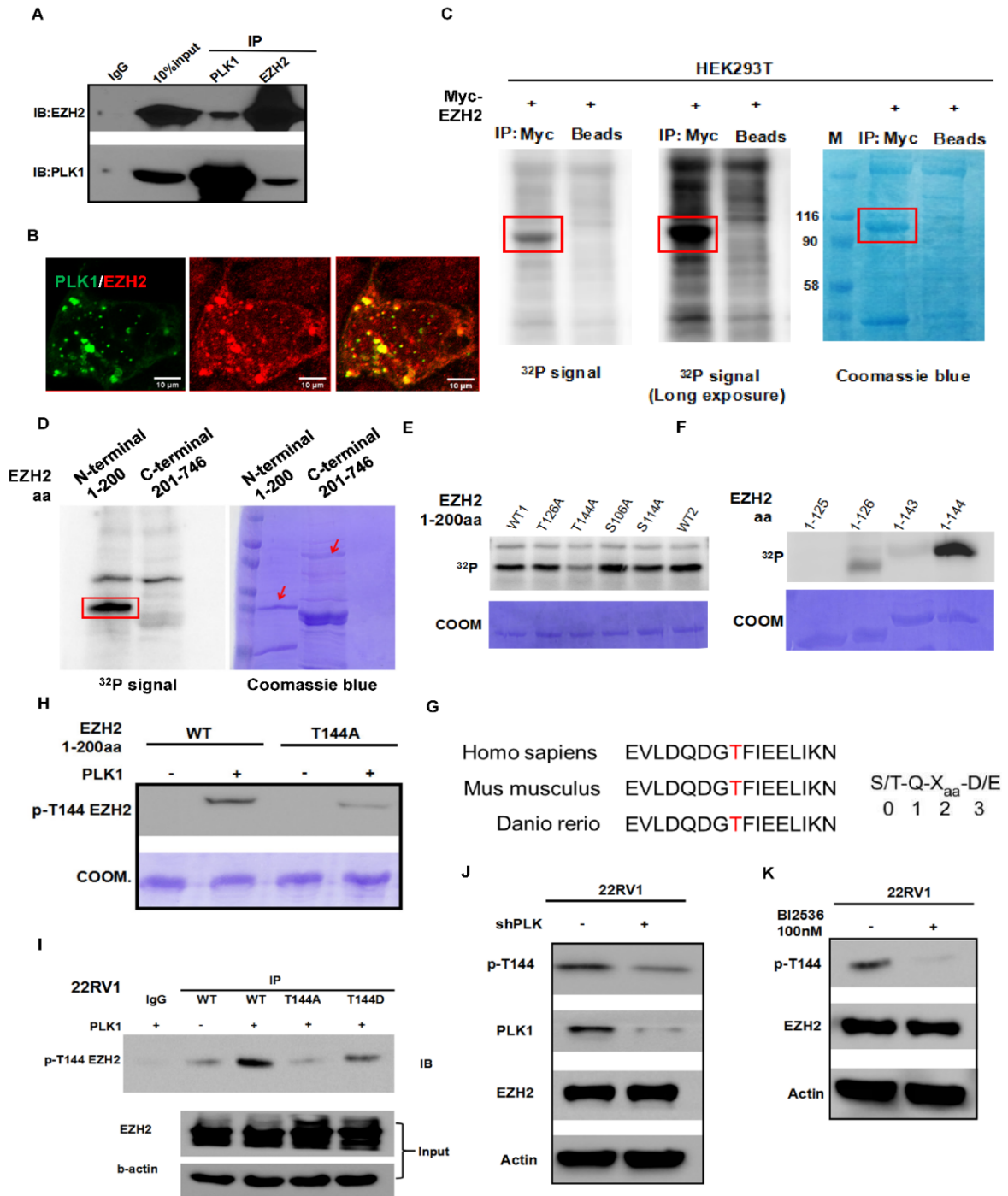


Figure 3.3 Blocking PLK1-mediated phosphorylation of EZH2 results in higher sensitization of CRPC cells to treatment of EZH2 inhibitors. (A) Knock-Out of endogenous EZH2 by CRISPR-cas9 technique in 22RV1 cells. (B) EZH2 knock-out 22RV1 cell line-A11 were re-transfected with different EZH2 constructs (WT, T144A or T144D), and then western blot was conducted against EZH2 and H3K27me3. (C) A11 cells carrying EZH2-WT, EZH2-T144A or EZH2-T144D were treated with 10 μ M GSK126, an EZH2 inhibitor, for 24 hrs. , and cell lysates were subjected to western blot against cleaved-PARP. (D) 1,000 A11 cells carrying with EZH2-WT or EZH2-T144A were treated with 5 μ M EPZ6438 or 5 μ M GSK126 for 10 days, and the colonies were fixed by 10% formalin and stained with 5% crystal violet. (E) LNCaP cells were infected with PLK1 KI lentivirus. After puromycin selection, western blot was performed showing the PLK1 overexpression in LNCaP cells. (F) LNCaP PLK KI cells were infected with shEZH2 lentivirous; after 1 week neomycin selection, cells were re-transfected with shRNA-resistant EZH2 constructs with WT, T144A or T144E, and western blot was conducted to confirm EZH2 expression. (G) The culture medium including 10% Fetal Bovine Serum (FBS) of indicated cell lines was replaced with hormone deprived medium (with 5% Charcoal Stripped Fetal Bovine Serum but without FBS) overnight. Cell growth of cells for 0 day, 3 days, 6 days and 9 days were measured (* $p < 0.05$, *** $p < 0.001$). Stv: hormone starvation.

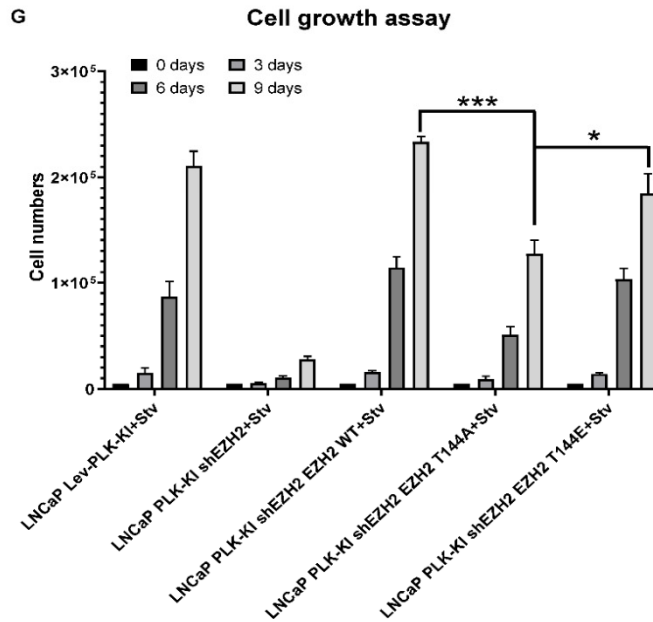
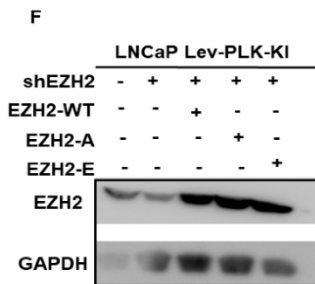
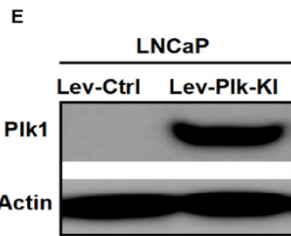
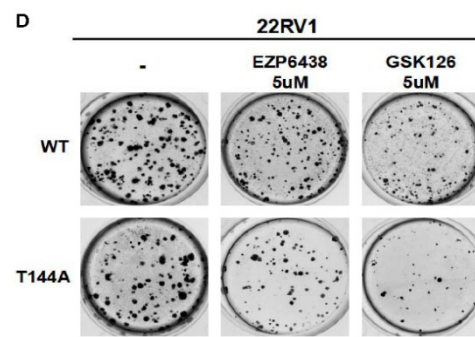
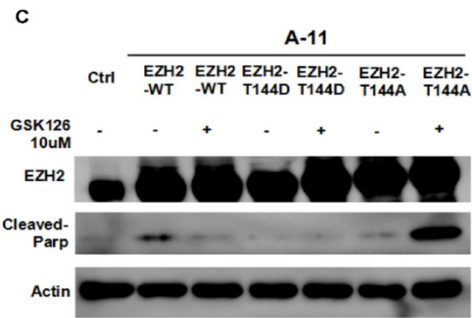
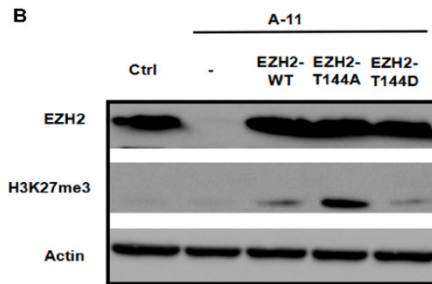
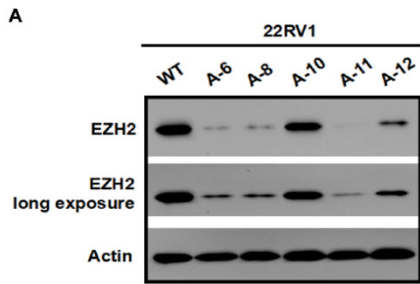
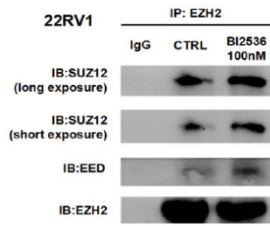
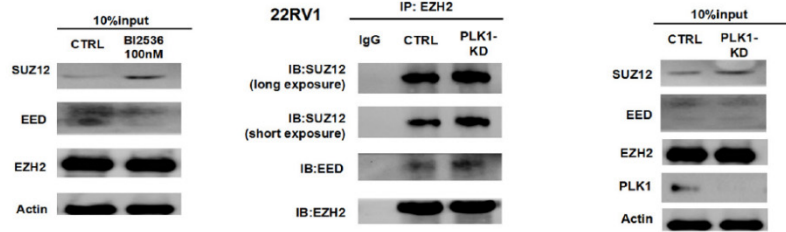


Figure 3.4 PLK1-mediated phosphorylation induce EZH2 functional switch from a repressor depending on PRC2 to a transcriptional co-activator of AR. (A-B) 22RV1 cells treated with BI2536 or lentivirus-based shPLK1 were subjected to co-IP of EZH2 with SUZ12 or EED. (C) 22RV1 cells with EZH2WT, EZH2-T144A or EZH2-T144D were subjected to co-IP of EZH2 with SUZ12 or EED. (D) The mRNA expression levels of the downstream target of PRC2 function-DAB2IP were measured by real-time PCR from 22RV1 cells with EZH2-KO or with re-transfected EZH2 WT, T144A or T144D after KO. (E) 22RV1 cells with EZH2WT, EZH2-T144A or EZH2-T144D were subjected to co-IP between EZH2 and AR. (F) 293TA cells were co-transfected with Flag-AR, PLK1 with KM mutation or TD mutation, HA-EZH2 with WT, T144A T144D or T144E, and then subjected to co-IP between EZH2 and AR. KM: K82M, kinase dead mutation; TD: T210D, constitutively active mutation. (G-J) The mRNA expression levels of TMEM48 and KIAA0101, whose transcriptions rely on PRC2-independent function of EZH2, were measured from 22RV1 cells treated with BI2536 or shPLK1.

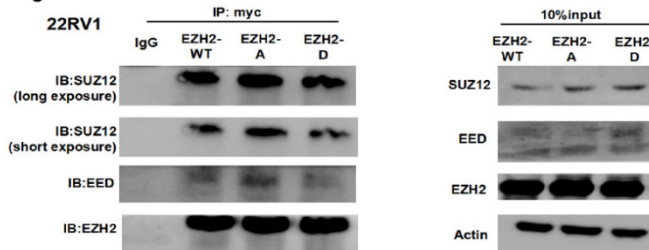
A



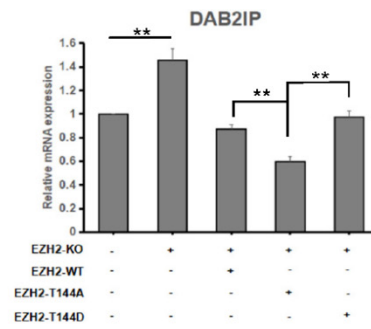
B



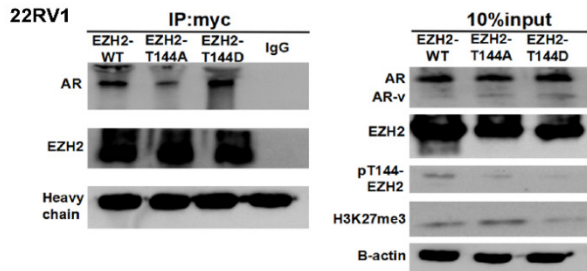
C



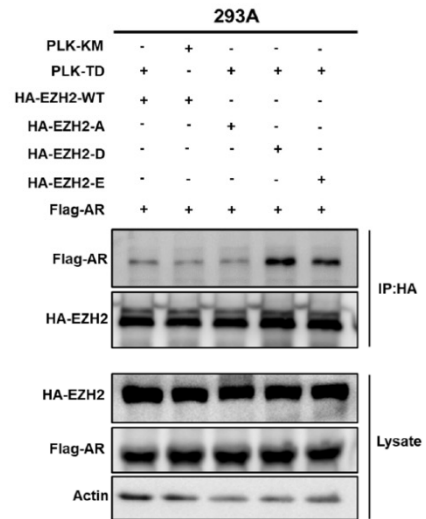
D



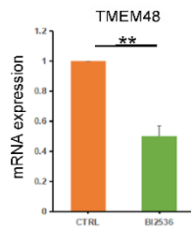
E



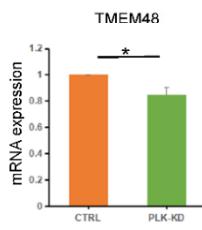
F



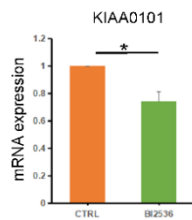
G



I



H



J

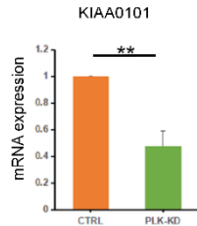


Figure 3.5 Co-targeting PLK1 and EZH2 shows a synergetic efficacy in CRPC cells. (A-C) C4-2 cells were treated with 5nM BI2536, indicated concentrations of EZH2 inhibitors (EPZ6438, GSK126, or DNZeP), or BI2536 combined with EZH2 inhibitors for 24 hrs., and cell lysates were subjected to western blot against cleaved-PARP. (D) RWPE1 cells were treated with 5nM BI2536, 10 μ M EPZ6438, or both for 24 hrs., or treated with Doxorubicin as a positive control; and cell lysates were subjected to western blot against cleaved-PARP. (E-F) C4-2 and 22RV1 cells were treated with 5nM BI2536, 10 μ M EPZ6438, or both for 6 days, and cell numbers were counted at 0 day, 3 days and 6 days. (G-H) C4-2 and 22RV1 cells were treated with 2nM BI2536, 1 μ M EPZ6438, or both for 10 days, and the colonies were fixed by 10% formalin and stained with 5% crystal violet.

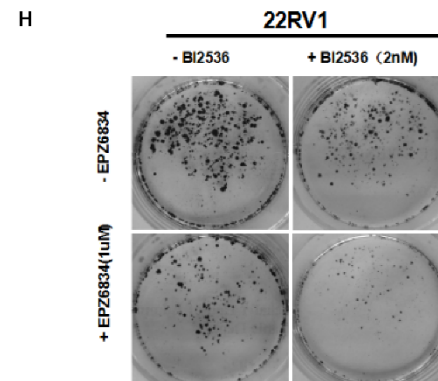
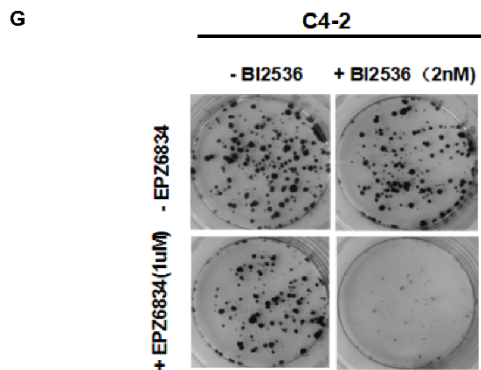
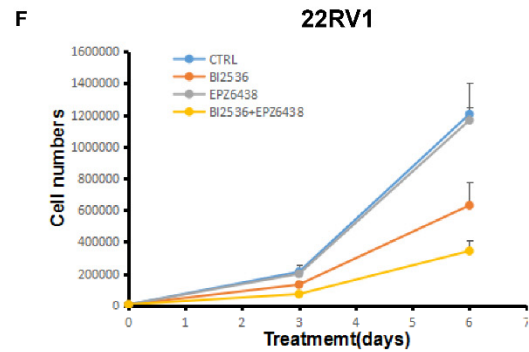
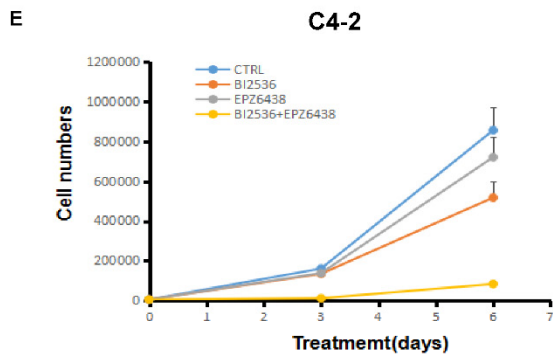
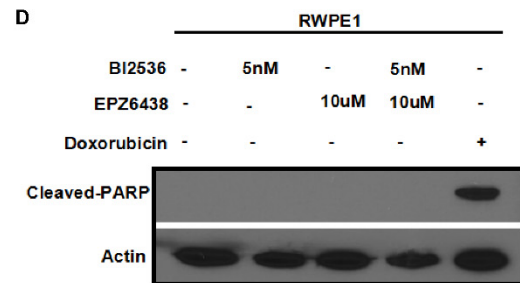
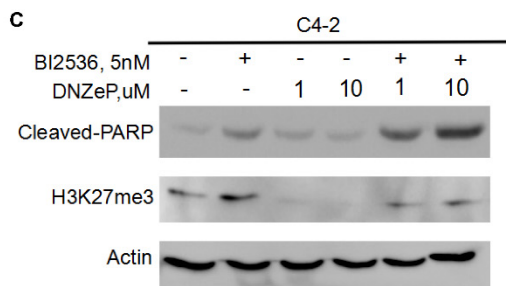
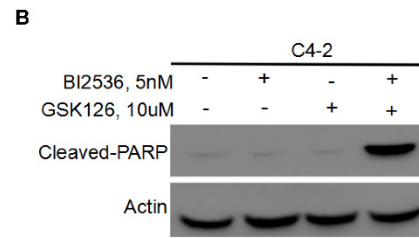
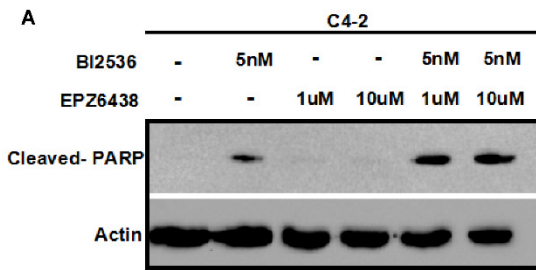
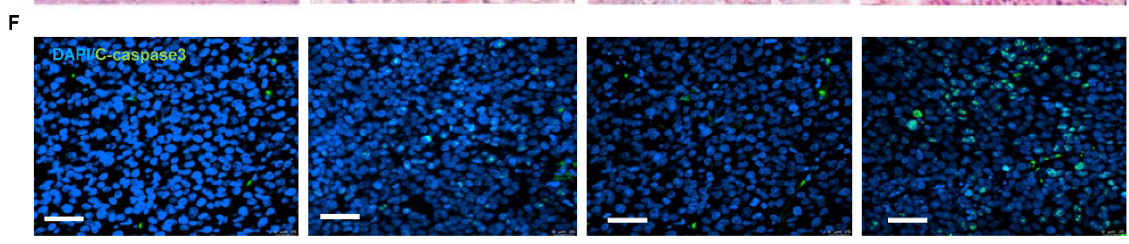
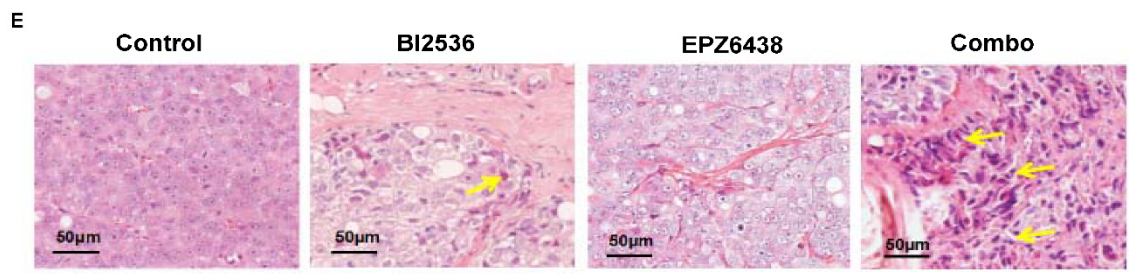
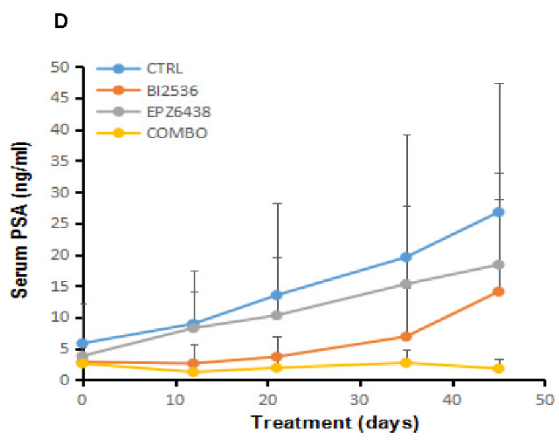
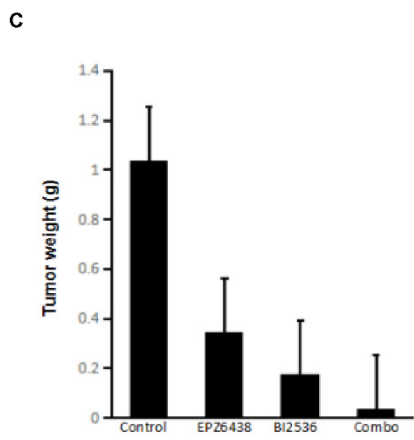
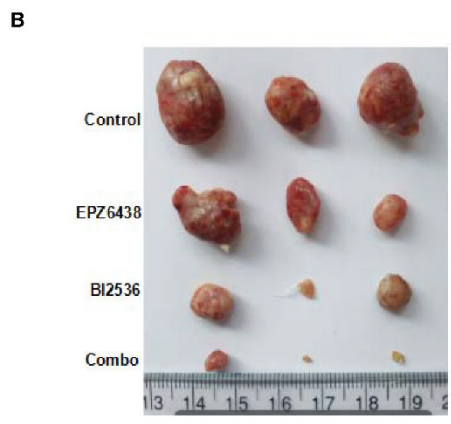
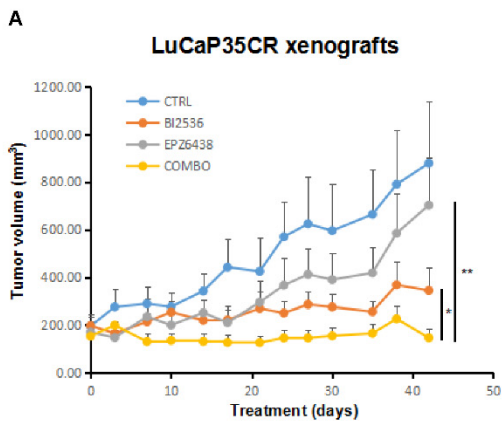


Figure 3.6 Co-treatment of BI2536 and EPZ6438 synergistically inhibit tumor growth in CRPC patient-derived xenograft. LuCaP35CR tumors were inoculated into NSG mice, which had been castrated 1 week earlier. After waiting for several weeks for tumors to reach a size of 200 to 300 mm³, mice were intravenously injected twice per week with BI2536 (15 mg/kg), EPZ6438 (40 mg/kg), or both, and monitored for 42 days. (A) Tumor growth curves (n=4; **P* < 0.05; ***P* < 0.01). (B) Images of tumors at the end of the study. (C) The weights of freshly dissected tumors were measured. (D) Mouse serum was harvested about every 10 days, and subjected to human PSA detection kit followed manufacture instruction. (E-F) Representative images of H&E and IFC staining for cleaved caspase 3 on formaldehyde-fixed, paraffin-embedded LuCaP35CR tumor sections from indicated treatment groups.



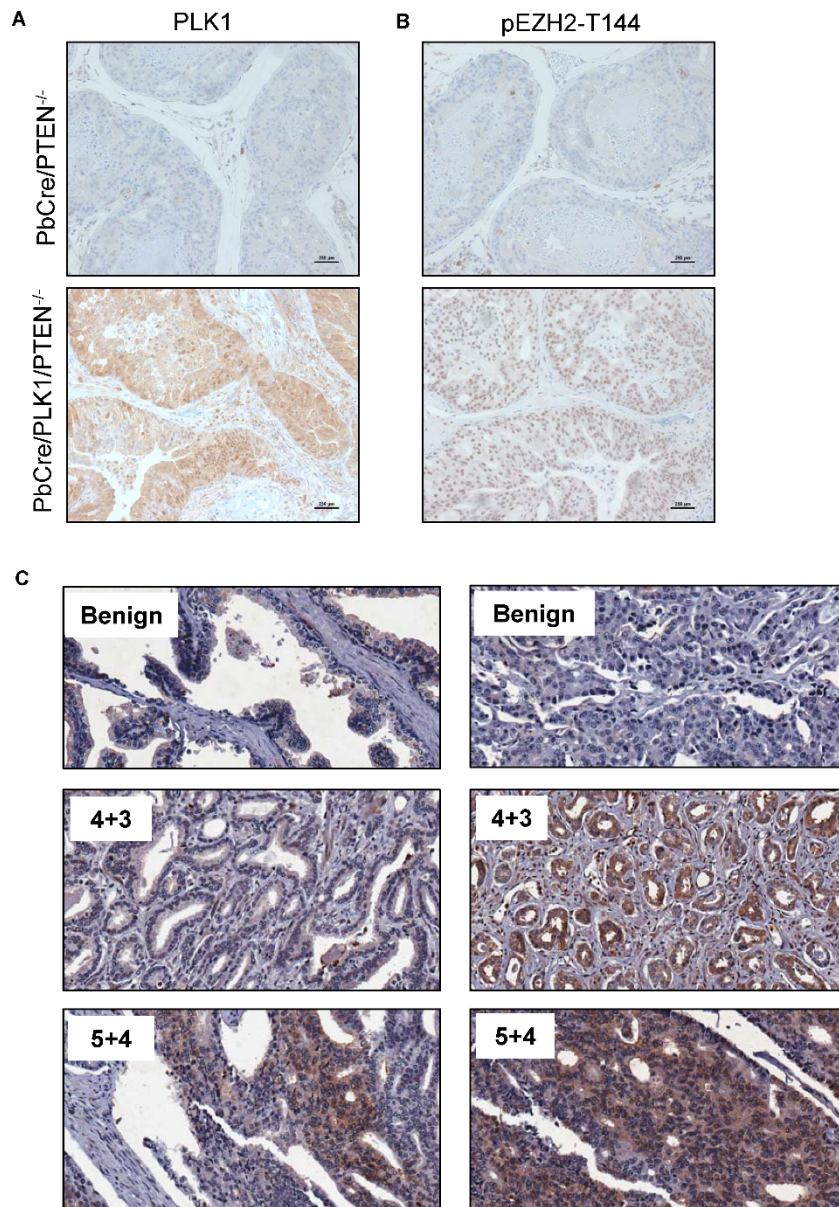


Figure 3.7 High phosphorylation of EZH2 at T144 can be detected in both PLK-overexpressing mouse prostates and human advanced prostate cancers. (A-B) Representative images of prostates from $PbCre/PTEN^{-/-}$ and $PbCre/PLK1/PTEN^{-/-}$ mice at the age of 12 weeks stained with PLK1 and pT144-EZH2. (C) Representative images of tissue microarray (TMA), which obtained from prostate cancer patients with different Gleason score and benign control, stained with pT144-EZH2 antibody.

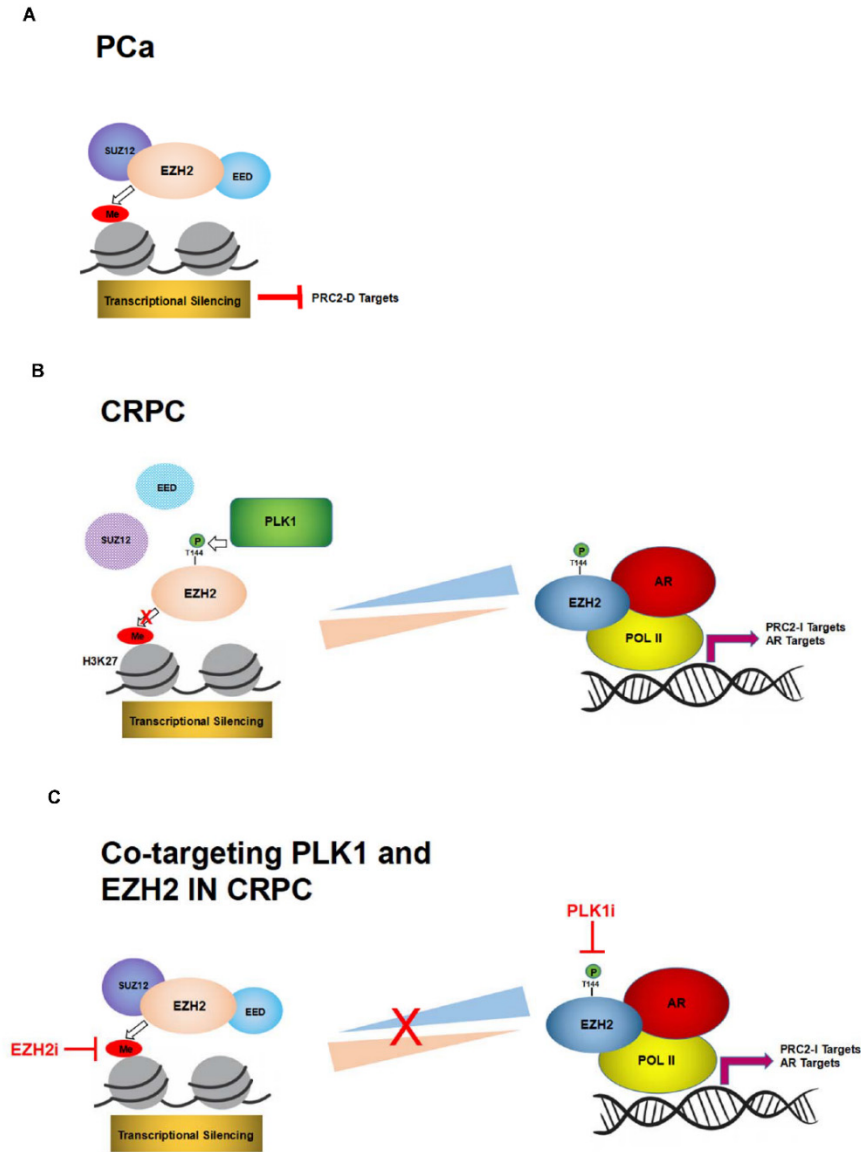


Figure 3.8 Model for EZH2 functional switch from a transcriptional repressor within PRC2 complex to a transcriptional activator working with AR in CRPC. (A) In non-CRPC PCa cells in which PLK1 expression is relatively low, EZH2 functions as a histone methyltransferase within PRC2 complex to catalyze trimethylation of H3K27 and consequently result in genes silence. PRC2-D: PRC2 dependent. (B) In contrast, for CRPC cells, high level of PLK1 mediates phosphorylation of EZH2 at T144; this phosphorylation event leads to disruption of PRC2 complex and a functional switch of EZH2 from a polycomb repressor to a transcriptional coactivator binding with AR. The novel oncogenic function of EZH2 promotes transcriptions of a series of oncogenes. PRC2-I: PRC2 independent. (C) Co-targeting PLK1 and EZH2 provides an effective therapeutic approach for CRPC treatment. Inhibition of PLK1 shuts down phosphorylation of EZH2 and ultimately restores EZH2 from PRC2-independence to PRC2-dependence, which upregulates methylation level at H3K27; and treatment of current EZH2 inhibitors can efficiently attenuate H3K27me3. Therefore, combinatory treatment of the PLK1 inhibitor with the EZH2 inhibitor indicates an enhanced efficacy on CRPC.

Table 3-1 Reagents

Designation	Source	Cat#
Primary antibodies		
AR Rabbit mAb	Cell Signaling Technology	5153
β -actin Mouse mAb	Cell Signaling Technology	3700
Cleaved Caspase-3 Rabbit mAb	Cell Signaling Technology	9579
Cleaved PARP Rabbit mAb	Cell Signaling Technology	5625
EED Rabbit polyAb	Santa Cruz	sc-28701
EZH2 Rabbit mAb	Cell Signaling Technology	5246
HA-tag Rabbit mAb	Cell Signaling Technology	3724
Histone H3 Rabbit mAb	Cell Signaling Technology	4499
H3K27me3 Mouse mAb	Active motif	61017
Myc-tag Mouse mAb	Cell Signaling Technology	2276
PLK1 Mouse mAb	Sigma Aldrich	05-844
SUZ12 Mouse mAb	Santa Cruz	sc-271325
Phospho-antibodies		
Phospho-EZH2 (Thr144) Rabbit polyAb	Proteintech (Chicago, IL)	
Plasmids		
pCMV-PLK-GFP	Chongli Yuan (Purdue University, IN)	
pCDNA3.0-EZH2-myc	Haojie Huang (Mayo Clinic)	
pCMV-EZH2-HA	Kristian Helin [36]	
pCMV-AR-FLAG	Elizabeth Wilson [37]	
Inhibitors		
BI2536	Selleckchem	S1109
EPZ6438	Selleckchem	S7128
GSK126	Selleckchem	S7061
DZNeP	Selleckchem	S7120
Critical reagents		
Human PSA ELISA Kit	Abnova	KA0208
Charcoal Stripped Fetal Bovine Serum	Thermo Fisher	12676029
EZH2 Human Gene Knockout Kit (CRISPR)	Origene	KN202054

Table 3-2 Primers

Designation	Forward oligo	Reverse oligo
qRT-PCR Primers		
DAB2IP	ACACGCCATGGAGCCCGACT	GAAGCCCGTGACCCGGAACG
TMEM48	AGGTCGCGGGACATACTGT	TGCAGATGGGTAGAAATAGCA CT
KIAA0101	ATGGTGCGGACTAAAGCAGAC	CCTCGATGAAACTGATGTCGA AT

REFERENCES

1. Feinberg, A.P., The epigenetics of cancer etiology. *Seminars in Cancer Biology*, 2004. 14(6): p. 427-432.
2. Egger, G., et al., Epigenetics in human disease and prospects for epigenetic therapy. *Nature*, 2004. 429: p. 457.
3. Biswas, S. and C.M. Rao, Epigenetic tools (The Writers, The Readers and The Erasers) and their implications in cancer therapy. *European Journal of Pharmacology*, 2018. 837: p. 8-24.
4. Jones, P.A. and S.B. Baylin, The fundamental role of epigenetic events in cancer. *Nature Reviews Genetics*, 2002. 3: p. 415.
5. Rodriguez, J., et al., Chromosomal Instability Correlates with Genome-wide DNA Demethylation in Human Primary Colorectal Cancers. 2006. 66(17): p. 8462-9468.
6. Clark, S.J. and J. Melki, DNA methylation and gene silencing in cancer: which is the guilty party? *Oncogene*, 2002. 21: p. 5380.
7. Baylin, S.B., DNA methylation and gene silencing in cancer. *Nature Clinical Practice Oncology*, 2005. 2: p. S4.
8. Fujita, T. and A. Aoike, CpG methylation inactivates the promoter activity of the human retinoblastoma tumor-suppressor gene. 1993.
9. Rideout, W., et al., 5-Methylcytosine as an endogenous mutagen in the human LDL receptor and p53 genes. 1990. 249(4974): p. 1288-1290.
10. Jin, B. and K.D. Robertson, DNA methyltransferases, DNA damage repair, and cancer. *Advances in experimental medicine and biology*, 2013. 754: p. 3-29.
11. Esteller, M., Epigenetics in Cancer. 2008. 358(11): p. 1148-1159.
12. Li, P., et al., Effects of DNA methyltransferase 1 inhibition on esophageal squamous cell carcinoma. *Diseases of the Esophagus*, 2011. 24(8): p. 601-610.
13. Peng, D.-F., et al., DNA methylation of multiple tumor-related genes in association with overexpression of DNA methyltransferase 1 (DNMT1) during multistage carcinogenesis of the pancreas. *Carcinogenesis*, 2006. 27(6): p. 1160-1168.
14. Zhao, Z., et al., Depletion of DNMT3A suppressed cell proliferation and restored PTEN in hepatocellular carcinoma cell. *Journal of biomedicine & biotechnology*, 2010. 2010: p. 737535-737535.
15. Butcher, D.T. and D.I. Rodenhiser, Epigenetic inactivation of BRCA1 is associated with aberrant expression of CTCF and DNA methyltransferase (DNMT3B) in some sporadic breast tumours. *European Journal of Cancer*, 2007. 43(1): p. 210-219.
16. Lin, H., et al., Suppression of intestinal neoplasia by deletion of Dnmt3b. *Molecular and cellular biology*, 2006. 26(8): p. 2976-2983.
17. Kobayashi, Y., et al., DNA methylation profiling reveals novel biomarkers and important roles for DNA methyltransferases in prostate cancer. *Genome research*, 2011. 21(7): p. 1017-1027.
18. Baylin, S.B. and P.A. Jones, A decade of exploring the cancer epigenome - biological and translational implications. *Nature reviews. Cancer*, 2011. 11(10): p. 726-734.
19. Kanai, Y., et al., Mutation of the DNA methyltransferase (DNMT) 1 gene in human colorectal cancers. *Cancer Letters*, 2003. 192(1): p. 75-82.

20. Neumann, M., et al., Whole-exome sequencing in adult ETP-ALL reveals a high rate of DNMT3A mutations. 2013. 121(23): p. 4749-4752.
21. Rodenhiser, D. and M. Mann, Epigenetics and human disease: translating basic biology into clinical applications. *CMAJ : Canadian Medical Association journal = journal de l'Association medicale canadienne*, 2006. 174(3): p. 341-348.
22. Haney, S.L., et al., Dnmt3a Is a Haploinsufficient Tumor Suppressor in CD8+ Peripheral T Cell Lymphoma. *PLoS genetics*, 2016. 12(9): p. e1006334-e1006334.
23. Zheng, Y., et al., Loss of Dnmt3b accelerates MLL-AF9 leukemia progression. *Leukemia*, 2016. 30: p. 2373.
24. Kouzarides, T., Chromatin Modifications and Their Function. *Cell*, 2007. 128(4): p. 693-705.
25. Chi, P., C.D. Allis, and G.G. Wang, Covalent histone modifications--miswritten, misinterpreted and mis-erased in human cancers. *Nature reviews. Cancer*, 2010. 10(7): p. 457-469.
26. Jenuwein, T. and C.D. Allis, Translating the Histone Code. 2001. 293(5532): p. 1074-1080.
27. Cohen, I., et al., Histone Modifiers in Cancer: Friends or Foes? *Genes & Cancer*, 2011. 2(6): p. 631-647.
28. Baxter, E., et al., Epigenetic regulation in cancer progression. *Cell & bioscience*, 2014. 4: p. 45-45.
29. Garraway, Levi A. and Eric S. Lander, Lessons from the Cancer Genome. *Cell*, 2013. 153(1): p. 17-37.
30. Schneider, R. and V. Di Cerbo, Cancers with wrong HATs: the impact of acetylation. *Briefings in Functional Genomics*, 2013. 12(3): p. 231-243.
31. Iyer, N.G., H. Özdag, and C. Caldas, p300/CBP and cancer. *Oncogene*, 2004. 23: p. 4225.
32. Dell'Aversana, C., I. Lepore, and L. Altucci, HDAC modulation and cell death in the clinic. *Experimental Cell Research*, 2012. 318(11): p. 1229-1244.
33. Busslinger, M. and A. Tarakhovskiy, Epigenetic control of immunity. *Cold Spring Harbor perspectives in biology*, 2014. 6(6): p. a019307.
34. Qi, J., Bromodomain and extraterminal domain inhibitors (BETi) for cancer therapy: chemical modulation of chromatin structure. *Cold Spring Harbor perspectives in biology*, 2014. 6(12): p. a018663-a018663.
35. Izzo, A. and R. Schneider, Chatting histone modifications in mammals. *Briefings in functional genomics*, 2010. 9(5-6): p. 429-443.
36. Valk-Lingbeek, M.E., S.W.M. Bruggeman, and M. van Lohuizen, Stem Cells and Cancer: The Polycomb Connection. *Cell*, 2004. 118(4): p. 409-418.
37. Kondo, Y., et al., Downregulation of histone H3 lysine 9 methyltransferase G9a induces centrosome disruption and chromosome instability in cancer cells. *PloS one*, 2008. 3(4): p. e2037-e2037.
38. Shi, Y.G. and Y. Tsukada, The discovery of histone demethylases. *Cold Spring Harbor perspectives in biology*, 2013. 5(9): p. a017947.
39. Oki, M., H. Aihara, and T. Ito, Role of histone phosphorylation in chromatin dynamics and its implications in diseases. *Subcell Biochem*, 2007. 41: p. 319-36.
40. Metzger, E., et al., Phosphorylation of histone H3 at threonine 11 establishes a novel chromatin mark for transcriptional regulation. *Nature cell biology*, 2008. 10(1): p. 53-60.
41. DeCarlo, D. and M.K. Hadden, Oncoepigenomics: Making histone lysine methylation count. *European Journal of Medicinal Chemistry*, 2012. 56: p. 179-194.

42. Hervouet, E., et al., Disruption of Dnmt1/PCNA/UHRF1 interactions promotes tumorigenesis from human and mice glial cells. *PLoS one*, 2010. 5(6): p. e11333-e11333.
43. Estève, P.-O., et al., A methylation and phosphorylation switch between an adjacent lysine and serine determines human DNMT1 stability. *Nature structural & molecular biology*, 2011. 18(1): p. 42-48.
44. Li, C., P.J.R. Ebert, and Q.-J. Li, T cell receptor (TCR) and transforming growth factor β (TGF- β) signaling converge on DNA (cytosine-5)-methyltransferase to control forkhead box protein 3 (foxp3) locus methylation and inducible regulatory T cell differentiation. *The Journal of biological chemistry*, 2013. 288(26): p. 19127-19139.
45. Deplus, R., et al., Regulation of DNA Methylation Patterns by CK2-Mediated Phosphorylation of Dnmt3a. *Cell Reports*, 2014. 8(3): p. 743-753.
46. Cha, T.-L., et al., Akt-Mediated Phosphorylation of EZH2 Suppresses Methylation of Lysine 27 in Histone H3. 2005. 310(5746): p. 306-310.
47. Bredfeldt, T.G., et al., Xenoestrogen-induced regulation of EZH2 and histone methylation via estrogen receptor signaling to PI3K/AKT. *Molecular endocrinology (Baltimore, Md.)*, 2010. 24(5): p. 993-1006.
48. Xu, K., et al., EZH2 oncogenic activity in castration-resistant prostate cancer cells is Polycomb-independent. *Science (New York, N.Y.)*, 2012. 338(6113): p. 1465-1469.
49. Wan, L., et al., Phosphorylation of EZH2 by AMPK Suppresses PRC2 Methyltransferase Activity and Oncogenic Function. *Molecular cell*, 2018. 69(2): p. 279-291.e5.
50. Chen, S., et al., Cyclin-dependent kinases regulate epigenetic gene silencing through phosphorylation of EZH2. *Nature cell biology*, 2010. 12(11): p. 1108-1114.
51. Wei, Y., et al., CDK1-dependent phosphorylation of EZH2 suppresses methylation of H3K27 and promotes osteogenic differentiation of human mesenchymal stem cells. *Nature cell biology*, 2011. 13(1): p. 87-94.
52. Yan, J., et al., EZH2 phosphorylation by JAK3 mediates a switch to noncanonical function in natural killer/T-cell lymphoma. 2016. 128(7): p. 948-958.
53. Liu, H., et al., Phosphorylation of MLL by ATR is required for execution of mammalian S-phase checkpoint. *Nature*, 2010. 467(7313): p. 343-346.
54. Liu, F., et al., JAK2V617F-Mediated Phosphorylation of PRMT5 Downregulates Its Methyltransferase Activity and Promotes Myeloproliferation. *Cancer Cell*, 2011. 19(2): p. 283-294.
55. Baba, A., et al., PKA-dependent regulation of the histone lysine demethylase complex PHF2-ARID5B. *Nature Cell Biology*, 2011. 13: p. 668.
56. Arteaga, Maria F., et al., The Histone Demethylase PHF8 Governs Retinoic Acid Response in Acute Promyelocytic Leukemia. *Cancer Cell*, 2013. 23(3): p. 376-389.
57. Barlev, N.A., et al., Repression of GCN5 Histone Acetyltransferase Activity via Bromodomain-Mediated Binding and Phosphorylation by the Ku-DNA-Dependent Protein Kinase Complex. 1998. 18(3): p. 1349-1358.
58. Kawasaki, H., et al., ATF-2 has intrinsic histone acetyltransferase activity which is modulated by phosphorylation. *Nature*, 2000. 405: p. 195.
59. Huang, W.-C. and C.-C. Chen, Akt Phosphorylation of p300 at Ser-1834 Is Essential for Its Histone Acetyltransferase and Transcriptional Activity. 2005. 25(15): p. 6592-6602.
60. Seto, E. and M. Yoshida, Erasers of histone acetylation: the histone deacetylase enzymes. *Cold Spring Harbor perspectives in biology*. 6(4): p. a018713-a018713.

61. Phosphorylation of Histone Deacetylase 6 within its C-terminal Region by Extracellular Signal Regulated Kinase 1. USF Dissertation, 2013.
62. Citro, S., et al., PI3K/mTOR mediate mitogen-dependent HDAC1 phosphorylation in breast cancer: a novel regulation of estrogen receptor expression. *Journal of Molecular Cell Biology*, 2015. 7(2): p. 132-142.
63. Hanigan, T.W., et al., Divergent JNK Phosphorylation of HDAC3 in Triple-Negative Breast Cancer Cells Determines HDAC Inhibitor Binding and Selectivity. *Cell chemical biology*, 2017. 24(11): p. 1356-1367.e8.
64. Siegel, R.L., K.D. Miller, and A. Jemal, *Cancer statistics, 2019*. CA: A Cancer Journal for Clinicians, 2019. 69(1): p. 7-34.
65. Karantanos, T., P.G. Corn, and T.C. Thompson, Prostate cancer progression after androgen deprivation therapy: mechanisms of castrate resistance and novel therapeutic approaches. *Oncogene*, 2013. 32(49): p. 5501-5511.
66. Ferraldeschi, R., et al., Targeting the androgen receptor pathway in castration-resistant prostate cancer: progresses and prospects. *Oncogene*, 2015. 34: p. 1745-1757.
67. Rodriguez-Vida, A., et al., Enzalutamide for the treatment of metastatic castration-resistant prostate cancer. *Drug design, development and therapy*, 2015. 9: p. 3325-3339.
68. Liu, C., et al., Intracrine Androgens and AKR1C3 Activation Confer Resistance to Enzalutamide in Prostate Cancer. *Cancer Research*, 2015. 75(7): p. 1413-1422.
69. Li, Y., et al., Androgen Receptor Splice Variants Mediate Enzalutamide Resistance in Castration-Resistant Prostate Cancer Cell Lines. *Cancer Research*, 2013. 73(2): p. 483-489.
70. Kong, Y., et al., Inhibition of cholesterol biosynthesis overcomes enzalutamide resistance in castration-resistant prostate cancer (CRPC). *Journal of Biological Chemistry*, 2018. 293(37): p. 14328-14341.
71. Tan, J.-z., et al., EZH2: biology, disease, and structure-based drug discovery. *Acta pharmacologica Sinica*, 2014. 35(2): p. 161-174.
72. Shi, B., et al., Integration of estrogen and Wnt signaling circuits by the polycomb group protein EZH2 in breast cancer cells. *Molecular and cellular biology*, 2007. 27(14): p. 5105-5119.
73. Lee, Shuet T., et al., Context-Specific Regulation of NF- κ B Target Gene Expression by EZH2 in Breast Cancers. *Molecular Cell*, 2011. 43(5): p. 798-810.
74. Gonzalez, M.E., et al., EZH2 expands breast stem cells through activation of NOTCH1 signaling. *Proceedings of the National Academy of Sciences*, 2014. 111(8): p. 3098-3103.
75. Jung, H.-Y., et al., PAF and EZH2 Induce Wnt/ β -Catenin Signaling Hyperactivation. *Molecular Cell*, 2013. 52(2): p. 193-205.
76. Xu, K., et al., EZH2 Oncogenic Activity in Castration-Resistant Prostate Cancer Cells Is Polycomb-Independent. 2012. 338(6113): p. 1465-1469.
77. Li, J., et al., Cotargeting Polo-Like Kinase 1 and the Wnt/ β -Catenin Signaling Pathway in Castration-Resistant Prostate Cancer. *Molecular and Cellular Biology*, 2015. 35(24): p. 4185.
78. Zhang, H., et al., PLK1 and HOTAIR Accelerate Proteasomal Degradation of SUZ12 and ZNF198 during Hepatitis B Virus-Induced Liver Carcinogenesis. *Cancer Res*, 2015. 75(11): p. 2363-74.
79. Seruga, B., A. Ocana, and I.F. Tannock, Drug resistance in metastatic castration-resistant prostate cancer. *Nature Reviews Clinical Oncology*, 2011. 8(1): p. 12-23.

80. Crawford, E.D. and D. Petrylak, Castration-Resistant Prostate Cancer: Descriptive Yet Pejorative? *Journal of Clinical Oncology*, 2010. 28(23): p. e408-e408.
81. De Marzo, A.M., et al., Inflammation in prostate carcinogenesis. *Nature Reviews Cancer*, 2007. 7(4): p. 256-269.
82. Shiao, S.L., G.C.-Y. Chu, and L.W.K. Chung, Regulation of prostate cancer progression by the tumor microenvironment. *Cancer letters*, 2016. 380(1): p. 340-348.
83. Hanahan, D. and Lisa M. Coussens, Accessories to the Crime: Functions of Cells Recruited to the Tumor Microenvironment. *Cancer Cell*, 2012. 21(3): p. 309-322.
84. Balkwill, F.R., M. Capasso, and T. Hagemann, The tumor microenvironment at a glance. *Journal of Cell Science*, 2012. 125(23): p. 5591.
85. Shimura, S., et al., Reduced Infiltration of Tumor-associated Macrophages in Human Prostate Cancer: Association with Cancer Progression. *Cancer Research*, 2000. 60(20): p. 5857.
86. Nonomura, N., et al., Infiltration of tumour-associated macrophages in prostate biopsy specimens is predictive of disease progression after hormonal therapy for prostate cancer. *BJU International*, 2011. 107(12): p. 1918-1922.
87. Lanciotti, M., et al., The role of M1 and M2 macrophages in prostate cancer in relation to extracapsular tumor extension and biochemical recurrence after radical prostatectomy. *BioMed research international*, 2014. 2014: p. 486798-486798.
88. Sica, A. and A. Mantovani, Macrophage plasticity and polarization: in vivo veritas. *The Journal of clinical investigation*, 2012. 122(3): p. 787-795.
89. Sica, A. and V. Bronte, Altered macrophage differentiation and immune dysfunction in tumor development. *The Journal of clinical investigation*, 2007. 117(5): p. 1155-1166.
90. Li, J., et al., Targeting Plk1 to Enhance Efficacy of Olaparib in Castration-Resistant Prostate Cancer. *Molecular cancer therapeutics*, 2017. 16(3): p. 469-479.
91. Zhang, Z., et al., Plk1 Inhibition Enhances the Efficacy of Androgen Signaling Blockade in Castration-Resistant Prostate Cancer. *Cancer Research*, 2014. 74(22): p. 6635.
92. Dabo, S., et al., Regulation of innate immunity and inflammation by the mitotic kinase PLK1 through inhibition of IKK ϵ activity. *Cytokine*, 2009. 48: p. 51-52.
93. Hu, J., et al., Polo-like kinase 1 (PLK1) is involved in toll-like receptor (TLR)-mediated TNF- α production in monocytic THP-1 cells. *PloS one*, 2013. 8(10): p. e78832-e78832.
94. Lesche, R., et al., Cre/loxP-mediated inactivation of the murine Pten tumor suppressor gene. *genesis*, 2002. 32(2): p. 148-149.
95. Wu, X., et al., Generation of a prostate epithelial cell-specific Cre transgenic mouse model for tissue-specific gene ablation. *Mechanisms of Development*, 2001. 101(1): p. 61-69.
96. Zhang, Q., et al., Interleukin-17 promotes formation and growth of prostate adenocarcinoma in mouse models. *Cancer research*, 2012. 72(10): p. 2589-2599.
97. Shappell, S.B., et al., Prostate Pathology of Genetically Engineered Mice: Definitions and Classification. The Consensus Report from the Bar Harbor Meeting of the Mouse Models of Human Cancer Consortium Prostate Pathology Committee. *Cancer Research*, 2004. 64(6): p. 2270.
98. Wang, H.-H., et al., Characterization of autoimmune inflammation induced prostate stem cell expansion. *The Prostate*, 2015. 75(14): p. 1620-1631.
99. Czimmerer, Z., et al., The Transcription Factor STAT6 Mediates Direct Repression of Inflammatory Enhancers and Limits Activation of Alternatively Polarized Macrophages. *Immunity*, 2018. 48(1): p. 75-90.e6.

100. Liao, C.-P., et al., Mouse prostate cancer cell lines established from primary and postcastration recurrent tumors. *Hormones & cancer*, 2010. 1(1): p. 44-54.
101. Wang, S., et al., Prostate-specific deletion of the murine Pten tumor suppressor gene leads to metastatic prostate cancer. *Cancer Cell*, 2003. 4(3): p. 209-221.
102. Hyun, S.-Y., H.-I. Hwang, and Y.-J. Jang, Polo-like kinase-1 in DNA damage response. *BMB reports*, 2014. 47(5): p. 249-255.
103. Liu, Z., Q. Sun, and X. Wang, PLK1, A Potential Target for Cancer Therapy. *Translational oncology*, 2017. 10(1): p. 22-32.
104. Deeraksa, A., et al., Plk1 is upregulated in androgen-insensitive prostate cancer cells and its inhibition leads to necroptosis. *Oncogene*, 2013. 32(24): p. 2973-2983.
105. Li, Z., et al., Polo-like kinase 1 (Plk1) overexpression enhances ionizing radiation-induced cancer formation in mice. *The Journal of biological chemistry*, 2017. 292(42): p. 17461-17472.
106. Shannon, R.L., et al., Sarcomatoid carcinoma of the prostate a clinicopathologic study of 12 patients. *Cancer*, 1992. 69(11): p. 2676-2682.
107. Harris, W.P., et al., Androgen deprivation therapy: progress in understanding mechanisms of resistance and optimizing androgen depletion. *Nature clinical practice. Urology*, 2009. 6(2): p. 76-85.
108. Wu, J., et al., Polo-like kinase 1 induces epithelial-to-mesenchymal transition and promotes epithelial cell motility by activating CRAF/ERK signaling. *eLife*, 2016. 5: p. e10734.
109. Drost, J., et al., Organoid culture systems for prostate epithelial and cancer tissue. *Nature Protocols*, 2016. 11: p. 347.
110. Karthaus, W.R., et al., Identification of multipotent luminal progenitor cells in human prostate organoid cultures. *Cell*, 2014. 159(1): p. 163-175.
111. Gao, D., et al., Organoid cultures derived from patients with advanced prostate cancer. *Cell*, 2014. 159(1): p. 176-187.
112. Martinez, F.O., et al., Genetic programs expressed in resting and IL-4 alternatively activated mouse and human macrophages: similarities and differences. *Blood*, 2013. 121(9): p. e57-e69.
113. Quelle, F.W., et al., Cloning of murine Stat6 and human Stat6, Stat proteins that are tyrosine phosphorylated in responses to IL-4 and IL-3 but are not required for mitogenesis. *Molecular and cellular biology*, 1995. 15(6): p. 3336-3343.
114. Dickensheets, H.L., et al., Interferons inhibit activation of STAT6 by interleukin 4 in human monocytes by inducing SOCS-1; gene expression. *Proceedings of the National Academy of Sciences*, 1999. 96(19): p. 10800.
115. Binnemars-Postma, K., et al., Targeting the Stat6 pathway in tumor-associated macrophages reduces tumor growth and metastatic niche formation in breast cancer. *The FASEB Journal*, 2017. 32(2): p. 969-978.
116. Barr, F.A., H.H.W. Silljé, and E.A. Nigg, Polo-like kinases and the orchestration of cell division. *Nature Reviews Molecular Cell Biology*, 2004. 5(6): p. 429-441.
117. Liu, X., Targeting Polo-Like Kinases: A Promising Therapeutic Approach for Cancer Treatment. *Translational oncology*, 2015. 8(3): p. 185-195.
118. Gutteridge, R.E.A., et al., Plk1 Inhibitors in Cancer Therapy: From Laboratory to Clinics. *Molecular cancer therapeutics*, 2016. 15(7): p. 1427-1435.
119. de Cárcer, G., The Mitotic Cancer Target Polo-Like Kinase 1: Oncogene or Tumor Suppressor? *Genes*, 2019. 10(3): p. 208.

120. de Cárcer, G., et al., Plk1 overexpression induces chromosomal instability and suppresses tumor development. *Nature communications*, 2018. 9(1): p. 3012-3012.
121. Mazzucchelli, R., et al., Rare and unusual histological variants of prostatic carcinoma: clinical significance. *BJU International*, 2008. 102(10): p. 1369-1374.
122. Domínguez, A., et al., Prostatic sarcoma after conservative treatment with brachytherapy for low-risk prostate cancer. *Acta Oncologica*, 2013. 52(6): p. 1215-1216.
123. Tseng, T.Y., et al., Prostatic carcinosarcoma 15 years after combined external beam radiation and brachytherapy for prostatic adenocarcinoma: a case report. *Prostate Cancer and Prostatic Diseases*, 2006. 9(2): p. 195-197.
124. Sun, Y., et al., Androgen Deprivation Causes Epithelial–Mesenchymal Transition in the Prostate: Implications for Androgen-Deprivation Therapy. *Cancer Research*, 2012. 72(2): p. 527.
125. Zhang, Z., et al., Plk1 inhibition enhances the efficacy of androgen signaling blockade in castration-resistant prostate cancer. *Cancer research*, 2014. 74(22): p. 6635-6647.
126. Nieto, M.A., et al., EMT: 2016. *Cell*, 2016. 166(1): p. 21-45.
127. Moustakas, A. and A.G. de Herreros, Epithelial-mesenchymal transition in cancer. *Molecular oncology*, 2017. 11(7): p. 715-717.
128. Jolly, M.K., et al., Implications of the Hybrid Epithelial/Mesenchymal Phenotype in Metastasis. *Frontiers in oncology*, 2015. 5: p. 155-155.
129. Marcucci, F., G. Stassi, and R. De Maria, Epithelial–mesenchymal transition: a new target in anticancer drug discovery. *Nature Reviews Drug Discovery*, 2016. 15: p. 311.
130. Park, J.W., et al., Prostate epithelial cell of origin determines cancer differentiation state in an organoid transformation assay. *Proceedings of the National Academy of Sciences of the United States of America*, 2016. 113(16): p. 4482-4487.
131. Li, X., et al., Oncogenic transformation of diverse gastrointestinal tissues in primary organoid culture. *Nature medicine*, 2014. 20(7): p. 769-777.
132. Dai, X., et al., Prostate cancer-associated SPOP mutations confer resistance to BET inhibitors through stabilization of BRD4. *Nature medicine*, 2017. 23(9): p. 1063-1071.
133. Chen, Y., W. Tan, and C. Wang, Tumor-associated macrophage-derived cytokines enhance cancer stem-like characteristics through epithelial-mesenchymal transition. *OncoTargets and therapy*, 2018. 11: p. 3817-3826.
134. Cassetta, L. and J.W. Pollard, Repolarizing macrophages improves breast cancer therapy. *Cell research*, 2017. 27(8): p. 963-964.
135. Pesu, M., et al., Interleukin-4-induced transcriptional activation by Stat6 involves multiple serine/threonine kinase pathways and serine phosphorylation of Stat6. *Blood*, 2000. 95(2): p. 494-502.
136. Zhang, Z., et al., Inhibition of Plk1 represses androgen signaling pathway in castration-resistant prostate cancer. *Cell cycle (Georgetown, Tex.)*, 2015. 14(13): p. 2142-2148.
137. Kim, K.H. and C.W.M. Roberts, Targeting EZH2 in cancer. *Nature Medicine*, 2016. 22: p. 128.
138. Yang, Y.A. and J. Yu, EZH2, an epigenetic driver of prostate cancer. *Protein & cell*, 2013. 4(5): p. 331-341.
139. Yan, J., et al., EZH2 phosphorylation by JAK3 mediates a switch to noncanonical function in natural killer/T-cell lymphoma. *Blood*, 2016. 128(7): p. 948-958.
140. Cao, R., et al., Role of Histone H3 Lysine 27 Methylation in Polycomb-Group Silencing. *Science*, 2002. 298(5595): p. 1039.

141. Yu, J., et al., An integrated network of androgen receptor, polycomb, and TMPRSS2-ERG gene fusions in prostate cancer progression. *Cancer cell*, 2010. 17(5): p. 443-454.
142. Kuruma, H., et al., A Novel Antiandrogen, Compound 30, Suppresses Castration-Resistant and MDV3100-Resistant Prostate Cancer Growth & In Vitro and In Vivo. *Molecular Cancer Therapeutics*, 2013. 12(5): p. 567.
143. Kim, K.H. and C.W.M. Roberts, Targeting EZH2 in cancer. *Nature Medicine*, 2016. 22(2): p. 128-134.
144. Xu, K., et al., EZH2 Oncogenic Activity in Castration-Resistant Prostate Cancer Cells Is Polycomb-Independent. *Science*, 2012. 338(6113): p. 1465-1469.
145. Chen, H. and J.t. Hsieh, Silencing of human DAB2IP gene expression mediated by polycomb EZH2 complex in prostate cancer. *Cancer Research*, 2005. 65(9 Supplement): p. 219.
146. Mostaghel, E.A., et al., Resistance to CYP17A1 Inhibition with Abiraterone in Castration-Resistant Prostate Cancer: Induction of Steroidogenesis and Androgen Receptor Splice Variants. *Clinical Cancer Research*, 2011. 17(18): p. 5913.
147. Donkena, K.V., H. Yuan, and C.Y. Young, Recent Advances in Understanding Hormonal Therapy Resistant Prostate Cancer. *Current Cancer Drug Targets*, 2010. 10(4): p. 402-410.
148. Varambally, S., et al., The polycomb group protein EZH2 is involved in progression of prostate cancer. *Nature*, 2002. 419: p. 624-629.

VITA

Ruixin Wang

Major Professor: Dr. Timothy Ratliff, Dr. Xiaoqi Liu

Date of entry into Graduate Program: Fall 2014

Date of entry into Biochemistry Department: Fall 2015

EDUCATION

08/2014-12/2019 PULSe Program & Department of Biochemistry, Purdue University, West Lafayette, IN, U.S.A.

Ph.D. degree

09/2009-07/2012 College of Marine Life Sciences, Ocean University of China, Qingdao, Shandong, China

Master of Science in Developmental Biology

09/2005-07/2009 Marine College, Shandong University, Shandong, China

Bachelor of Science in Biotechnology

AWARDS

06/2018-05/2019 Purdue Research Foundation Grant, Department of Biochemistry

06/2018 Miles Graduate Scholarship, Purdue University Center for Cancer Research

03/2018-03/2019 Bird Stair Graduate Research Fellowship, Department of Biochemistry

04/2017-04/2018 Spring 2017 Beach Travel Award, Department of Biochemistry

02/2017-02/2018 Bird Stair Graduate Research Fellowship, Department of Biochemistry

PUBLICATIONS

Bai Y, Zhang Z, Cheng L, **Wang R**, Chen X, Kong Y, Feng F, Ahmad N, Li L, Liu X*. Inhibition of enhancer of zeste homolog 2 (EZH2) overcomes enzalutamide-resistance in castration-resistance prostate cancer. *J Biol Chem*. 2019 Jun 21; 294(25):9911-9923.

Mao F, Li J, Luo Q, **Wang R**, Kong Y, Carlock C, Liu Z, Elzey B, Liu X*. Plk1 inhibition enhances the efficacy of BET epigenetic reader blockade in castration-resistant prostate cancer. *Mol Cancer Ther*. 2018 Jul; 17(7):1554-1565

Li J[¶], **Wang R**[¶], Kong Y[¶], Broman M, Carlock C, Chen L, Li Z, Farah E, Ratliff TL, Liu X*. Targeting Plk1 to enhance efficacy of Olaparib in castration-resistant prostate cancer. *Mol Cancer Ther*. 2017, 16(3):469-479.

¶ Contribution equal

Li J, **Wang R**, Schweickert PG, Karki A, Yang Y, Kong Y, Ahmad N, Konieczny SF, Liu X*. Plk1 inhibition enhances the efficacy of gemcitabine in human pancreatic cancer. *Cell Cycle*. 2016, 15(5):711-9.

Wang R, and Liu X. Epigenetic regulation of prostate cancer. *Genes & Diseases*. 2019 Nov 9.